TABLE OF CONTENTS

ABOUT THE COVER: Blue diamonds are among the rarest and most highly valued of gemstones. The lead article in this issue examines the history, sources, and gemological characteristics of these diamonds, as well as their distinctive color appearance. Relationships between their color, clarity, and other properties were derived from hundreds of samples—including such famous blue diamonds as the Hope and the Blue Heart (or Unzue Blue)—that were studied at the GIA Gem Trade Laboratory over the past several years. The diamonds shown here range from 0.69 to 2.03 ct.

Photo © Harold & Erica Van Pelt—Photographers, Los Angeles, California.

LETTERS

GIA "Cut" Report Flawed?

The long-awaited GIA report on the ray-tracing analysis of round brilliant diamonds appeared in the Fall 1998 *Gems & Gemology* ("Modeling the Appearance of the Round Brilliant Cut Diamond: An Analysis of Brilliance," by T. S. Hemphill et al., pp. 158–183). The writer initially saw this article as an opportunity to qualitatively validate his own SAS2000 two-dimensional ray-tracing facility, but soon realized that this report on the brilliance aspect of cut grade analysis, based on GIA's weighted light return (WLR) metric, contains what appears to be an unintentional fatal flaw in its design: The hemispherical lighting model chosen by GIA for this study is not an unbiased benign source, and as a result it probably invalidates any conclusions presented in the article. The use of any comparisons in the *G&G* article should be strictly avoided, as the illumination model chosen apparently (based on limited SAS2000 two-dimensional analyses) weighs the results toward favoring shallower crown angles and possibly larger tables.

A scientific perturbation analysis such as that attempted in GIA's report is intended to show the effect on some output parameter (such as GIA's defined WLR) as a function of a change in a given parameter or combination of parameters. The model chosen by GIA was apparently intended to present a uniformly (diffuse) distributed set of input ray incident angles to the modeled diamond, each emanating from the hemisphere's internal surface. The amount of light entering the diamond (that which can potentially contribute to WLR) is dependent on the angle of incidence, and the researchers sought a uniform distribution of this angle of incidence.

Figure 1A shows a ray incident on the table (RO), originating from the hemisphere, with angle of incidence i defined by ROP. For the table, any ray such as ROP can have an angle of incidence bounded by the 90° angles defined by POA and POB, where PO is a normal to the table.

For any other crown facet, such as the crown main shown in figure 1B, rays originating from the hemisphere, such as R'O' (defined by the angle R'O'P'), are limited as to angle of incidence i', by the angles defined by P'O'A' and P'O'B', where P'O'A' is less than the 90° angle defined by P'O'B'. P'O' is a normal to the crown main shown. With this model, the allowed angular inputs for any facet below the table change as the facet angle changes—hardly the uniform, unchanging, angular distri-
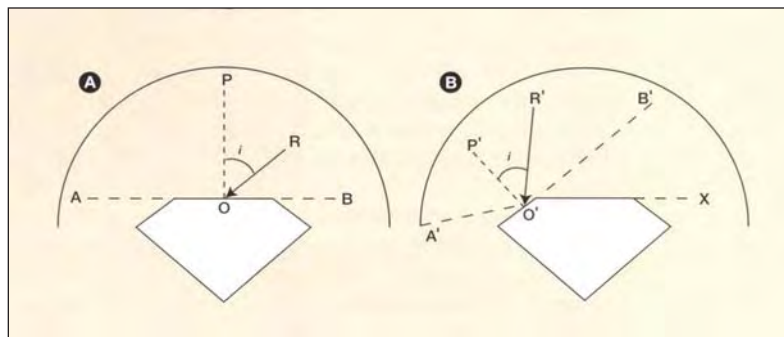

Figure 1. GIA's hemispherical input model.

bution applied to the table facet. Theoretically at least, the allowed angular range within a given point in a particular crown facet also changes, the magnitude of the change dependent on the radius chosen for the illuminating hemisphere. The angle defined by P'O'A' is, in the limit defined by an infinite hemispherical radius, equal to 90° minus the crown angle. Likewise, in GIA's three-dimensional model, the star and break facets will each have similarly defined angular ranges, with an individual angular cutoff on one side of the range.

What does all this mean? To this writer, it mandates an immediate retraction of the *G&G* article by GIA and a republication of results with a corrected model.

GIA should also, to eliminate what is a perceived bias in their report, include in an amended table 3 comparison of GIA's "Make Grade" system, which is taught in their own educational courses, regardless of the results shown: good, bad, or indifferent.

Martin Haske
*Adamas Gemological Laboratory
Boston, Massachusetts*

Authors' Reply

We thank Mr. Haske for drawing attention to these issues. We believe that many of his concerns stem from the difference between two-dimensional and three-dimensional analysis of the appearance of a diamond.

Mr. Haske states that he examined our results for the purpose of comparison with his own two-dimensional (SAS2000) analytical system. He evidently suspects that our diffuse hemispherical illumination condition is the

likely cause of the apparent disagreement between his analyses and our results, rather than the difference in the number of dimensions used in the two approaches. We chose this lighting condition because we believe that it represents the best average of the many ambient light conditions in which diamonds are viewed. A diffuse hemisphere of light at infinite distance is exactly that: Light rays of all angles emanate from all points on the inside of this hemisphere. We sought a uniform distribution of light with regard to the diamond as a whole, not over each facet independent of the other facets.

The "apparent flaw" Mr. Haske shows in his diagram is in fact the expected result of illuminating the diamond from above the girdle with a hemispherical source. Like all three-dimensional objects, a round brilliant diamond throws some small shadow on itself, and our model captures this aspect of real diamonds. All of the crown facets, including the table, are partly in the shadow of other facets (e.g., for rays originating between points B' and X in his figure 1B, the far bezel is in the "shadow" of the table and near bezel facet). One of the differences between a 2D model and a 3D model is the extent of this shadowing. In three dimensions, light rays coming from in front and behind impinge the particular "crown main" (bezel) facet at many of the angles that appear blocked in a two-dimensional view, for which the light source is an arc rather than a hemisphere. We know of no publication in the scientific literature on SAS2000 analyses of diamond cut appearance, and so do not know what other differences there might be between the two approaches, or whether such differences would be relevant.

Note also that the paths of some rays through the diamond cannot be represented in two dimensions, as was shown in figure A-2 of the original paper (p. 167). Given the different effects from two-dimensional and three-dimensional models, we do not believe Mr. Haske's geometrical argument applies to (three-dimensional) round, brilliant-cut diamonds.

Mr. Haske also writes that we attempted a "perturbation analysis." In fact, we did no such thing. Perturbation analysis is used to evaluate a mathematical function, to find out whether any particular point (in however many parameter dimensions) is a local maximum (a bump), a local minimum (a divot), or something else (such as a saddle point, which is a peak in one direction but a valley in another). It works by evaluating that function at that point, and then examining how the value changes as you move slightly away from that point. Although this technique could be used to find the exact location of the various local maxima in the WLR surfaces, we did not think this was necessary at this time.

Finally, Mr. Haske refers to a "Make Grade" system taught in the GIA courses. The GIA Diamond Grading Course (see, e.g., Assignment 9, 1994, pp. 15–17, 20–21) describes four general classes of cut as a teaching tool, but never proposes that they be used as a grading system. Thus, it was not appropriate to include them in table 3. The approximate values of WLR across the range of proportions described by these classes can be readily seen from the data given in the article.

In conclusion, we stand behind our study as published in *Gems & Gemology*, and do not feel that any correction is necessary.

<div align="right">

T. Scott Hemphill, Ilene M. Reinitz,
Mary L. Johnson, and James E. Shigley
Gemological Institute of America

</div>

CHARACTERIZING NATURAL-COLOR TYPE IIB BLUE DIAMONDS

By John M. King, Thomas M. Moses, James E. Shigley, Christopher M. Welbourn, Simon C. Lawson, and Martin Cooper

Although rarely encountered, blue diamonds are among the most famous, and most distinctive, of fine gemstones. To better understand these unique gems, more than 400 were studied at the GIA Gem Trade Laboratory over several years to reveal additional information about the relationships between their color, clarity, and other gemological properties. The overwhelming majority of natural-color blue diamonds are type IIb. The color appearance varies widely from light to dark, but there is a limited range of color saturation. As a result, color appearance between neighboring GIA GTL color grades can be subtle. Of the blue diamonds examined at GIA GTL, few had any solid inclusions. Nevertheless, internal features such as graining and color zoning can make the processing of these diamonds a challenge.

Because of their great beauty and rarity, blue diamonds are both intriguing and highly valued (figure 1). Such important historic diamonds as the Hope, the Blue Heart (also called the Unzue or Eugénie Blue), and the Idol's Eye have greatly added to the fascination and mystery surrounding blue diamonds throughout history.

In recent years, auction sales have also placed blue diamonds in the forefront of industry interest. The current record per-carat price paid for a blue diamond at auction, $569,000, was set in November 1995, for a 4.37 ct Fancy Deep blue oval shape which sold at Christie's Geneva. Only three diamonds have sold at auction for higher per-carat prices; indeed, of the 10 highest per-carat prices paid for colored diamonds at auction, six have been for blue diamonds (*World Diamond Industry Directory & Yearbook, 1997/98*, p. 56).

Even with their high profile, blue diamonds have long been considered among the rarest of gems (Federman, 1989, 1998). The De Beers Polished Division, in their published compilation *Important Diamond Auction Results 1997*, noted only 18 blue diamonds offered for sale that year at the auction houses of Christie's, Sotheby's, and Phillips (in contrast to 143 predominantly yellow diamonds noted for the same period). Of the numerous colored diamonds submitted for grading reports to the GIA Gem Trade Laboratory (GIA GTL) during the first half of 1998, only 0.3% were described as predominantly blue. Although such diamonds are much sought after, dealers indicate that only a couple of new blue diamonds come to their attention during the course of a year (K. Ayvazian and I. Gol, pers. comm., 1998). This observation is consistent with the current mining recovery rate. Of all the De Beers South African rough production, there is on average "only one significant blue" mined per year. When they occur, such finds are said "to cause excitement along the chain from the discovery at the mine to the sorting" (M. Semple, pers. comm., 1998).

In GIA GTL's color grading of colored diamonds, there

Figure 1. Blue diamonds are among the most highly prized objects in contemporary society. The connoisseur of such stones appreciates the subtle differences and nuances of color. Shown here are a range of appearances from the strongly colored heart shape in the ring to the gray-blue marquise shape at the upper left. The diamonds range from 0.48 ct to 2.01 ct; the 1.04 ct blue diamond in the ring is surrounded by approximately 2 carats of near-colorless diamonds. Loose stones courtesy of Rima Investors Corp.; the ring is courtesy of Martin Kirschenbaum Trading, Inc. Composite photo © Harold & Erica Van Pelt.
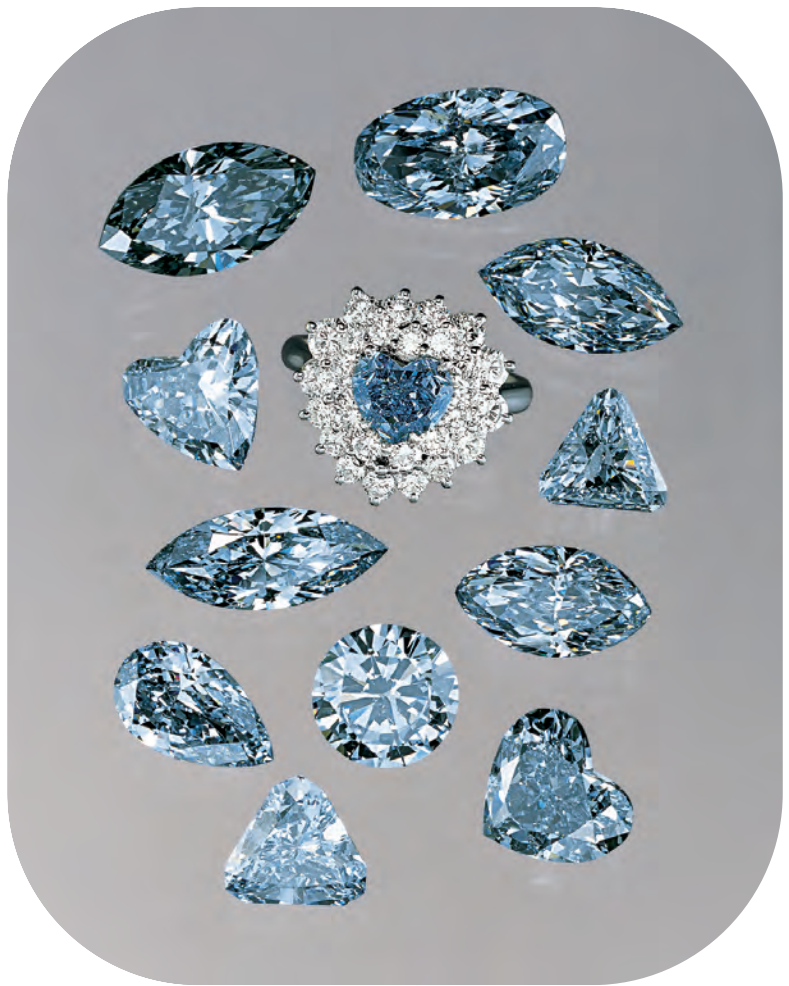
are other natural colors that are more rarely encountered than blue (such as purple or red). However, it is the combination of *relative* rarity (although the numbers are small, they are sufficient to enable a recognized market to be established), high value, and trade enthusiasm that makes it critical to expand our knowledge of blue diamonds. In particular, precisely because blue diamonds are so rare, few dealers understand their full range of color appearances. This is important to accurately assess the relationship of one blue diamond to another. As is the case with other aspects of diamond valuation, subtle differences in color appearance (reflected in differences in grading terminology)* can result in large differences in value. Therefore, understanding and consistently describing color in blue diamonds is critical.

To this end, GIA GTL and GIA Research have been compiling for several years (as well as drawing on the Laboratory's more than 40 years of reporting on these stones) information based on a significant quantity of blue diamonds they have graded and/or otherwise documented. This study represents the largest number of blue gem diamonds ever examined by a single organization, including some of the most famous diamonds known.

Following a discussion of the history of blue diamonds and a mention of some of the main localities where they are found, the present article reports on the relationship of the various color appearances of blue diamonds, as reflected in their GIA GTL color grades, to their other gemological properties.

Note that this article contains a number of photos illustrating subtle distinctions in color. Because of the inherent difficulties of controlling color in printing (as well as the instability of inks over time), the color in an illustration may differ from the actual color of the diamond.

Figure 2. The excitement generated by the historic 45.52 ct Hope diamond, now on display at the Smithsonian Institution, is due as much to its Fancy Deep color as to the dramatic events associated with its various owners. Photo © Harold & Erica Van Pelt.

BACKGROUND

History and Geographic Origin. Historically, blue diamonds have been recovered from several localities. Early accounts cite the Kollur mine (and possibly other mines) along the Krishna River valley near Golconda, in the Indian state of Hyderabad (now called Andhra Pradesh; Scalisi and Cook, 1983). This region was described by noted French traveler and gem dealer Jean-Baptiste Tavernier (1676). Over the course of almost 40 years (1631–1668), Tavernier made six journeys from Europe to India. At that time, India was the source of almost all gem diamonds. During these visits, Tavernier saw many spectacular rough diamonds, a number of which he purchased and brought back to Europe.

Tavernier is widely believed to have acquired one of the world's most famous diamond crystals, the 112.5 ct stone that became known as the Tavernier Blue, in India in 1642 (Tillander, 1975).

He sold this rough diamond to Louis XIV of France in 1669, who had the diamond cut into a triangular shape of 67.12 ct (possibly with additional smaller cut stones). In 1792, during the French Revolution, this and other diamonds were stolen from the collection of the French Crown Jewels housed in the Garde Meuble palace. It is believed that, to avoid detection, subsequent owners had the Tavernier Blue recut twice, ultimately to a weight of 45.52 ct, before Henry Philip Hope purchased it in 1830 (figure 2). Currently on exhibit in the Harry Winston gallery at the Smithsonian Institution in Washington, DC, the Hope diamond is seen by more than four million museum visitors each year (J. E. Post, pers. comm., 1998).

The 70.21 ct Idol's Eye is also reported to have been found in the Golconda district in the early 17th century. Like the Hope, it is a classic example of a diamond with a history surrounded by myths and legends (Krashes, 1993). It was claimed to have been set in the eye of an idol in the Temple of Benghazi, rumored to have been seized from its original owner for payment of debts, and disappeared for 300 years before resurfacing. This light blue diamond was rediscovered in the possession of Abdul Hamid II (1842–1918) in 1906, who became the 34th Ottoman Sultan.

A number of other important blue diamonds have published histories (see, for example, Balfour, 1997) and specific names that have lasted for many years. Table 1 presents a list of some of these notable blue diamonds, with their weights, color descriptions, cut shapes, and the most recent year that individual stones were examined by GIA staff members.

Today, there is little production at the Indian mines. The Premier mine in South Africa is now considered the most significant source of the blue diamonds entering the market (Federman, 1989; G. Penny, pers. comm., 1998).

The Premier Mine. Discovered in 1903, the Premier mine was initially worked by open-pit methods (figure 3); in 1905, it yielded the largest rough diamond ever found, the 3,106 ct Cullinan. In celebration of the gift of this diamond to King Edward VII of England, Thomas Cullinan, then chairman of the Premier mine, presented his wife with a necklace that contained several blue diamonds, including a 2.60 ct center stone (illustrated in Janse, 1995, p. 240).

The open-pit operations were closed in 1932, but De Beers reopened the Premier in 1946 as an under-

ground mine, with full production attained in 1949. Underground operations continue to the present time (figure 4).

Since mining began at the Premier in 1903, 278 million tons of ore have been processed and 90.5 million carats of gem and industrial diamonds recovered. Current production is approximately 1.6 million carats per year. The yield is 50 carats per 100 tons of ore, or approximately 0.50 ct per ton. Of this production, diamonds with any evidence of blue color (but that would not necessarily color grade as blue once cut and polished) represent less than 0.1% (H. Gastrow, pers. comm., 1998). The Premier mine is well known as a source not only of blue diamonds, but also of large, colorless diamond crystals. Indeed, it is the three or four blue and/or colorless "specials" recovered each year that make the Premier mine a viable operation (G. Penny, pers. comm., 1998). To date, there is no known correla-

tion between the geologic conditions of the host rock and the type or color of diamond recovered from the Premier mine or elsewhere; the recovery of blue diamonds is random and very sporadic (D. E. Bush, pers. comm., 1998).

Other South African mines that have produced blue diamonds include the Jagersfontein and Koffiefontein (both near Kimberley); the Bellsbank mine near Barkly West; and the Helem mine at Swartsruggens. Very rarely, blue diamonds have been found in alluvial deposits at Lichtenburg in the Western Transvaal. Guinea, in western Africa, is also known to have produced blue diamonds (Webster, 1994). Historically, central Africa has been rumored to be a source of blue diamonds, especially Sierra Leone for lighter blues (A. Arslanian, pers. comm., 1997). Outside of Africa, blue diamonds have been reported from Kalimantan on the island of Borneo in Indonesia (Spencer et al., 1988),

TABLE 1. Notable blue diamonds.[a]

Name	Weight (carats)	Color description[b]	Shape	Date of the most recent GIA Gem Trade Laboratory report/examination
Brazilia	176.2	"light blue"	Rough	ne[e]
Idol's Eye	70.21	Light blue	Modified triangle	1995
Mouawad Blue	49.92	Fancy Dark blue	Pear	1984
Copenhagen Blue	45.85	"blue"	Emerald	ne
Hope[c]	45.52	Fancy Deep grayish blue	Cushion	1996
Tereschenko	42.92	"blue"	Pear	ne
Graff Imperial Blue	39.31	Fancy Light blue	Pear	1984
Wittlesbach	35.50	"blue"	Oval	ne
Sultan of Morocco	35.27	"bluish gray"	Cushion	ne
North Star	32.41	"blue"	Pear	ne
Blue Heart (Unzue Blue)[c]	30.62	Fancy Deep blue	Heart	1997
Blue Lili	30.06	Fancy blue	Cushion	1980
Transvaal Blue	25.00	"blue"	Pear	ne
Howeson	24	"blue"	nr[d]	ne
Begum Blue[c]	13.78	Fancy Deep blue	Heart	1995
Brunswick Blue	13.75	"blue"	Pear	ne
Graff Blue	6.19	Fancy Dark blue	Round	1990
Marie Antoinette Blue	5.46	"blue"	Heart	ne
Cullinan Blue necklace (center stone)	2.60	"blue"	Cushion	1993

[a] Information obtained from GIA GTL reports or examination of individual diamonds (as indicated by a date given in the last column), as well as from the GIA Diamond Dictionary (1993), Christie's Jewellery Review 1995 (1996), and Balfour (1997).

[b] Color descriptions for diamonds graded by GIA GTL (i.e., those that are not set off by quotation marks) represent the color grading terminology that prevailed at that time. Modifications to the GIA GTL colored diamond color grading system and its nomenclature were introduced in 1995.

[c] Diamonds that were examined as part of this study.

[d] nr = not recorded.

[e] ne = not examined.

Figure 3. Opened in 1903, the Premier mine in South Africa is considered the principal producer of blue diamonds today. Note the original open-pit mine in the background and the modern processing plant in the foreground. Photo courtesy of De Beers.

from several regions in Brazil (Cassedanne, 1989), and from areas of Guyana and Venezuela (Webster, 1994; also see Bruton, 1978).

Past Studies of Blue Diamonds. Although blue diamonds have been known for centuries, only relatively recently have they become the subject of scientific study (see Box A). One of the results of such study was the identification of most blue diamonds as type IIb. Historically, the classification of diamond into two types has been determined by the differences in the diamond's transparency to ultraviolet (UV) radiation and in its infrared spectra (Robertson et al., 1934). In a type I diamond, UV

radiation is not transmitted substantially below about 300 nm, whereas type II diamonds transmit UV down to 230 nm. Because only simple equipment is needed, UV transparency is commonly used by gemologists to separate diamonds into these two basic categories.

The region of the infrared spectrum that is used to determine type (1000–1400 cm^{-1}) is referred to as the "nitrogen" region. Type I diamonds (which comprise most gem-quality stones) contain significant amounts of nitrogen, whereas type II diamonds do not. (For a discussion of diamond types, see Fritsch and Scarratt, 1992.) A further distinction within the type II classification was made in 1952 (see Box A). In the 1950s, irradiation and annealing of "off-color" diamonds began to be used commercially for the color treatment of gem diamonds, some of which turned blue (see, e.g., Schulke, 1962). As a result, concerns quickly arose in the trade about how a treated-color blue diamond could be identified by jewelers. During this period, J. F. H. Custers reported that natural-color blue diamonds display electrical conductivity with an efficiency capacity somewhere between that of a conductor (such as copper) and a nonconductor (such as glass or typical near-colorless diamonds); this capacity is referred to as semi-conductivity (Custers, 1954, 1955). Because of their electrical conductivity and their lack of substantial nitrogen, and because they exhibit a mid-infrared spectrum that is quite different from the spectra of other diamonds, these semi-conducting blue diamonds were designated as type IIb (again, see Box A).

On the basis of this electrical conductivity, early cooperation between GIA and De Beers resulted in the development of a simple conductometer in 1959 (Crowningshield, 1959; Benson, 1959). This proved very effective in distinguishing natural-color type IIb blue diamonds from treated-color blues of other diamond types (Custers and Dyer, 1954; Custers et al., 1960).

Recently, gemological researchers have recognized the existence of two other categories of natural-color blue diamonds (figure 5): (1) blue to green-blue type Ia or IIa diamonds that owe their color to natural radiation exposure (Fritsch and Shigley, 1991); and (2) gray-blue to gray-violet type Ia diamonds, in which the color is associated with the presence of hydrogen (Fritsch and Scarratt, 1992). These other two groups of natural-color blue diamonds are not electrically conductive, and their gemological properties differ from those of type IIb diamonds. In our experience, these two categories of

diamonds are rarely described as simply "blue" (without a modifier) in the GIA GTL grading system. Those non-IIb diamonds that are described as "blue" represent a miniscule number of the blue diamonds examined in GIA GTL. For these reasons, they are not part of this study. In addition, because the overwhelming majority of diamonds described as blue by GIA GTL are natural-color type IIb, this article deals only briefly with their separation from treated-color diamonds. (The latter are typically green-blue, not blue, and are never electrically conductive). Likewise, although gem-quality synthetic type IIb blue diamonds have been produced experimentally (Crowningshield, 1971), they are not commercially available. Therefore, they are not a significant part of this study either.

Some information on blue diamonds is presented in books by, for example, Liddicoat (1987, p. 230), Webster (1994), and Hofer (1998). A brief summary of the gemological properties of natural-color type IIb blue diamonds was presented as part of a natural/synthetic diamond identification chart by Shigley et al. (1995). To date, however, we know of no previous systematic study in which the gemological characteristics of a large number of blue diamonds have been documented.

MATERIALS AND METHODS

Samples. Over the course of the past 40 years, and in particular during the 1990s, staff members at the GIA Gem Trade Laboratory and GIA Research have examined hundreds of natural-color type IIb blue diamonds. For the present study, we gathered data from a representative sample of more than 400 of these diamonds, each of which was described as predominantly blue (i.e., blue, grayish blue, and gray-blue), to explore their color relationships with each other and with their gemological properties. The polished diamonds ranged from 0.07 to 45.52 ct (65 weighed more than 5 ct). Based on their infrared spectra and/or electrical conductivity, the diamonds in this study were all type IIb. Because of time constraints or other restrictions, it was not possible to gather all data on all of the blue diamonds included in this study. Some data (such as duration of phosphorescence) are not typically recorded in the course of routine gemological testing, as it is the absence or presence of the phenomenon that is most relevant. In specific cases, some tests could not be performed due to the conditions under which we were required to grade. For example, we typically cannot perform comprehensive testing (e.g., for

the Hope diamond) when the grading must be done off the GIA GTL premises. Also, because GIA GTL offers different reporting services for colored diamonds, different data are captured for different stones. For example, laboratory clients do not request a clarity grading on all colored diamonds. Consequently, we collected data on random subsets of blue diamonds for some properties (e.g., duration of phosphorescence). The number of stones examined for some key characteristics are listed in table 2; other sample numbers are given in the Results section.

Grading and Testing Methods. We used standard GIA GTL colored diamond color-grading methodology to determine the color descriptions and rela-

Figure 4. Since 1946, the Premier mine has been operated underground. The occasional recovery of blue diamonds helps make the expensive underground mining viable. Photo courtesy of De Beers.

BOX A: THE PHYSICS OF BLUE TYPE IIb SEMICONDUCTING DIAMONDS

The classification "type IIb" was suggested by Custers (1952) for type II diamonds that displayed phosphorescence after excitation with short-wave UV radiation. He noted that these diamonds also showed higher electrical conductivity than usual. The diamonds studied in this initial work were described as "water white" or light brown. However, in a note, Custers mentioned that similar characteristics had been seen in a diamond that was "a diluted bluish color." Further work by Custers (1954) showed that blue diamonds did indeed consistently exhibit high electrical conductivity and phosphorescence.

It was initially believed that the impurity responsible for the characteristic features of type IIb diamonds was aluminum (Austin and Wolfe, 1956; Dean et al., 1965; Lightowlers and Collins, 1966). However, when Wentorf and Bovenkerk (1962) produced synthetic diamonds doped with boron, they found that depth of blue color increased with boron content. They proposed that boron was responsible for the characteristic features of type IIb diamonds. Subsequently, Collins and Williams (1971) and Chrenko (1973) found that aluminum concentrations could not account for type IIb characteristics in diamonds, whereas Chrenko (1973) and Lightowlers and Collins (1976) showed that there was a good correlation between boron concentra-

tion and electrical conductivity in diamonds.

Electrical measurements (Leivo and Smoluchowski, 1955; Custers, 1955; Brophy, 1955; Austin and Wolfe, 1956; Dyer and Wedepohl, 1956; Wedepohl, 1956; Collins and Williams, 1971) showed that type IIb diamonds behave as semiconductors: The electrical conductivity *increases* with increasing temperature. These measurements also revealed that the conductivity is *p*-type. In *p*-type semiconductors, electrical current is carried by positively charged "holes," whereas in *n*-type semiconductors it is carried by negatively charged electrons.

A "hole" is what is left behind when an electron is missing from the normal bonding structure of a semiconductor. If an electron moves in to fill the hole, then another hole is left at that electron's original position. Although it is actually the negatively charged electron that has moved, the effect is the same as if a positively charged hole had moved in the opposite direction. Holes result when impurities known as acceptors are present. An acceptor can "accept" an electron from the bonding structure of the semiconductor, leaving a hole behind. In diamonds, boron acts as an acceptor; a boron atom contributes only three electrons to the bonding structure of the diamond crystal, whereas a carbon atom contributes four electrons (thus there is a deficiency of one electron per boron atom).

Figure A-1. The UV-Vis-IR spectrum of a natural type IIb diamond is shown in blue and, for comparison, that of a natural type IIa diamond is in red. The IR absorption of the type IIb below 1332 cm^{-1} results from lattice vibrations induced by boron impurities. The bands at 2455, 2802, and 2928 cm^{-1} are due to transitions of holes from the ground state to excited states of the boron acceptors. The absorption starting at 2985 cm^{-1} and continuing with decreasing intensity into the visible range corresponds to electrons being excited from the valence band to neutral acceptors. The fact that this absorption extends into the visible part of the spectrum, and decreases in intensity from the red end toward the blue end, gives rise to the blue color in type IIb diamonds.
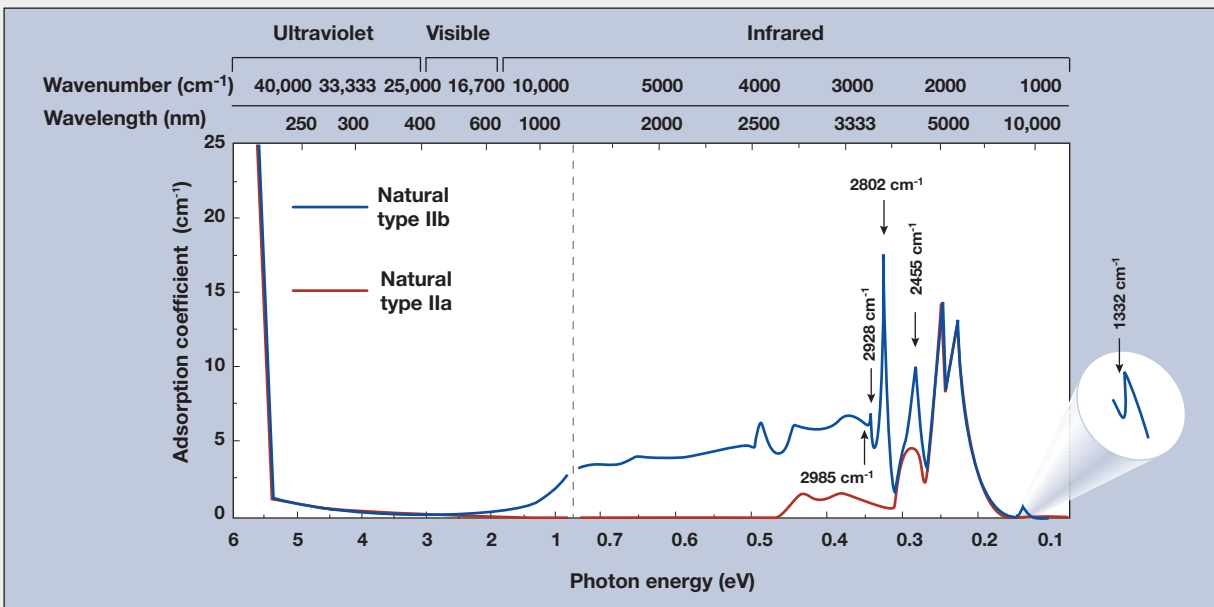
Analysis of the electrical measurements cited above implied that not all of the boron acceptors present in diamonds contribute to the semiconducting behavior. Even in type II diamonds, there are sufficient concentrations of nitrogen (although typically less than 0.1 ppm) to influence the electrical behavior. Nitrogen, which contributes five electrons to the bonding structure of a diamond crystal, acts as an electron donor. They donate electrons to boron acceptors, which become permanently ionized. These acceptors are said to be "compensated" by an electron from the nitrogen. Only the uncompensated acceptors contribute to semiconductivity, so the strength of this behavior depends on the difference between the boron and nitrogen concentrations, not on boron concentration alone.

The blue color of type IIb diamonds results from the decreasing edge of a region of absorption that is centered in the infrared and extends into the visible region of the spectrum. In addition to the intrinsic absorption exhibited by all diamonds, the infrared spectrum of type IIb diamonds, when measured at room temperature, has a series of bands located at 2455, 2802, and 2928 cm^{-1} (figure A-1). These bands were first observed by Blackwell and Sutherland (1949). Austin and Wolfe (1956) and Wedepohl (1957) found that their intensity is related to the concentration of neutral (i.e., uncompensated) boron acceptors. Smith and Taylor (1962) found that when the infrared spectrum was recorded at low temperature (–188°C), it was evident that these bands were composed of numerous sharp lines, the details of which are still not completely understood.

The basic shape of this spectrum can be explained in terms of the energy-level diagram shown in figure A-2. The energy level of the boron acceptor is located 0.37 electron volts (eV) above the valence band. The continuum absorption above 2985 cm^{-1} results from the capture of electrons by boron acceptors at various depths in the valence band; this leaves holes in the valence band that can take part in electrical conduction, a process called photoconduction. Thermal stimulation of electrons from the valence band onto the acceptors also results in holes in the valence band being available for electrical conduction. The higher the temperature, the greater the number of acceptors that are ionized, the greater the number of holes in the valence band, and so the higher the electrical conductivity will be.

Phosphorescence in boron-doped synthetic diamond has recently been studied in some detail. Whereas natural type IIb diamonds are known to exhibit both red and blue phosphorescence, synthetic type IIb diamonds always exhibit blue phosphorescence, occasionally accompanied by orange. Both may exhibit a greenish blue fluorescence when excited by electrons (cathodoluminescence) or short-wave UV radiation. This luminescence has been attributed to transitions between a donor and the boron acceptor, where the donor is believed to be nitrogen related (see Klein et al., 1995). It has been observed that whereas the fluorescence is also a characteristic of diamonds that have been so heavily boron doped as to be very dark blue or black, the phosphorescence is only dominant and long lived in lightly boron-doped diamonds (containing less than about 10 ppm of uncompensated boron and appearing pale blue to dark blue).

Watanabe et al. (1997) have proposed a model to explain this phosphorescence behavior. Essentially, their recombination model shows that following short-wave UV excitation and the rapid fluorescence decay, the rate of electron transition from the donor to the boron acceptor is limited by the availability of holes in the valence band. At room temperature, only about 0.2% of the boron acceptors are ionized; the lower the concentration of these acceptors is, the lower is the probability that the donor-to-acceptor transition can occur. Such low-probability transitions are characterized by long decay times, so strong, long-lived phosphorescence is a characteristic only of lightly boron-doped material. Boron concentrations in natural type IIb diamonds are usually a few ppm at most, and often considerably less than this, so their phosphorescence behavior is similar to that of the lightly boron-doped synthetic diamonds.

Figure A-2. In this schematic energy-level diagram for the boron acceptor in diamond, the acceptor ground state is located 0.37 eV above the top of the valence band. The excited-state energy levels are shown in simplified form for clarity. In fact, they are split into a number of sublevels. Bound-hole transitions from the ground state to these excited states give rise to the bands in the infrared spectrum at 2455, 2802, and 2928 cm^{-1}. If a hole is excited from the acceptor ground state into the valence band, either thermally or by photons of energy greater than 0.37 eV, it becomes available for electrical conduction.
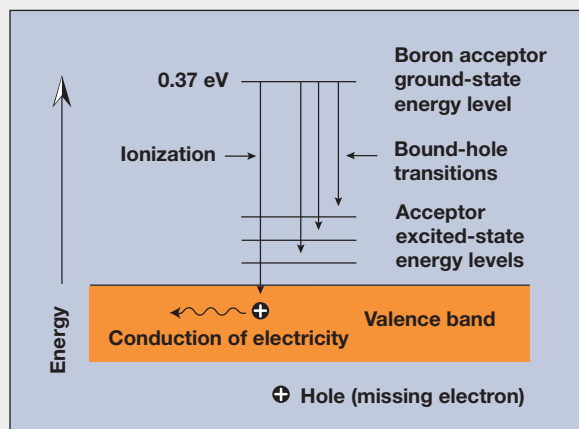
GIA GTL color grade		Clarity					SW UV phosphorescence intensity						SW UV phosphorescence duration (seconds)							
Grade	No.	FL/IF	VVS	VS	SI/I	No.	None	Wk	Med	St	VSt	No.	<5	6–15	16–25	26–35	36–45	45+	Avg	No.
Faint	**9**	2	3	0	4	**9**	0	1	1	0	0	**2**	—	—	—	—	—	—	—	**0**
Very Light	**10**	2	2	2	3	**9**	0	2	1	0	1	**4**	—	—	—	—	—	—	—	**0**
Light	**27**	5	3	6	3	**17**	1	7	4	0	0	**12**	2	0	0	1	0	0	12	**3**
Fancy Light	**44**	3	6	7	5	**21**	2	16	0	0	0	**18**	4	2	1	0	0	0	6	**7**
Fancy	**226**	35	28	55	18	**136**	5	70	16	2	1	**94**	9	6	2	0	0	0	8	**17**
Fancy Intense	**84**	29	12	14	9	**64**	1	14	3	0	0	**18**	8	1	0	1	0	0	7	**10**
Fancy Dark	**10**	1	2	0	0	**3**	1	3	1	0	0	**5**	1	2	0	0	0	0	6	**3**
Fancy Deep	**46**	6	7	12	5	**30**	4	12	4	1	0	**21**	1	3	0	1	1	0	18	**6**
Fancy Vivid	**6**	3	0	2	0	**5**	0	5	1	0	0	**6**	2	4	0	0	0	0	8	**6**
Totals	**462**	86	63	98	47	**294**	14	130	31	3	2	**180**	27	18	3	3	1	0	—	**52**

[a] *Abbreviations: No. = number of samples tested in each subcategory, Wk = weak, Med = medium, St = strong, VSt = very strong, Avg = average. The clarity grade ranges follow the standard GIA GTL system for clarity grading of diamonds.*

tionships of the study diamonds (see King et al., 1994). We have continued to look into instrumental measurement to assist in color determinations. To date, however, we have not identified instrumentation that can adequately describe the complex face-up color appearance of a colored diamond with the perspective that an experienced observer can pro-vide in a controlled grading environment such as that used in our laboratory.

Standard equipment was used for gemological documentation, including a Gemolite Mark VII binocular gemological microscope, a GIA GEM Instruments ultraviolet unit with long-wave (365 nm) and short-wave (254 nm) lamps, a desk-model spectroscope, and a GIA GEM Instruments conductometer. Electrical conductivity measurements were made by placing the diamond on a metal base plate and touching a probe carrying an electric current to various surfaces of the polished diamond. Because we found that in some diamonds the measured conductivity values varied from one location to the next, we made several measurements on each stone and recorded the highest conductivity reading in our database. When documenting conductivity and reporting the results here, we used a numerical value that expresses the electrical current that passed through the diamond relative to the current measured when the probe was touched to the metal base plate (which, in this study, was always 135). This was also done to compensate for minor variations in line current. Because of the difficulty of making good, consistent contact between the instrument and the diamond, these values do not represent a precise measurement of the electrical conductivity. At best, they provide a relative indication of differences in conductivity among the blue diamonds tested.

A Hitachi U-4001 spectrophotometer was used to collect visible absorption spectra, from 400 nm to 800 nm, at low (liquid nitrogen) temperatures. To

Figure 5. Three categories of diamonds have been associated with a natural blue color: (1) type IIb, which are colored by boron impurities; (2) those type Ia or IIa that owe their color to radiation exposure; and (3) those type Ia in which the color is associated with hydrogen. Of these, only type IIb diamonds (like that in the center) are typically described as blue (without a hue modifier) in the GIA GTL colored diamond color-grading system. Those naturally colored by exposure to radiation are usually described as green-blue (left), whereas those colored by color centers associated with hydrogen are described as gray-violet to gray-blue (right). The photo of the 1.01 ct blue marquise is by Shane F. McClure; those of the 0.28 ct gray-violet heart shape and the 0.15 ct green-blue round brilliant are by Robert Weldon.

Electrical conductivity values[b]							GIA GTL color grade
10–30	31–50	51–70	71–90	90+	Avg	No.	Grade
—	—	—	—	—	—	**0**	Faint
—	—	—	—	—	—	**0**	Very Light
3	4	2	0	0	41	**9**	Light
4	7	11	3	1	56	**26**	Fancy Light
12	31	35	17	8	60	**103**	Fancy
3	7	7	8	3	64	**28**	Fancy Intense
0	0	5	2	1	76	**8**	Fancy Dark
1	3	6	6	6	77	**22**	Fancy Deep
2	1	1	1	1	62	**6**	Fancy Vivid
25	53	67	37	20	—	**202**	Totals

[b] *All 462 samples were electrically conductive.*

investigate the relationship between the depth of color and the visible absorption spectra, we selected four diamonds of similar size and shape but different depths of blue color (GIA GTL grades Very Light, Fancy Light, Fancy, and Fancy Intense). We also tested a Fancy Light gray diamond for comparison. We recorded the spectrum of each diamond with the light directed into a bezel facet and emerging from the pavilion facet on the opposite side. We then corrected the measured absorbance values for the approximate size of the diamond. Light passing through a diamond does not follow a straight path without any internal reflections, and a large portion of the diamond is illuminated in the instrument. Therefore, to simulate the direction and length of the light path through the diamond, we calculated an approximate sample thickness as the average of the girdle width and the table-to-culet thickness.

For the purposes of this study, infrared absorption spectra were recorded with a Nicolet Model 510 FTIR spectrometer over a range of 6000 to 400 wavenumbers (cm^{-1}) on the same five diamonds for which visible spectra were recorded. Laser Raman microspectrometry and energy-dispersive X-ray fluorescence (EDXRF) analysis were attempted to identify the inclusions in two other blue diamonds.

RESULTS

Color Appearance. One of the most important parts of this study was the unique opportunity to document the range of color appearances of blue diamonds. The study samples covered the entire range of GIA GTL fancy grades, as shown in figure 6.

Details of the hue (such as blue in this case), tone (the lightness or darkness of a color), and saturation (the strength of a color) of the diamonds—that is, their location in color space—are described below (again, for details on this color-grading system, see King et al., 1994).

Hue. The diamonds in this study typically occur in a restricted region of the hue circle (figure 7). This supports our past observations that the hue of type IIb blue diamonds *does not transition smoothly* into the neighboring color hues (i.e., their hue does not extend into violetish blue in one direction around the hue circle, or into greenish blue in the other direction). Within this region of the hue circle, there are two narrow populations. The fact that type IIb blue diamonds occur within such narrow ranges is very different from the situation with yellow diamonds, in which subtle hue shifts are seen throughout its hue range.

Tone and Saturation. Figure 8 shows the general location of the blue diamonds in our study on a tone and saturation grid. Of the three color attributes, blue diamonds showed the greatest variation in tone: The samples covered a broad light-to-dark range.

Compared to other colors in diamond, however, a relatively narrow range of appearance distinctions was seen for the saturation of blue diamonds. For example, at its widest region—i.e., corresponding to such GIA GTL fancy grades as Fancy, Fancy Intense

Figure 6. This pie chart illustrates the percentages of the 462 blue diamonds studied that appeared in each GIA GTL fancy grade category.
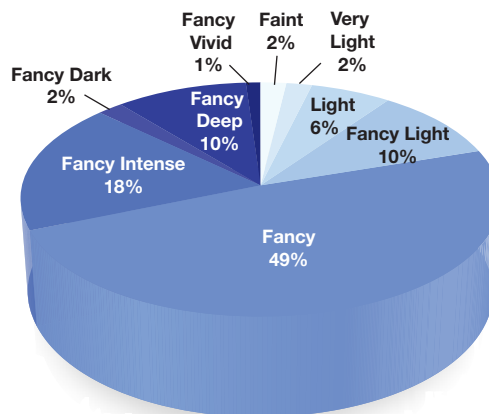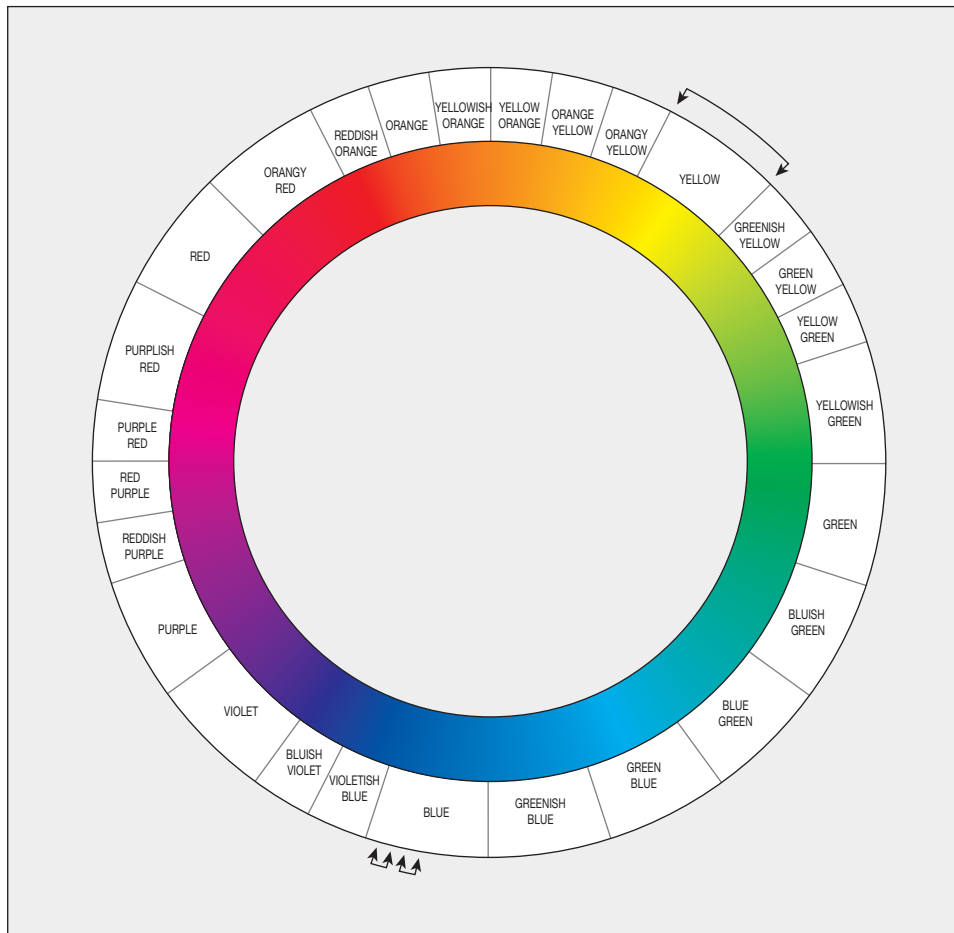
Figure 7. The blue diamonds studied appear to group into two narrow, restricted populations (indicated by the arrows) within the range of color GIA GTL associates with the term blue. This is unlike the broader occurrence within the hue ranges of other colored diamonds, such as yellow, that we have encountered.
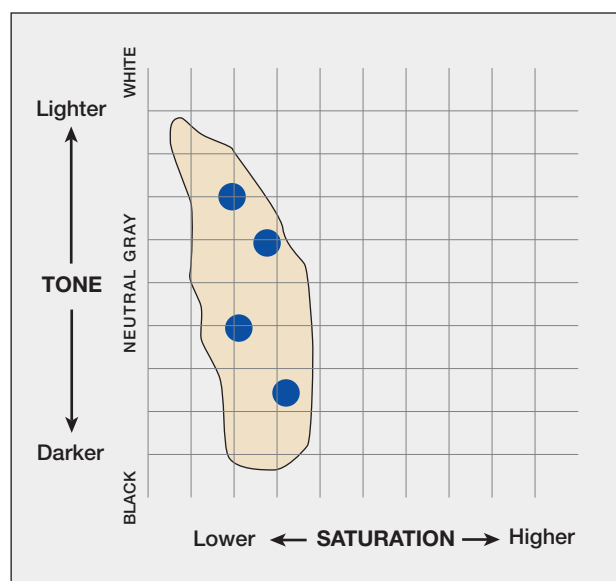
or Fancy Deep, and Fancy Vivid—the saturation range for blue diamonds is less than one third that in which yellow diamonds occur. *This compressed saturation range means that the degree of difference in color appearance within each GIA GTL fancy grade is much narrower for blue diamonds than for yellow diamonds.* For example, the range of appearances between Fancy Deep yellow and Fancy Vivid yellow is broader than the range between Fancy Deep blue and Fancy Vivid blue.

For the diamonds in our study, and in our general experience, we found that there are four smaller clusters in color space where blue diamonds most commonly occur. These are indicated on the grid in

figure 8 by the circles.

GIA GTL fancy grades represent a combined effect of tone and saturation (King et al., 1994). Figure 9 shows the general relationship of the

Figure 8. The beige area on this grid illustrates the tone and saturation range observed for the blue diamonds in this study. Note that the tone values occur over a broader range than the saturation values. Within this area are four smaller clusters (here, shown as circles) in which the colors of blue diamonds are typically observed.

FAINT

VERY LIGHT

LIGHT

FANCY LIGHT

FANCY

FANCY INTENSE
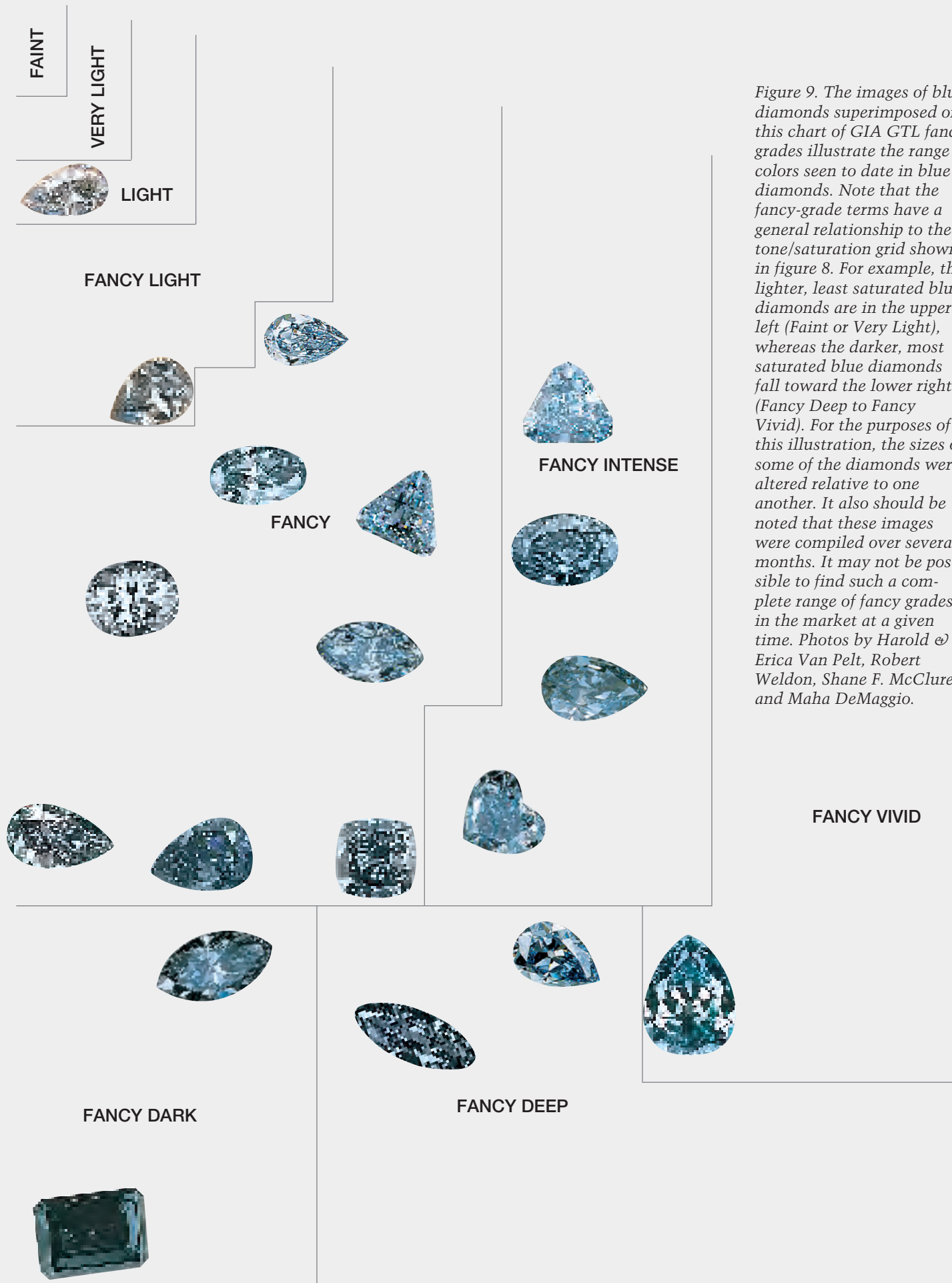
FANCY VIVID

FANCY DARK

FANCY DEEP

Figure 9. The images of blue diamonds superimposed on this chart of GIA GTL fancy grades illustrate the range of colors seen to date in blue diamonds. Note that the fancy-grade terms have a general relationship to the tone/saturation grid shown in figure 8. For example, the lighter, least saturated blue diamonds are in the upper left (Faint or Very Light), whereas the darker, most saturated blue diamonds fall toward the lower right (Fancy Deep to Fancy Vivid). For the purposes of this illustration, the sizes of some of the diamonds were altered relative to one another. It also should be noted that these images were compiled over several months. It may not be possible to find such a complete range of fancy grades in the market at a given time. Photos by Harold & Erica Van Pelt, Robert Weldon, Shane F. McClure, and Maha DeMaggio.

images of several blue diamonds superimposed on a chart of the GIA GTL fancy-grade categories. Such a chart illustrates the subtle distinctions in color appearance between the various "fancy" terms.

Microscopic Examination. *Clarity.* As shown in figure 10, 29% of the 294 diamonds analyzed for clarity were Flawless or Internally Flawless; 84% were VS or higher (these data include diamonds in which clarity could potentially be improved even further by the removal of shallow imperfections). These percentages are much higher than we have observed in other diamonds. The high clarity grades of these polished blue diamonds are consistent with the high "purity" (i.e., clarity) of the rough as compared to most other diamonds (D. E. Bush, pers. comm., 1998).

Inclusions. In the subset of 62 diamonds that we examined specifically for inclusions, we found that approximately 35% (22) had no inclusions. Of the remaining stones, 78% had fractures or cleavages and only 25% had solid inclusions (and, in some cases, fractures or cleavages as well). In the small percentage of blue diamonds that contained solid inclusions, the tendency was for the inclusions to have a consistent shape and appearance. The inclusions in figure 11 are typical of those observed.

Figure 10. This pie chart illustrates how the 294 blue diamonds in this study that were clarity graded fit into the various GIA GTL clarity grade ranges. Although marketing factors may influence these results, the most surprising feature of this diagram is the very high percentage of diamonds in the Flawless/Internally Flawless category (much greater than for other diamonds).
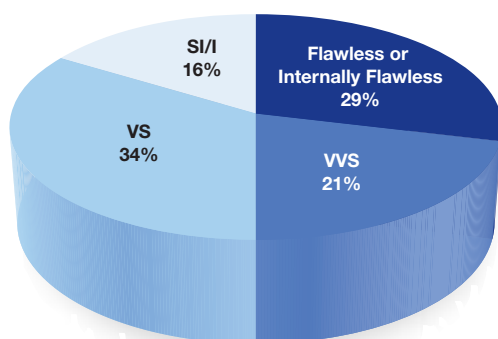
They tend to be opaque, dark, platy in habit, and would best be described as "flakes" with a slightly rough surface. They have an almost hexagonal, somewhat geometric outline. At magnification higher than 10×, the outlines are jagged and appear to be composed of interconnected and overlapping plates. When examined with reflected fiber-optic illumination, the inclusions appear gray and the roughness of the surface becomes most apparent.

With magnification and polarized light, the opaque inclusions are surrounded by visible strain halos composed of low-order interference colors. The inclusions do not align with any linear strain pattern of the host diamond. Instead, they seem to interfere with the otherwise orderly arrangement of the crystal structure, causing additional strain to the host crystal.

Since GIA acquired its Raman spectroscopy system in the fall of 1997, there has been limited opportunity to analyze the solid inclusions in blue diamonds. Raman analysis of solid inclusions in two diamonds proved inconclusive because of the small size of the inclusions and the fact that their rough surfaces caused the laser beam to scatter rather than return to the detector. The resulting Raman spectra were of poor quality and such weak intensity that they could not be matched with the spectral features of likely inclusion materials (such as graphite or a sulfide mineral inclusion; see following paragraph). EDXRF chemical analysis of the inclusions also was not diagnostic. For both techniques, the composition and size of the inclusion, its depth below the surface of the diamond, and its location within the diamond were all factors that prevented successful analysis.

From our visual observations of these inclusions with respect to their luster, dark color, morphology, and lack of transparency, we believe that the inclusions are either a sulfide or graphite (see, e.g., Harris, 1972; Meyer and Tsai, 1976). The fact that the inclusions are positioned in seemingly random directions, and they cut across distinct linear strain planes in the diamond, suggests that they are sulfides, because graphite forms most commonly along cleavage planes as a result of diamond alteration (see Harris, 1972; Harris and Vance, 1972; and Meyer and Tsai, 1976). Graphite inclusions would be expected to follow the planar structures in a diamond, rather than cutting across those layers. The excessive strain surrounding each of these inclusions also supports their identification as sulfides. Graphite forming as an alteration product along
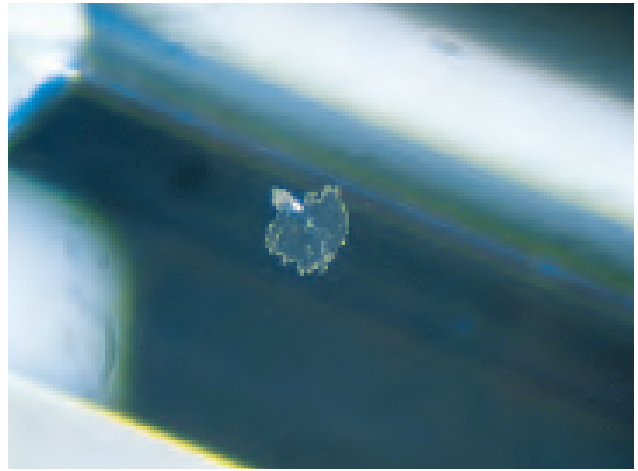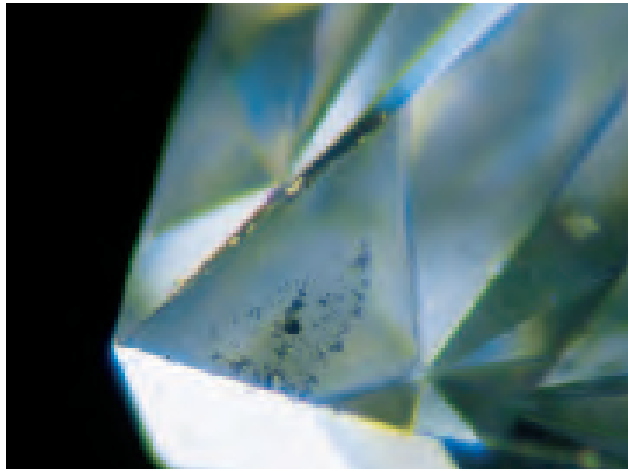
Figure 11. In 10 of the blue diamonds examined for inclusions in this study, we observed dark solid inclusions. On the left are several such inclusions in a 1.22 ct Fancy blue diamond. On the right is an isolated example of a flattened inclusion in a 4.57 ct Fancy Intense blue emerald cut. Visual examination suggests that these are probably sulfide mineral inclusions. Photomicrograph on the left is by Nick DelRe, magnified 30×; right, by Vincent Cracco, magnified 63×.

planes in the diamond would not be expected to produce detectable strain in the host, whereas visible strain halos around sulfide inclusions are typical (J. I. Koivula, pers. comm., 1998).

Graining. Internal graining is more common in blue diamonds than in near-colorless type Ia diamonds. Readily noticeable graining—which would carry a comment of "internal graining is present" on the report—was seen in approximately one-fourth of the 40 sample diamonds that had internal features. Graining is commonly believed to result from irreg-

ularities in the crystal structure that form during or after crystallization. In our samples, the graining most often appeared as whitish bands (figure 12) or reflective internal planes.

Color Zoning. We saw color zoning, often very subtle, in more than 30 of the 62 diamonds in the inclusion subset. This zoning was most easily seen with diffused lighting and darkfield illumination. It typically appeared as discrete blue and colorless areas or parallel bands (figure 13). When cutting such a diamond, manufacturers try to locate the

Figure 12. This Fancy Deep blue diamond, which weighs more than 10 ct, exhibits parallel bands near the culet. Such graining is not uncommon in blue diamonds. When graining is this extensive, it affects the clarity grade. Photo by Vincent Cracco; magnified 10×.

Figure 13. Color zoning is often observed in blue diamonds. This photograph, taken at 10× magnification, shows parallel banding of colorless and blue areas. The position of the zones can have a significant impact on the face-up color (but typically not the clarity) of the diamond. Photo by Stephen Hofer, © GIA.

Box B: Manufacturing Blue Diamonds

Like many other aspects of blue diamonds, the manufacturing processes (planning, cutting, and polishing) often follow a path different from those used for near-colorless diamonds and even other fancy colors. Several factors must be considered. First, the rough usually lacks a symmetrical form (figure B-1), unlike type Ia diamonds which often occur in common habits such as octahedra or dodecahedra. Thus, it may be more difficult than normal to determine appropriate cleaving and polishing directions. Second, the blue color may be unevenly distributed: Color zoning frequently occurs along growth directions or in isolated regions, often as alternating blue and near-colorless bands. Orienting these color zones to obtain the best face-up color appearance is a challenge similar to the cutting and polishing of blue sapphire, but the much higher value of blue diamonds (in which every point removed could mean a loss of thousands of dollars) means that the consequences are far more serious. Third, the surfaces of strongly asymmetric diamonds are commonly sculpted and translucent (Orlov, 1977). Thus, the cutter must polish several "windows" on the crystal to see any color zoning and inclusions before planning the cut.

These manufacturing challenges make modern computer-assisted cutting programs such as the Sarin Dia-Expert (Caspi, 1997) less useful in planning cuts for blue rough. Larger blue rough sometimes is shaped first in a rudimentary manner, maintaining flexibility regarding the final shape until the cutter can see the internal features more clearly. One may start out with plans for an oval or perhaps a pear shape, but make the final decision late in the faceting process. Weight recovery is often less than that typically obtained with colorless to near-colorless octahedral diamond rough.

The final face-up color of a blue diamond is much less predictable than most diamonds in the D-to-Z range or even than other fancy colors because of such features as color zoning. However, modern cutting and polishing techniques used to retain, improve, and spread color in all fancy-color diamonds also apply to blue diamonds. These techniques include the adaptation of "half-moon" facets and French culets to nearly all known brilliant-cut designs and shapes (figure B-2). Half-moon-shaped facets are cut along the girdle on the pavilion (on straight or curved sides), usually at high angles relative to the girdle plane. These half-moon facets create more internal reflection, which produces a more intense face-up color appearance. A French culet distributes the color more evenly throughout. Conventional pavilion faceting typically concentrates the color in the points, corners, or heads of longer shapes such as ovals and pears. The color in the center (under the table) is weaker, creating an uneven two-tone effect. The French culet reduces this collection of color at the point and, with the half-moon facets, can prevent loss of color in the center of the faceted diamond.

Because of the irregular shape of the rough, the polishing directions are often difficult to orient. A cutter must be conscious of heat build-up and surface burning from misorientation on the polishing wheel, especially when working on large facets such as the table.

The fact that blue diamonds occupy a small region of color space means that subtle changes in appearance can influence the color description or grade. After deciding on a final shape, the cutter methodically adjusts the pavilion and crown angles, factoring in any previous experience with those angles in similarly colored rough. Often each side is cut to different angles, and the resulting effects on color appearance are compared. In fact, in some cases this asymmetrical faceting is left on the finished stone. Manufacturing blue diamonds is often a slow, arduous process that requires careful inspection of the face-up color appearance at each stage.
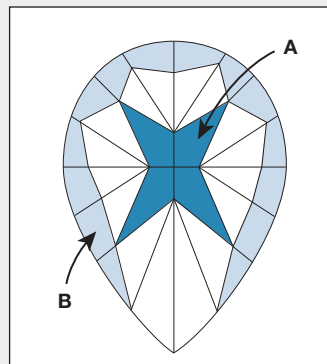
Figure B-1. These rough blue diamonds (approximately 0.75 to 2.00 ct) are typical of the irregular shapes, color zoning, and sculpted, translucent surfaces associated with this material.

Figure B-2. The use of a French culet (A) and half-moon facets (B) on the pavilion often creates a blue diamond with a stronger, more evenly colored face-up appearance.

Figure 14. Type IIb blue
diamonds are electrically
conductive. In some cases,
different locations on the
surface of the diamond
differ in conductivity.
Shown here are the results
of conductivity measure-
ments recorded for vari-
ous locations on the
famous Hope diamond.
On the basis of our con-
vention to record the high-
est number obtained
through repeated mea-
surements, the number
recorded for the Hope was
70:135.

DIAMOND POSITION 1

40:135

30:135

DIAMOND POSITION 2

45:135

65:135

70:135

Metal Base Plate
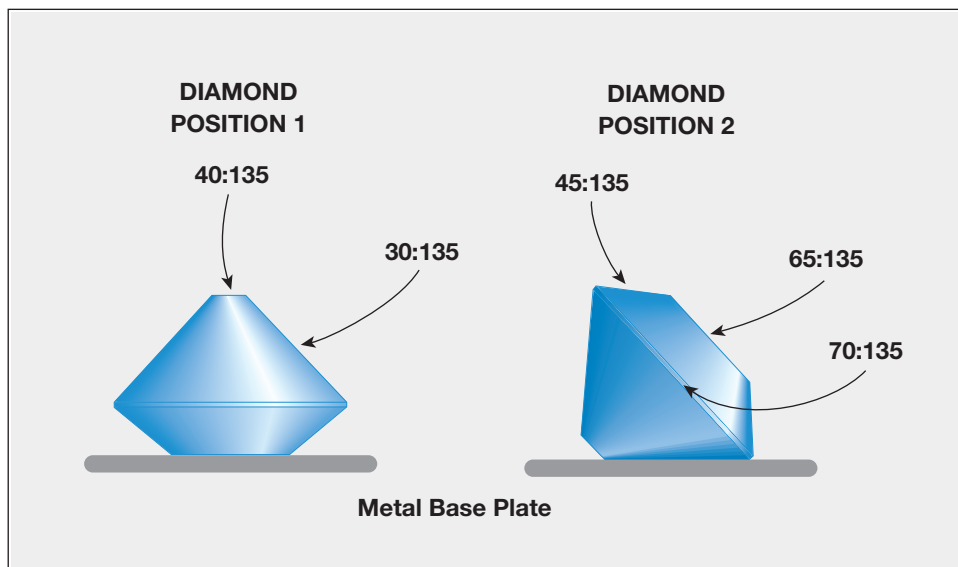
color zoning strategically to give the stone a uni-
form, more saturated blue appearance when it is
viewed face-up (see Box B).

Fluorescence/Phosphorescence. Ninety-eight per-
cent of the diamonds in this study showed no
observable fluorescence to long-wave UV, and 91%
showed no observable fluorescence to short-wave
UV. However, subtle fluorescence was difficult to
observe because of the blue bodycolor combined
with the purple surface reflections from the UV
lamps. Of the small number of diamonds that did
show a readily observable fluorescence to long- or
short-wave UV radiation, the reaction was chalky
blue to green or, rarely, red; the intensity was weak.
It should be mentioned that extremely weak fluo-
rescence in a diamond could be recorded as "none"
on a GIA GTL report. Thus, the actual percentages
of diamonds that fluoresce is likely to be higher
than the values given above.

As is typical of type IIb blue diamonds, there was
almost never a phosphorescence to long-wave UV,
but a reaction to short-wave UV was common
(again, see table 2). In fact, it was usually much easi-
er to see phosphorescence from our samples than to
see fluorescence. Of the blue diamonds that phos-
phoresced (92%), the reaction varied from very
weak to very strong, with almost three-quarters
showing a very weak or weak reaction. The most
common color was the same as the fluorescence
color, chalky blue to green; rarely, it was red or
orangy red. Because the important criterion in our
typical gemological examinations of blue diamonds

is whether or not a phosphorescent reaction is
noted, for this study we recorded the duration of the
phosphorescence in a random subset of 52 blue
diamonds. The duration varied from a few seconds to
as long as 45 seconds. Within the subset, we also
noted that the Fancy Deep diamonds had the most
persistent phosphorescence, at an average of 18 sec-
onds. During our most recent examination of the
(Fancy Deep) Hope diamond, we checked this feature
closely and noted that the total phosphorescence,
which was red, actually lasted almost 45 seconds.

Electrical Conductivity. All the diamonds in our
study were electrically conductive. The samples
showed a wide range of measured values, both in
general and within each fancy-grade category (see
table 2). The lowest value measured among our
samples was 10:135, and the highest was 120:135
(again, reading on the diamond and reading on the
metal plate).

As mentioned above, we sometimes noted a
variation in conductivity within individual stones
by touching the probe to different areas. A good
example is the data we recorded for the Hope dia-
mond in 1996, as shown in figure 14.

Visible Absorption Spectrum. Type IIb blue dia-
monds lack sharp absorption bands in their visible
spectra. Rather, they exhibit a gradually increas-
ing absorption toward the red end of the spec-
trum. Figure 15 shows the absorption spectra of
four blue diamonds of differing intensities and a
gray diamond.

Infrared Absorption Spectrum. Figure 16 shows the mid-infrared spectra of the same five diamonds for which the visible spectra were illustrated in figure 15. The features that are characteristic of a type IIb diamond were more intense in the two diamonds with a stronger blue color relative to the other diamonds.

DISCUSSION

Type IIb blue diamonds are unique in a number of their gemological properties, such as their electrical conductivity together with their phosphorescence to short-wave UV. This allows for their separation from other materials more readily than is the case for many gems. In addition, diamonds of other types that are described as blue typically are not of the same hue, nor do they have similar reactions to other gemological tests. Therefore, this study focused less on the identification of natural from treated or synthetic blue diamonds and more on understanding their distinctive color appearance. Because of the critical role that color plays in the evaluation of type IIb blue diamonds, the following discussion will examine the relationship of the various color appearances to the characteristics documented in natural type IIb blue diamonds.

**Color Relationships Among Blue Diamonds.** An important goal of this study was to better understand how blue diamonds relate to one another in color space—that is, hue, tone, and saturation—especially as these relationships are articulated in the GIA GTL color grading system for colored diamonds.

Hue. From the tight hue clustering found in the type IIb blue diamonds studied, it appears that boron, the element that causes the color (again, see Box A), creates a very limited range of color appearance.

Tone and Saturation. For many people, tone and saturation are the most difficult aspects to discriminate in the face-up color appearance of a faceted gemstone. Because the hue range is limited, the variation in color appearance among blue diamonds is mainly determined by the tone and saturation of their colors. In the GIA GTL grading system, a variety of color appearances can be included within the same fancy grade. The system uses the same set of fancy grades for describing all colored diamonds, but for blue diamonds, these grades are compressed into a smaller region of color space.

As the results of this study indicate, the colors of type IIb blue diamonds occur in a relatively wide tone range (i.e., light to dark) but a narrower saturation range (i.e., weak to strong intensity) in color space (see again figure 8). Because of this distribution, the color appearances that one usually sees in blue diamonds are more likely to result from differences in tone (see figure 17). For an unfamiliar

Figure 15. The visible spectra of blue diamonds lack sharp absorption bands; rather, they have gradually increasing absorption toward the red end of the spectrum. Spectra A to D are for blue diamonds of differing color intensity (A = Fancy Intense, B = Fancy, C = Fancy Light, and D = Very Light); spectrum E is for a Fancy Light gray diamond. These spectra were recorded at low (liquid nitrogen) temperature. The diamonds, all oval or marquise shapes of similar weights and proportions, were positioned so that light entered a bezel facet and exited an opposite pavilion facet. Each of these spectra was normalized to the approximate sample path length, so the spectra could be compared. Because of the similarity of the spectra from one sample to the next, we could not correlate them with the depth of color in the five diamonds. However, this similarity in spectra is consistent with the narrow range of color appearances in which blue diamonds occur.
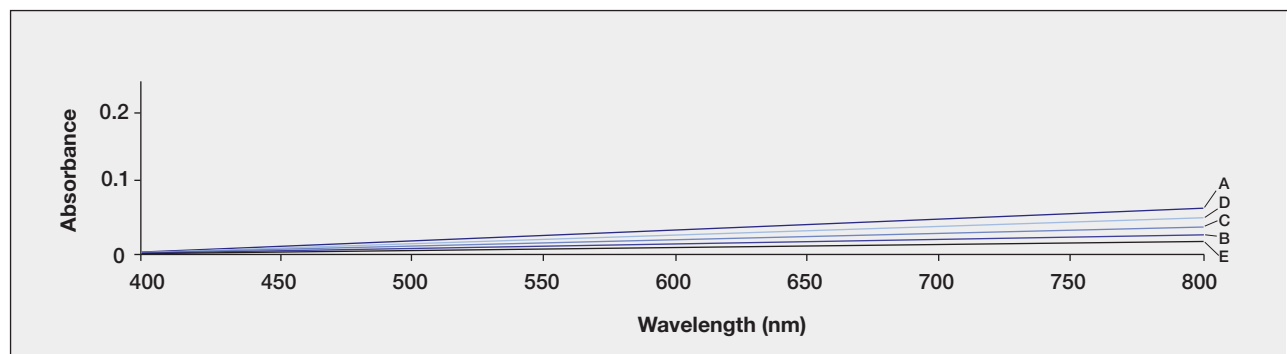
observer of blue diamonds, differences in tone can be misinterpreted as saturation differences.

As mentioned earlier, the colors of most blue diamonds tend to be concentrated around four clusters on the tone/saturation grid (see again figure 8). This clustering can cause misconceptions about the color grades of blue diamonds. For example:

1. Some of these clusters fall across grade boundaries. In this situation, subtle differences in color appearance between two blue diamonds can result in their being described with different fancy grades (figure 18). Judging from the more common situation involving yellow diamonds, some people may expect the differences in color appearance for some blue diamonds with different grades to be more pronounced than is actually the case.

2. When one looks at two blue diamonds that fall within the same cluster on the tone/saturation grid, at first these two colors may look sufficiently different that the observer feels that two grades are warranted. However, when the colors of these two blue diamonds are compared to that of a third diamond that is noticeably different in appearance, the close correspondence in color of the first two becomes apparent (figure 19). In this situation, use of two grades to describe the colors of blue diamonds that occur within the same cluster is not warranted.

3. In contrast to the colors of blue diamonds that fall within a cluster, a situation can occur where the color of a less-commonly seen blue diamond falls outside one of the four clusters. Despite the differences in appearance, these blue diamonds could still be assigned the same grade.

It is also important to recognize that the narrow saturation range in which blue diamonds occur is relatively close to the neutral gray region of color space. In general, the eye can discern fewer color distinctions in this region. Again, though, the trade expects—and an orderly description system implies—an equal number of grades for blue diamonds as for other colors despite the inequality between respective areas of color space. For a blue diamond and a yellow diamond in the same grade, the color of the yellow diamond is relatively stronger so the color differences between grades are more readily perceived.

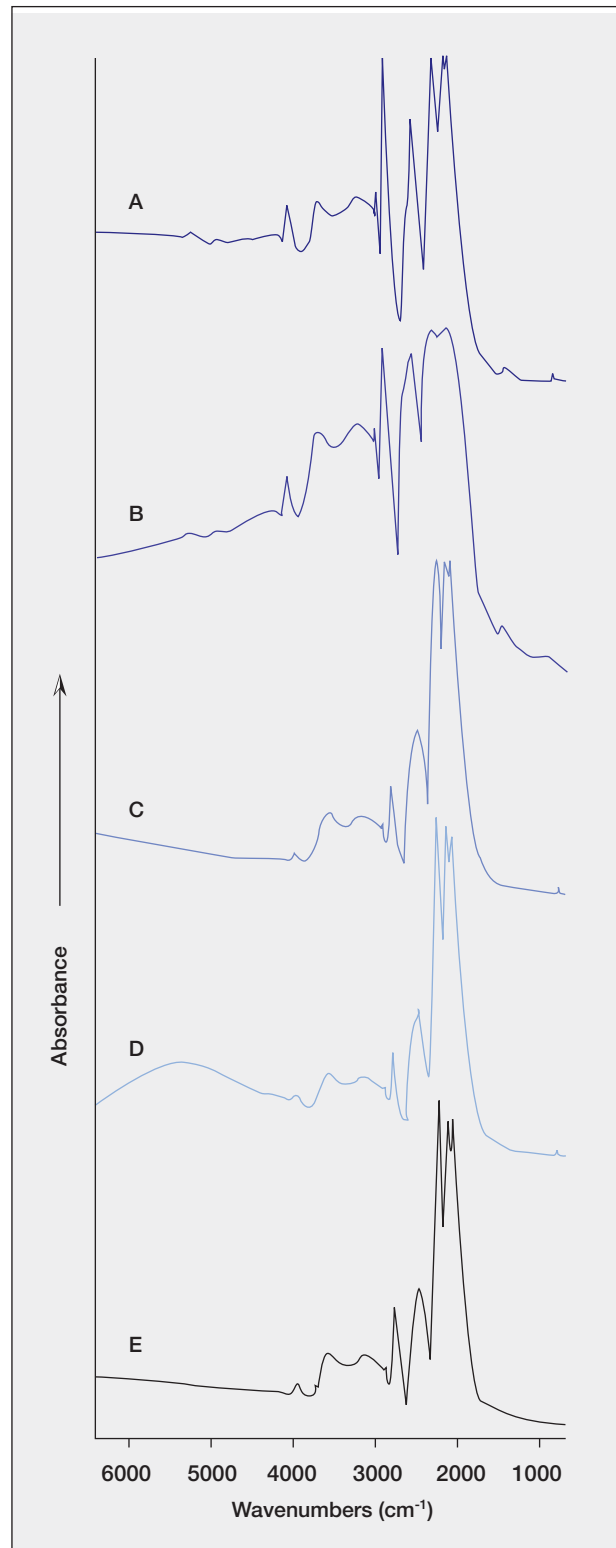Consequently, our experience with blue diamonds suggests the following:

Figure 16. The mid-infrared spectra of the five diamonds for which visible spectra are presented in figure 15 reveal the pattern of absorption features that is characteristic of type IIb diamonds. These features are most intense for the two stronger-blue diamonds (spectra A and B).
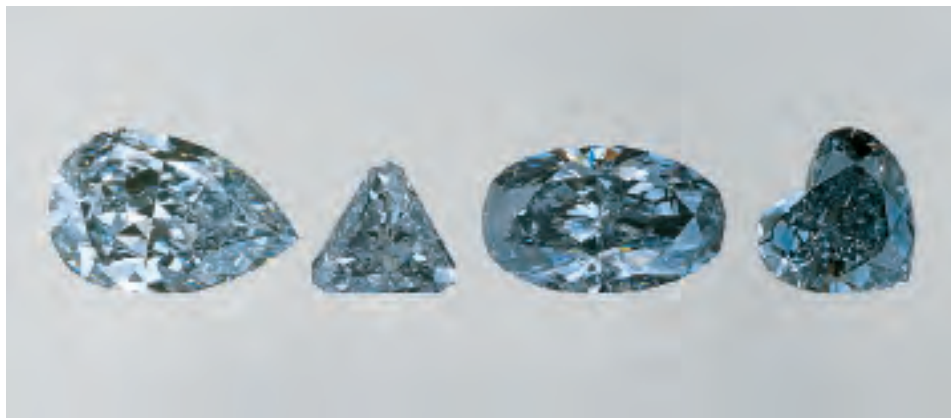
Figure 17. These four Fancy blue diamonds (from left to right, 2.03, 0.48, 2.01, and 1.15 ct) are similar in saturation, but they differ in tone; that is, they become progressively darker from left to right. These differences might be misinterpreted as increasing saturation by an inexperienced observer. Photo © Harold & Erica Van Pelt.

1. Color grading of blue diamonds requires use of a controlled methodology and grading environment to ensure the maximum consistency and repeatability.
2. To evaluate the significance of a difference between two colors, it is important to have references of known color location in color space for bracketing (see figure 20).

Clarity. The fact that blue diamonds are generally of high clarity is related to their type, not their color. Other type II diamonds, such as colorless type IIa diamonds, as well as some pink diamonds from India (Scarratt, 1987), show the same high clarity.

Figure 19. Because of the clustering in tone and saturation encountered with blue diamonds, those in similar clusters (such as the two diamonds on the left, 1.19 and 2.03 ct) may initially appear to differ in depth of color more than they actually do, since the observer has a natural tendency to make distinctions. When a diamond of different tone and saturation (far right, 1.82 ct) is placed next to them, the similarities between the first two become clearer. Unlike the situation in figure 18, these first two diamonds were not near a grade boundary, so both were graded Fancy blue. Photo © Harold & Erica Van Pelt.
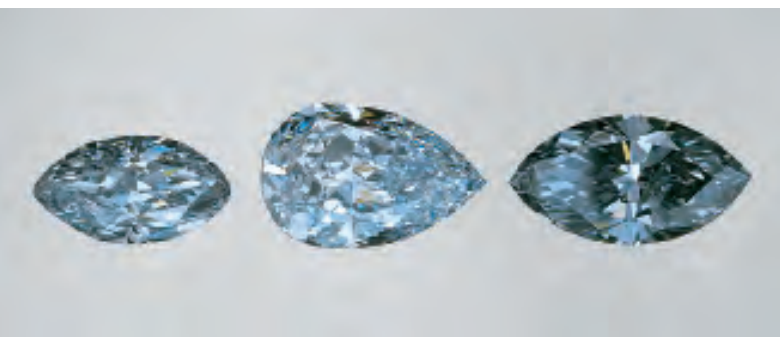

Figure 18. Colored diamonds located near fancy-grade terminology boundaries may appear similar yet still be described differently in the GIA GTL grading system. Because of the narrow saturation range in which blue diamonds occur, this effect is heightened, as the fancy-grade saturation boundaries are closer together than for other colored diamonds. The two diamonds shown here are of similar tone and differ slightly in saturation. Because they are near a fancy-grade boundary, the 1 ct marquise shape diamond on the left is described as Fancy blue and the (more saturated) 0.78 ct pear shape on the right is Fancy Intense blue. Photo © Harold & Erica Van Pelt.

Marketing decisions made by the manufacturer also probably influence this high clarity. That is, in some sizes, it may be that some markets prefer blue diamonds that are smaller but flawless to those that are larger and of lower (SI and below) clarity (M. Kirschenbaum, pers. comm., 1998). Ultimately, as with other colored diamonds, color is by far the most important factor.

Correlations of Depth of Blue Color and Other Gemological Properties. With the large number of blue diamonds available for study, we were able to establish some general correlations between depth of color and other properties (again, see table 2).

Figure 20. For centuries, people have devised ways to understand color appearance relationships through various order systems such as those shown in the background of this photograph. Understanding the color ordering of gems is particularly important for grading blue diamonds. The bracelet contains a 3.56 ct Fancy Dark gray-blue oval brilliant with 30.87 carats of D-color, internally flawless pear brilliants. In the three rings are a 2.87 ct Fancy Deep blue emerald cut, a 1.64 ct Fancy gray-blue marquise, and a 12.38 ct Fancy blue rectangular modified brilliant. The three unmounted pear brilliants are a 1.02 ct Fancy blue, a 4.02 ct Fancy Intense blue, and a 15.29 ct Fancy blue. Courtesy American Siba Corp. and Rima Investors Corp. Photo by Robert Weldon.
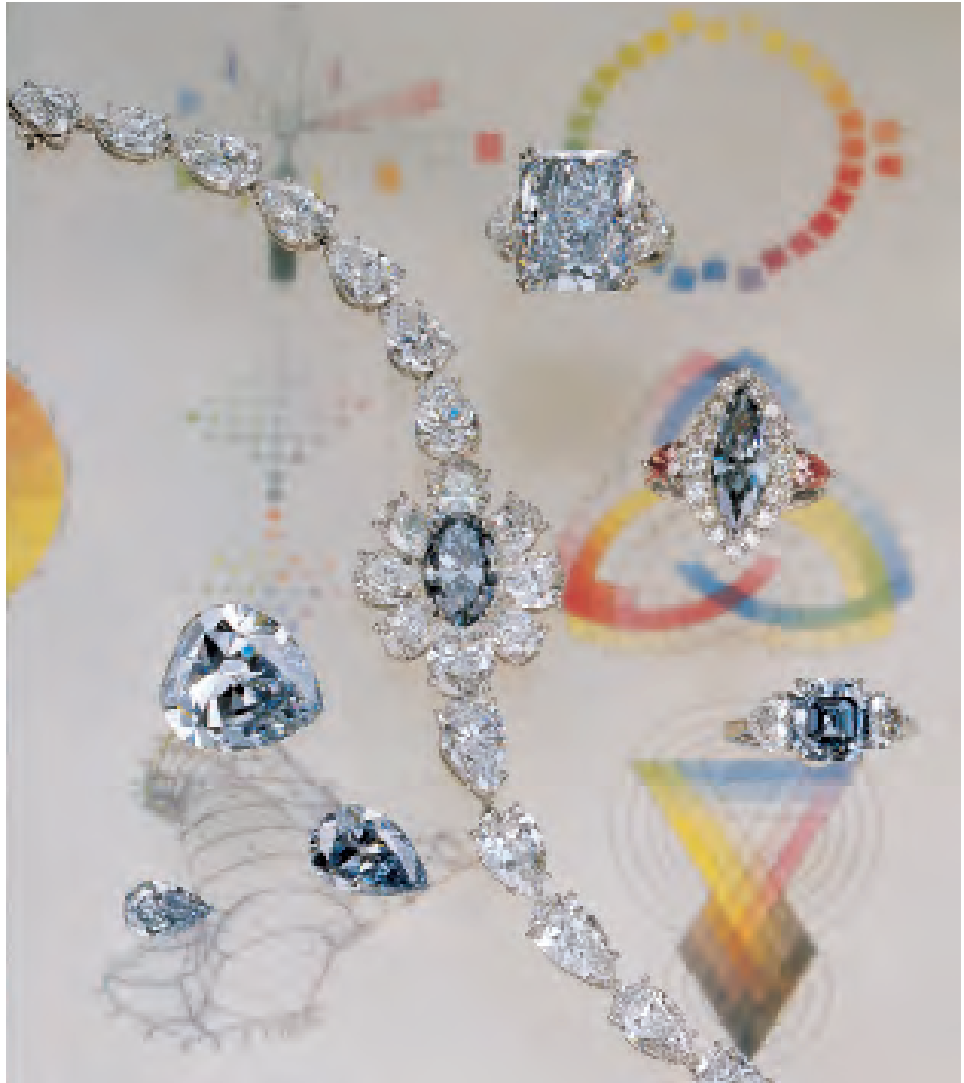
Phosphorescence. In general, the Fancy Deep blue diamonds had the longest lasting phosphorescence. There was no clear correlation between intensity of phosphorescence and strength of color (more than 50% across all grades showed weak phosphorescence).

Electrical Conductivity. While it is difficult to establish a direct relationship (partly due to the problems encountered in obtaining consistent measurements, as mentioned above), the general trend among our samples was for the blue color to be darker and/or stronger as the electrical conductivity increased. There are exceptions to this behavior, as can be seen by the measurements recorded for individual diamonds within a grade range (see table 2). Also, we have noted several highly conductive dark gray (i.e., unsaturated) diamonds, and we recently

encountered a Fancy Light blue diamond with a conductivity value that was similar to those of many of the blue diamonds graded as Fancy Deep or Fancy Dark.

Although electrical conductivity is not a completely accurate indicator, diamond manufacturers occasionally use strength of conductivity to identify potentially stronger and weaker areas of color in the rough diamond (K. Ayvazian, pers. comm., 1998). They believe that in combination with visual observations of color zoning, this can be helpful in producing the most saturated face-up color appearance possible in the finished diamond (again, see Box B).

Visible and Infrared Spectra. Comparison of the five spectra in figure 15 shows very little difference in absorption. We could not completely correlate the intensity of the face-up color of these five dia-

TABLE 3. Blue diamond identification.

Property	Natural diamond[a]	Natural diamond[a]	Treated diamond[b]	Synthetic diamond[c]
Type	IIb	IIa or Ia	IIa or Ia	IIb
Color	Pale to deeply colored blue	Pale to deeply colored green-blue and, rarely, blue to violet	Pale to deeply colored green-blue and, rarely, blue	Pale to deeply colored blue
Cause of color	Trace amounts of boron	Radiation exposure	Radiation exposure	Trace amounts of boron
Size of cut stones	To more than 50 ct	Up to 20 ct	Depends on sample selected for treatment	Less than 1 ct
Features seen with magnification				
Color distribution	Often even, sometimes uneven with blue/colorless zoning	Even, sometimes uneven with blue and near-colorless zones; color zoning may be located near surface radiation stains	Even, sometimes uneven with blue and near-colorless zones; color zoning may follow faceted shape—often concentrated at the culet	Usually uneven, with blue and near-colorless zones related to internal growth sectors; may form cross-shaped pattern
Graining	Sometimes whitish reflective or transparent graining	Occasional planar graining, sometimes colored or, rarely, whitish	Not diagnostic	Planar graining marking boundaries of color zoning, may form cross- or hourglass-shaped patterns
Inclusions	Usually free of mineral inclusions; sometimes opaque black inclusions	Sometimes mineral inclusions	Sometimes mineral inclusions	Elongated or rounded opaque metal inclusions, isolated or in small groups; occasional pinpoints
Other internal features	Occasional fractures or cleavages	Occasional fractures, cleavages, pinpoints, clouds	Occasional fractures, cleavages, pinpoints, clouds	Generally free of fractures and cleavages
Strain	Weak to strong anomalous double refraction, sometimes in parallel or cross-hatched patterns	Weak to strong anomalous double refraction, sometimes in parallel or cross-hatched patterns	Weak to strong anomalous double refraction, sometimes in parallel or cross-hatched patterns	Weak anomalous double refraction, sometimes in a cross pattern
Visible absorption spectra	No sharp bands, increasing absorption toward the red end of the spectrum	Sometimes weak to strong bands (415, 478, 496, 504, 595 nm)	Sometimes weak to strong bands (415, 478, 496, 504, 595 nm)	No sharp bands, increasing absorption toward the red end of the spectrum
Ultraviolet luminescence	Usually none, rarely weak red to orange-red, occasionally blue to greenish blue to SWUV	Sometimes weak to strong blue, greenish blue, green, yellow, or orange	Sometimes weak to strong blue, greenish blue, or green	Weak to moderate blue to greenish blue to SWUV; uneven distribution related to internal growth sectors
Phosphorescence	Blue to green, rarely red to orangy red	None	None	Moderate to strong blue, sometimes with orange; persistent duration
Cathodoluminescence	Usually greenish blue, sometimes shows cross-hatched pattern	Not examined	Not examined	Weak to strong greenish blue; sometimes with uneven distribution related to internal growth sectors; some sectors show no reaction
Other features	Electrically conductive	Green or brown radiation stains on surface or along open fractures	May exhibit residual radioactivity	Electrically conductive, may be attracted by a strong magnet

[a] Adapted from Shigley et al. (1995) and (for natural type IIb blue diamonds) based on data gathered for this study.

[b] Based on data accumulated at the GIA Gem Trade Laboratory and GIA Research.

[c] Based on observations by GIA Research and the DTC Research Centre.

monds (as expressed by the fancy grade description) and their spectra. This lack of correlation can be attributed to several factors. First, these spectra were recorded for a light path through the bezel and pavilion facets of the stone in an attempt to measure the bodycolor. The color grade, however, was established by visual observation of the face-up color. Second, the face-up color appearance of a col-

ored diamond is determined not just by the bodycolor but also by effects of the faceting style and the lighting and observation conditions. Nonetheless, the overall similarity of these five spectra lends support to the results of the visual observation portion of this study, that the range of color appearances from gray to gray-blue to blue is limited.

Although the infrared spectra of all 5 stones were similar, we did note that the type IIb features were most prominent in the two diamonds with the strongest blue color.

Identification and Separation. The properties and appearance of type IIb blue diamonds do not typically overlap with those of treated blues, and synthetic type IIb blue diamonds are not available on the commercial market. Still, it is valuable to understand the separation of these diamonds. Table 3 presents a brief comparison of the gemological properties of natural, treated, and synthetic blue diamonds.

SUMMARY AND CONCLUSION

The special qualities of blue diamonds, and the rich history associated with many of them, has made such diamonds highly valued and desirable in the gem and jewelry industry today. The earliest references to blue diamonds came centuries ago, when the Tavernier Blue was brought from India. Although blue diamonds have occasionally been reported from sources other than the Premier mine in South Africa, this historic mine has produced most of the blue diamonds seen in the marketplace. Currently an underground operation, the Premier mine is viable primarily because of the handful of blue or large colorless "specials" that are recovered each year.

Because virtually all the diamonds described as blue by the GIA Gem Trade Laboratory are type IIb, we chose to focus on this type for our study. In addition to their unique color attributes, type IIb diamonds have distinctive traits such as electrical conductivity, boron as the coloring agent, and a characteristic phosphorescent reaction to short-wave UV. Fancy Deep blue diamonds had the longest phosphorescence, but there was no correlation to intensity of the phosphorescence. Also, there was a trend among the samples for diamonds that were a stronger and/or darker blue to have higher electrical conductivity. We have found that blue diamonds typically are of higher clarity than other diamonds. However, the fact that the rough may be color zoned and is typically irregular in shape makes the manufacturing of these diamonds challenging.

A key goal of this study was to provide a better understanding of the narrow color range in which type IIb blue diamonds occur and the color appearances associated with their various GIA GTL fancy grades. Blue diamonds are unique among colored diamonds in that they occupy isolated regions in their hue range and primarily occur in four small tone/saturation clusters. If we understand this, we can understand how these diamonds relate to one another and to diamonds of other colors.

REFERENCES

Austin I.G., Wolfe R. (1956) Electrical and optical properties of a semiconducting diamond. *Proceedings of the Physical Society of London B*, Vol. 69, pp. 329–338.

Balfour I. (1997) *Famous Diamonds.* Christie, Manson and Woods Ltd., London.
Benson L. (1959) Highlights at the Gem Trade Lab in Los Angeles—Electrical conductivity in blue diamonds. *Gems & Gemology*, Vol. 9, No. 10, pp. 296–298.

Blackwell D.E., Sutherland G.B.B.M. (1949) The vibrational spectrum of diamond. *Journal de Chimie*, Vol. 46, pp. 9–15.

Brophy J.J. (1955) Preliminary study of the electrical properties of a semiconducting diamond. *Physical Review*, Vol. 99, pp. 1336–1337.

Bruton E. (1978) *Diamonds*, 2nd ed. Chilton Book Co., Radnor, PA.

Caspi A. (1997) Modern diamond cutting and polishing. *Gems & Gemology*, Vol. 33, No. 2, pp. 102–121

Cassedanne J.P. (1989) Diamonds in Brazil. *Mineralogical Record*, Vol. 20, No. 5, pp. 325–336.

Chrenko R.M. (1973) Boron, the dominant acceptor in semiconducting diamond. *Physical Review B*, Vol. 7, No. 10, pp. 4560–4567.

Christie's Jewellery Review 1995 (1996) Christie's International Jewellery Dept., Geneva and New York.

Collins A.T., Williams A.W.S. (1971) The nature of the acceptor centre in semiconducting diamond. *Journal of Physics C: Solid State Physics*, Vol. 4, pp. 1789–1800.

Crowningshield G.R. (1959) Highlights at the Gem Trade Lab—Electrical conductivity meter. *Gems & Gemology*, Vol. 9, No. 10, p. 291.

Crowningshield G.R. (1971) General Electric's cuttable synthetic diamonds. *Gems & Gemology*, Vol. 13, No. 10, pp. 302–314.

Custers J.F.H. (1952) Unusual phosphorescence of a diamond. *Physica*, Vol. 18, No. 8–9, pp. 489–496.

Custers J.F.H. (1954) Letter to the editor—Type II-b diamonds. *Physica*, Vol. 20, pp. 183–184.

Custers J.F.H. (1955) Semiconductivity of a type II-b diamond. *Nature*, Vol. 176, No. 4473, pp. 173–174.

Custers J.F.H., Dyer H.B. (1954) Discrimination between natural blue diamonds and diamonds coloured blue artificially. *Gems & Gemology*, Vol. 7, No. 2, pp. 35–37.

Custers J.F.H., Dyer H.B., Raal F. (1960) A simple method of differentiating between natural blue diamonds and diamonds coloured blue artificially. *Journal of Gemmology*, Vol. 7, No. 8, pp. 291–293.

Dean P.J., Lightowlers E.C., Wight D.R. (1965) Intrinsic and extrinsic recombination radiation from natural and synthetic aluminium-doped diamond. *Physical Review*, Vol. 140, No. 1A, pp. A353–A386.

Dyer H.B., Wedepohl P.T. (1956) Electrical measurements on type IIb diamonds. *Proceedings of the Physical Society, London, Section B*, Vol. 69, pp. 410–412.

Federman D. (1989) Gem profile: Fancy blue diamonds—Rarer than pink. *Modern Jeweler*, Vol. 88, No. 10, p. A20.

Federman D. (1998) Gem profile: Blue Heart diamond. *Modern Jeweler*, Vol. 97, No. 12, pp. 21–22.

Fritsch E., Scarratt K. (1992) Natural-color, nonconductive gray-to-blue diamonds. *Gems & Gemology*, Vol. 28, No. 1, pp. 35–42.

Fritsch E., Shigley J.E. (1991) Optical properties of some natural-color and laboratory-irradiated green to blue diamonds. In R. Messier, J.T. Glass, J.E. Butler, and R. Roy, Eds., *Proceedings of the Second International Conference—New Diamond Science and Technology, Washington DC, September 23–27, 1990*; Materials Research Society, Pittsburgh, Pennsylvania, pp. 677–681.

GIA Diamond Dictionary, 3rd ed. (1993) Gemological Institute of America, Santa Monica, CA.

Important Diamond Auction Results (1997) De Beers Polished Division, London, 49 pp.

Harris J.W. (1972) Black material on mineral inclusions and in internal fracture planes in diamonds. *Contributions to Mineralogy and Petrology*, Vol. 35, pp. 22–23.

Harris J.W., Vance E.R. (1972) Induced graphitisation around crystalline inclusions in diamonds. *Contributions to Mineralogy and Petrology*, Vol. 35, pp. 227–234.

Hofer S.C. (1998) *Collecting and Classifying Colored Diamonds: An Illustrated Study of the Aurora Collection*. Ashland Press, New York, 742 pp.

Janse A.J.A. (1995) A history of diamond sources in Africa, Part I. *Gems & Gemology*, Vol. 31, No. 4, pp. 228–255.

King J.M., Moses T.M., Shigley J.E., Liu Y. (1994) Color grading of colored diamonds in the GIA Gem Trade Laboratory. *Gems & Gemology*, Vol. 30, No. 4, pp. 220–242.

Klein P.B., Crossfield M.D., Freitas J.A. Jr., Collins A.T. (1995) Donor-acceptor pair recombination in synthetic type IIb semiconducting diamond. *Physical Review B*, Vol. 51, No. 15, pp. 9634–9642.

Krashes L.S. (1993) *Harry Winston, the Ultimate Jeweler*, 4th ed. Harry Winston Inc., New York, and the Gemological Institute of America, Santa Monica, CA.

Leivo W.J., Smoluchowski R. (1955) A semiconducting diamond. *Bulletin of the American Physical Society*, Vol. 30, No. 2, p. 9.

Liddicoat R.T. Jr. (1987) *Handbook of Gem Identification*, 12th ed.. Gemological Institute of America, Santa Monica, CA.

Lightowlers E.C., Collins A.T. (1966) Electrical-transport measurements on synthetic diamond. *Physics Review*, Vol. 151, No. 2, pp. 685–688.

Lightowlers E.C., Collins A.T. (1976) Determination of boron in natural semiconducting diamond by prompt particle nuclear microanalysis and Schottky barrier differential-capacitance measurements. *Journal of Physics D (Applied Physics)*, Vol. 9, pp. 951–963.

Meyer H.O.A., Tsai H. (1976) The nature and significance of mineral inclusions in natural diamonds: A review. *Minerals Science and Engineering*, Vol. 8, No. 4, pp. 242–261.

Orloff Yu.O. (1977) *The Mineralogy of the Diamond*. John Wiley & Sons, New York.

Robertson R., Fox J.J., Martin A.E. (1934) Two types of diamond. *Philosophical Transactions of the Royal Society of London*, Vol. A232, London, pp. 463–535.

Scalisi P., Cook D. (1983) *Classic Mineral Localities of the World—Asia and Australia*. Van Nostrand Reinhold, New York, 226 pp.

Scarratt K. (1987) Notes from the laboratory—10. *Journal of Gemmology*, Vol. 20, No. 6, pp. 358–361.

Schulke A.A. (1962) Artificial coloration of diamonds. *Gems & Gemology*, Vol. 10, No. 8, pp. 227–241.

Shigley J.E., Fritsch E., Reinitz I., Moses T.M. (1995) A chart for the separation of natural and synthetic diamonds. *Gems & Gemology*, Vol. 31, No. 4, pp. 256–264.

Smith S.D., Taylor W. (1962) Optical phonon effects in the infra-red spectrum of acceptor centres in semiconducting diamond. *Proceedings of the Physical Society, London*, Vol. 79, No. 512, pp. 1142–1153.

Spencer L.K., Dikinis S.D., Keller P.C., Kane R.E. (1988) The diamond deposits of Kalimantan, Borneo. *Gems & Gemology*, Vol. 24, No. 2, pp. 67–80.

Tavernier J.-B. (1676) *Travels in India*. Translated into English by V. Ball, published in two volumes in 1977 by Oriental Books Reprint Corp., New Delhi, India.

Tillander H. (1975) The "Hope" diamond and its lineage. International Gemmological Conference, Smithsonian Institution, Washington DC, October 1975.

Watanabe K., Lawson S.C., Isoya J., Kanda H., Sato Y. (1997) Phosphorescence in high-pressure synthetic diamond. *Diamond and Related Materials*, Vol. 6, pp. 99–106.

Webster R. (1994) *Gems: Their Sources, Descriptions, and Identification*, 5th ed. Rev. by P.G. Read, Butterworth-Heinemann, Oxford.

Wedepohl P.T. (1957) Electrical and optical properties of type IIb diamonds. *Proceedings of the Physical Society, London, Section B*, Vol. 70, pp. 177–185.

Wentorf R.H., Jr., Bovenkerk H.P. (1962) Preparation of semiconducting diamond. *Journal of Chemical Physics*, Vol. 36, No. 8, pp. 1987–1990.

World Diamond Industry Directory & Yearbook 1997/98, 3rd ed. (1998) CRU Publishing, London, pp. 51–56.

FINGERPRINTING
OF TWO DIAMONDS
CUT FROM THE SAME ROUGH

By Ichiro Sunagawa, Toshikazu Yasuda, and Hideaki Fukushima

If it can be determined that two faceted diamonds came from the same piece of rough, romantic value is added to the stones. X-ray topography and cathodoluminescence (CL) tomography were used to prove that a round brilliant and a pear-shaped brilliant were cut from the same piece of rough. With these techniques, the internal imperfections and inhomogeneities that reflect the distinctive growth history of the original diamond crystal can be seen. X-ray topography is a powerful tool for imaging the distribution of lattice defects; CL tomography is more sensitive for detecting faint chemical inhomogeneities. By combining the two methods, the sophisticated gemologist can view both physical and chemical characteristics of a crystal, and thus its growth history, and use this information to fingerprint a given stone.

ABOUT THE AUTHORS

Dr. Sunagawa is principal of the Yamanashi Institute of Gemology and Jewellery Arts in Kofu, Japan, and professor emeritus of mineralogy at Tohoku University, Sendai, Japan. Mr. Yasuda recently retired from the Geological Survey of Japan in Tsukuba, Ibaraki Prefecture, where he was a specialist in the X-ray topography of crystals. Mr. Fukushima is a member of the Education Department at the Gemmological Association of All Japan in Tokyo, where he has taken thousands of cathodoluminescence tomographs of faceted diamonds.

Typically, two faceted stones are cut from one well-formed diamond crystal. Yet each takes a different route in the market, with little chance of both diamonds being set together in a single piece or related pieces of jewelry. However, if two such diamonds were set in two pieces of jewelry worn, for example, by a mother and a daughter, this might provide additional sentimental value to the stones. Keeping two such diamonds together is possible only when the piece of rough is cut under the dealer's control. Even so, scientific documentation is necessary to prove this shared origin. Plotting a diamond's internal features (as in a diamond grading report) may help identify a single stone, but it cannot prove that two diamonds came from the same rough. More advanced techniques are needed for this task.

Natural crystals do not grow at a constant rate or under constant conditions. Rather, crystals may experience growth-rate fluctuations, gentle or abrupt changes in growth parameters, or partial dissolution and regrowth during their formation. As a result, physical imperfections and chemical inhomogeneities—such as inclusions, lattice defects (point defects, dislocations, and planar defects), and chemical impurities—are induced in crystals during their growth and postgrowth histories. These characteristics are uniquely distributed within each crystal as growth sectors (zonal structures), intrasectorial zoning, growth banding, and nonuniform distributions of elements, color, or luminescence; these features are not modified during later cutting and polishing processes (Sunagawa, 1984a, 1988; Scandale, 1996; and the references therein). Consequently, they are the most reliable diagnostic features for fingerprinting stones (and for distinguishing natural from synthetic gem minerals; see, e.g., Sunagawa, 1995), provided they can be determined nondestructively.

We report in this article how we verified that two diamonds—a round brilliant and a pear-shaped brilliant—came from the same piece of rough, by revealing the spatial distri-

Figure 1. These three diamonds, all from the same manufacturer, were studied to determine which two, if any, were cut from the same piece of rough. All of the diamonds were graded as E color and VS$_1$ clarity. Sample A (left) weighs 1.08 ct, sample B (center) is 0.81 ct, and sample C (right) weighs 1.05 ct. Samples B and C were proved to originate from the same rough diamond.

bution of lattice defects (using X-ray topography) and those of cathodoluminescence-emitting centers (using CL tomography). Both methods were applied without any damage to the stones.

The study was initiated when a dealer claimed that two brilliant-cut diamonds he was offering were from the same rough. After X-ray topography proved otherwise, the dealer traced the route the two stones had taken from the cutter, and eventually he found another brilliant that produced an X-ray topograph that matched one of the previous brilliants. After establishing the characteristics of these three diamonds by X-ray topography, the authors applied CL tomography to provide supporting evidence for the initial conclusions. The characteristics observed with these two techniques vividly demonstrate the different growth histories of different diamond crystals. This example also demonstrates the usefulness and applicability of X-ray topography and CL tomography in gemology.

MATERIALS AND METHODS

Samples. The first pair of diamonds offered by the dealer, samples A and B, had the following characteristics recorded on their GIA Gem Trade Laboratory (GIA GTL) grading reports:

Sample A: Round brilliant; 1.08 ct; 6.59–6.62 × 4.10 mm; E color; VS$_1$ clarity; 62.1% depth, 56% table, thin-to-medium faceted girdle, no culet; excellent polish; very good symmetry; no fluorescence (report dated February 9, 1993).

Sample B: Pear-shaped brilliant; 0.81 ct; 8.03 × 5.54 × 2.93 mm; E color; VS$_1$ clarity; 52.9%

depth, 55% table, thin-to-thick faceted girdle, very small culet; good polish; good symmetry; no fluorescence (report dated January 4, 1993).

As described below, it was proved that these two diamonds were not cut from the same piece of rough. Subsequently, the dealer traced the stones back to the manufacturer and submitted the following diamond, sample C:

Sample C: Round brilliant; 1.05 ct; 6.43–6.67 × 4.01 mm; E color; VS$_1$ clarity; 60.3% depth, 59% table, very thin-to-thin faceted girdle, small culet; excellent polish; very good symmetry; no fluorescence (report dated January 25, 1993).

Samples A, B, and C are shown in figure 1. They are very clean to the naked eye and, as evident from the GIA GTL grading reports, no internal flaws are discernible with the microscope, other than pinpoint inclusions. Nevertheless, X-ray topography and CL tomography (as described below) revealed distinctive internal heterogeneities and imperfections.

Experimental Procedures. *X-Ray Topography.* By identifying contrasts in X-ray reflection, X-ray topography can detect and record the spatial distribution of strain fields associated with various linear defects (e.g., dislocations) and planar defects (e.g., stacking faults and twin planes) in single crystals. In other words, X-ray topography reveals the distribution of deviations from the ideal lattice plane. The term *topography* is used to describe the three-dimensional nature of these data.
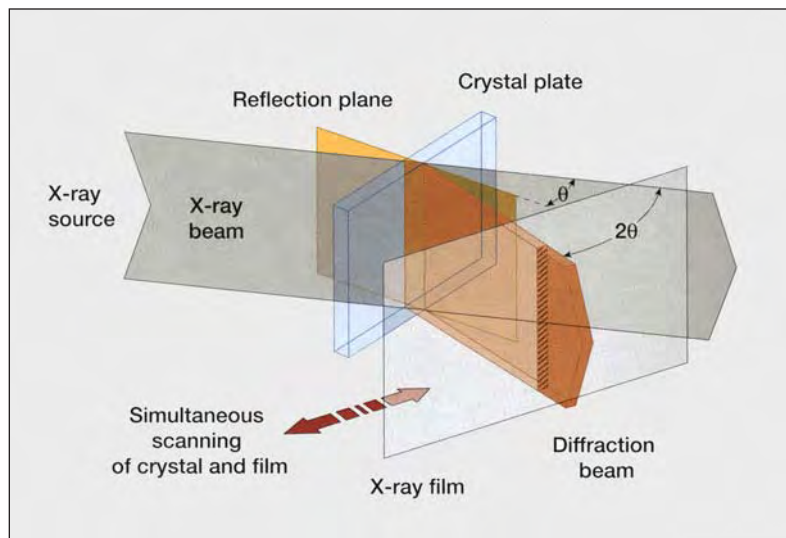
Since X-ray topography is a well-established

Figure 2. This schematic diagram illustrates the geometry generally adopted to obtain X-ray topographs (after Lang, 1978). In the present study, a faceted diamond was used in place of the crystal plate, with the table facet parallel or perpendicular to the plate (see figure 3). X-rays are passed through a narrow slit and reflected through the sample, off one selected lattice reflection plane, to produce a three-dimensional image of the crystallographic imperfections and inhomogeneities on the X-ray film. The three-dimensional image is obtained by scanning the entire sample, through synchronous movement of both sample and film.

method, this article will not give a detailed description of its principles and methods. Interested readers may refer to review papers by Frank and Lang (1965) or Lang (1978, 1979).

In the present study, the Lang method (1978) was used to record the X-ray topographs (see figure 2). The sample is typically cut into a plate for analysis, but complete crystals or faceted stones can be used if the sample is small; good topographs can be obtained for diamonds up to about 2 ct. A narrow, ribbon-like beam of X-rays with a fixed wavelength is passed through a narrow slit and scanned over the sample at a fixed incident angle (i.e., in a reflection orientation). Only those X-ray beams that match the ideal reflection of the lattice plane are reflected off this plane and recorded on the X-ray film. Distorted lattice portions (i.e., those that deviate from the ideal reflection plane) appear as contrasting images on the film (white on the negative, or black on the print), thus revealing the spatial distribution of lattice defects in the sample. The X-rays used in this study were produced with an accelerat-

Figure 3. For this study, {110} and {111} crystallographic planes (dashed lines) were selected as the lattice reflection planes (left). The orientation of two of the a-axes are shown. Two directions of the incident X-ray beams were used in this study—parallel and perpendicular to the table facet (horizontal and vertical, respectively). The schematic diagram on the right shows the viewing geometry for the samples. The round brilliant indicates the positions of samples A and C, and the pear-shaped brilliant indicates sample B. The two directions of view in the corresponding X-ray topographs are indicated by the eyes. Note that the reflection plane {220} is expressed as {110} for simplicity in this article; {110} does not reflect X-ray beams, but {220} does.
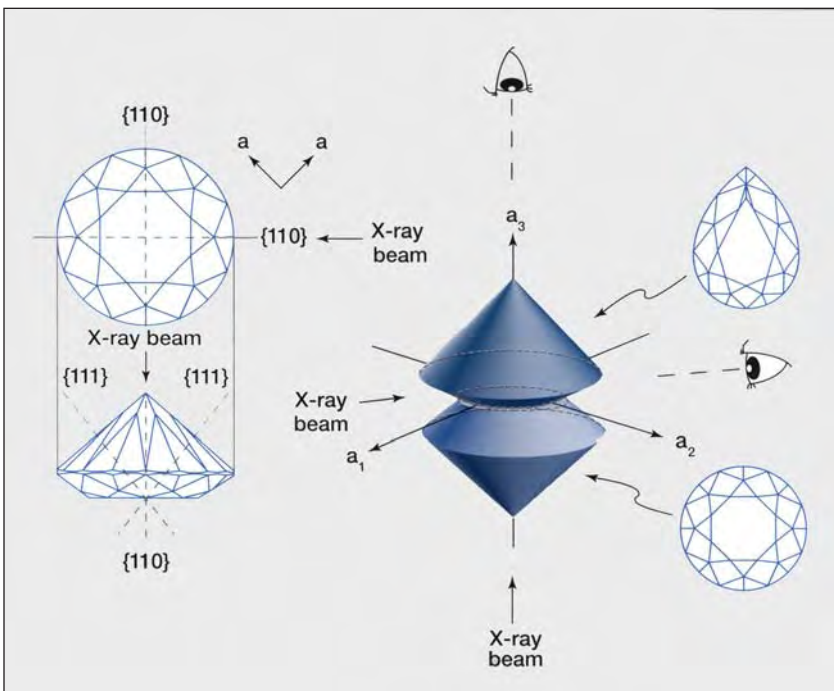
ing voltage of 50 kV and a current of 1 mA.

For X-ray topography, the system operator must select appropriate lattice reflection planes, taking into consideration the angles and intensities of reflecting beams and the distortion of images caused by the oblique scanning angle. Assuming that the table facet in each stone was approximately parallel to a (100) plane, we selected {110} and {111} directions as reflection planes. (Note that the reflection plane {220} is expressed as {110} for simplicity in this article; according to the extinction rule, {110} does not reflect X-ray beams, but {220} does.) This is shown schematically in figure 3. As figure 4 illustrates, the images are distorted depending on the direction of the reflection. This distortion must be taken into consideration when the X-ray topographs for two different stones are compared. To obtain images with good contrast, the researcher usually prepares a plate from the sample that is of appropriate thickness (depending on the material, e.g., 1 mm for quartz). This, of course, is not possible with polished gemstones. However, because good topographs can be achieved with relatively thick samples of diamond, we were able to obtain useful images from the faceted stones examined for this study.

Cathodoluminescence Tomography. After we had analyzed all three samples by X-ray topography, we used CL tomography as a supporting method. With this technique, one can see the heterogeneous distribution of CL-emitting centers in a solid material, up to a few micrometers below the surface. Because of the limited depth of penetration, this technique is referred to as *tomography,* since it reveals only the two-dimensional distribution of the CL-emitting centers in a plane near the surface. CL tomography has been used widely in solid-state physics and the earth sciences (see, e.g., Davies, 1979; Lang, 1979), and Ponahlo (1992) has also applied it to gemology.

A scanning electron microscope (SEM) or optical microscope is used to observe the images generated by CL tomography. The present study used the latter, a Premier American Technologies Co. Luminoscope. Because of its lower vacuum, the Luminoscope is not as sensitive as an SEM system, but it is adequate for this type of problem. Also, the samples do not need to be carbon-coated (as they would for SEM analysis). CL tomography does not automatically identify the elements responsible for the CL emission; nor does it give quantitative data
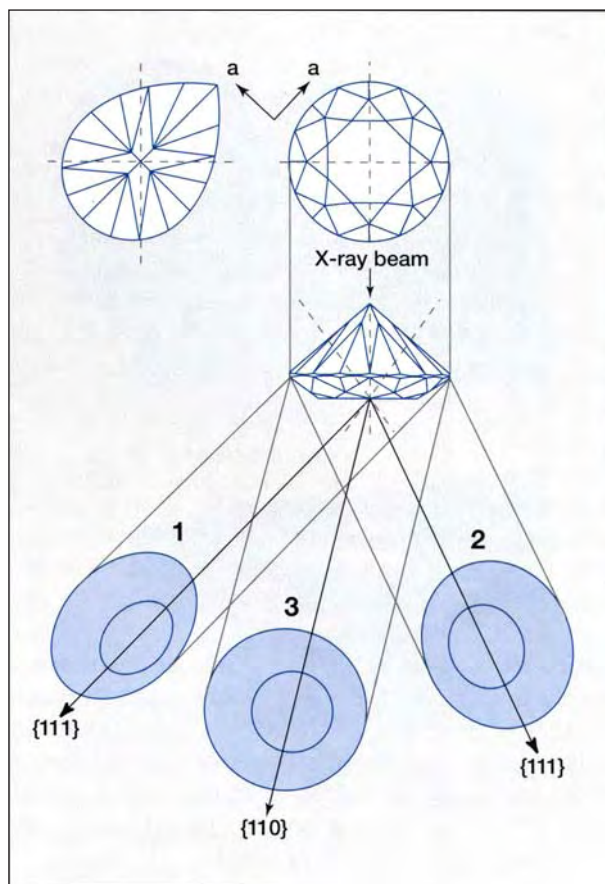

Figure 4. X-ray topographic images are distorted because of the oblique reflection of the vertical X-ray beam. Here, three schematic diagrams—each labeled with the corresponding reflection plane—{110} or {111}—illustrate the positions of the table facet (small circles) and the girdle outline; the profile of each stone is also shown. All three images are produced using the same (vertical) incident X-ray direction; the particular image obtained depends on the reflection plane selected. Note that the image in 2 is inverted relative to 1. Actual X-ray topographs corresponding to these three images are shown in figure 5.

for their concentrations. The CL intensities may correspond semi-quantitatively to the concentrations of the CL-emitting centers, but other methods, such as spectroscopy, are required to identify the chemical elements or obtain quantitative data. However, for the purpose of this study—that is, visualizing the distribution of CL-emitting centers in different diamonds—quantitative analyses were not needed.

RESULTS

X-Ray Topography. *Samples A and B.* X-ray topographs of sample A, taken with {110} and {111}
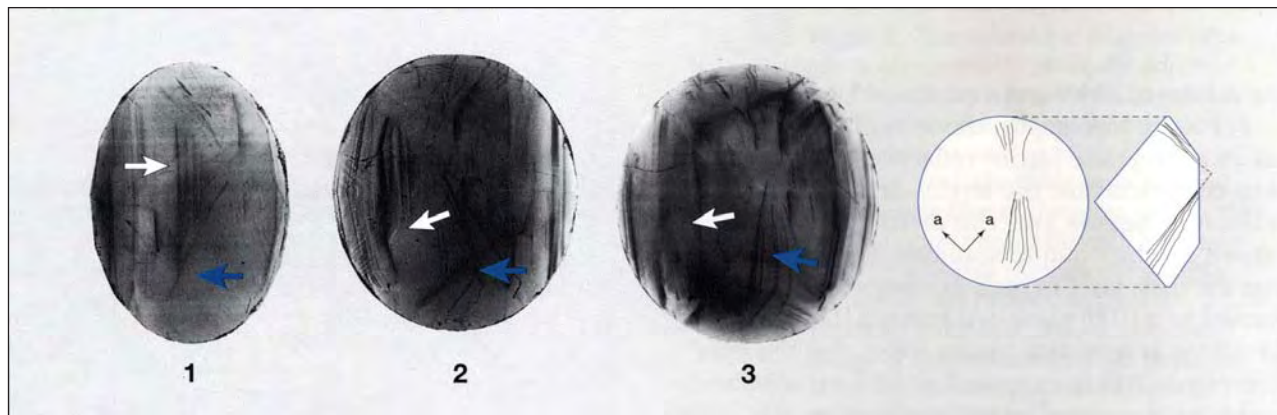
Figure 5. These three X-ray topographs of sample A were taken with different reflection planes, as shown in figure 4 (images 1, 2, and 3). The green arrows indicate dislocations, and the white arrows indicate growth banding. An idealized illustration of the dislocations is shown for topograph 3, in plan view and in profile. The two dislocation bundles are inferred to meet at a position slightly above the table facet.

lattice reflections, show a few dislocations that are nearly parallel to {110}, and straight growth bands parallel to {111}, planes (figure 5). The dislocations radiate from a point slightly above the table facet; this point marks the center of an octahedral crystal, from which the dislocations progressed nearly perpendicular to the growing octahedral {111} faces.

X-ray topographs of sample B (figure 6) are markedly different from those of sample A. The

sample B topographs reveal dislocation bundles that are much greater in number and density than those in sample A. Moreover, the dislocations in sample B are parallel to <100>, not to {110} as in sample A. The dislocation bundles originate not from a point center, but from the boundary of a square-shaped core. Faint growth banding is discernible in areas between the dislocation bundles, but these are more evident on CL tomographs (see below). The growth

Figure 6. These two X-ray topographs of sample B were taken with two (110) reflection planes. A large number of dislocations (dark heavy lines) originate from the boundaries of a square-shaped core, and form bundles nearly parallel to the a-axes. Faint zigzag patterns are also visible between the dislocations. Note the marked difference of these topographs from those of sample A shown in figure 5, with respect to the presence of a core portion, the number and orientation of dislocations, and the modes of growth banding.
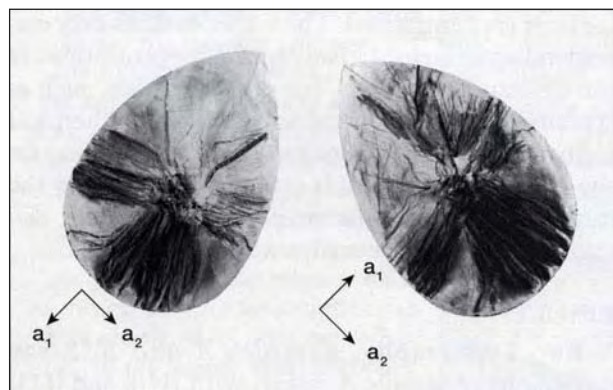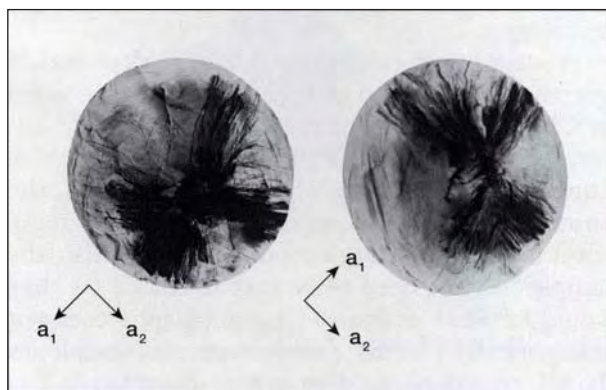
Figure 7. These X-ray topographs of sample C correspond to the same orientation and reflection planes as those shown in figure 6 for sample B. Note the close similarity to sample B in the presence of a square-shaped core portion, the density and orientation of dislocation bundles, and the faint zigzag patterns between the dislocations. The close resemblance shown by these topographs (considering that both diamonds had some material polished away) indicates that samples B and C came from the same rough.

banding is not straight, but rather shows a zigzag pattern. The differences in the X-ray topographs of samples A and B suggest that they could not have originated from the same piece of rough.

Sample C. X-ray topographs of sample C (figure 7) show dislocation bundles originating from the boundary of a square-shaped core and running parallel to <100>, as well as faint zigzag patterns in the areas between the dislocation bundles. By comparing the topographs of samples B and C, one can see that the presence of the square-shaped core, the orientation and spatial distribution of the dislocations, and the faint zigzag growth banding seen in these diamonds, are essentially the same. This implies that these two diamonds were cut from the same piece of rough.

Closer observation of the core portions of samples B and C confirms their similarity (figure 8). In both samples, the dislocation densities are much higher in the surrounding portion than in the core. Although most of the dislocations in the core continue into the surrounding portion of the diamond, it is clear that most of the dislocations outside the core are generated along the boundary between the core and the surrounding diamond. It is also evident that the core portion was bounded by somewhat rugged cuboid faces. The characteristics and sizes of the core portions of samples B and C match perfectly, if the volume of the portion that was polished away from both samples is taken into consideration.

In profile view, X-ray topographs of samples B and C at the same orientation also show good correlation in the morphology and position of the core and the spatial distribution of dislocation bundles (figure 9). In addition, one notices that the table facets of the two stones are inclined slightly (about 6°–7°) from the (100) face. This inclination may be due to the cutter's desire to avoid inclusions that were originally present in the rough, or simply to obtain a higher yield from odd-shaped rough.

The results of our X-ray topographic investigations are summarized in figure 10. The images conclusively indicate that samples B and C came from the same diamond rough, whereas sample A came from a different piece of rough.

CL Tomographs. By comparing CL tomographs of samples A, B, and C (figure 11) with their X-ray topographs, one immediately notices the following:

1. Only blue cathodoluminescence of varying intensities was observed; no yellow, green, or red.
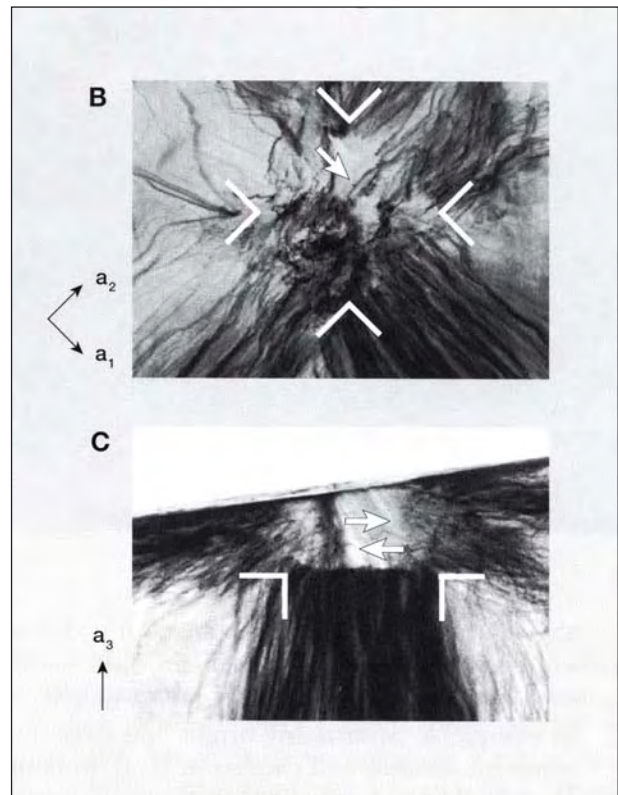

Figure 8. These X-ray topographs have been enlarged to show the core portions of samples B and C. Sample B is shown in plan view (X-ray beam perpendicular to the table facet), and sample C is shown in profile view (X-ray beam parallel to the table facet), as in figure 9. The truncation of sample C near the top of the topograph corresponds to the surface of the table facet, which shows a slight inclination relative to the (100) face. The white lines indicate the corners of the boundary of the square-shaped core, and the white arrows indicate dislocations that begin in the core and continue into the surrounding diamond. Enlarged approximately 30×.

2. Straight (sample A) or zigzag (samples B and C) growth banding, which was faintly visible on the X-ray topographs, was more readily seen on the CL tomographs (as alternating bright and dark bands).

3. The square-shaped core present on the CL tomographs of samples B (at the center of the table facet) and C (at the upper left of the table facet) is not visible in sample A, on either the X-ray topographs or the CL tomographs.

4. Although growth banding typically is easier to see on CL tomographs than on X-ray topographs,
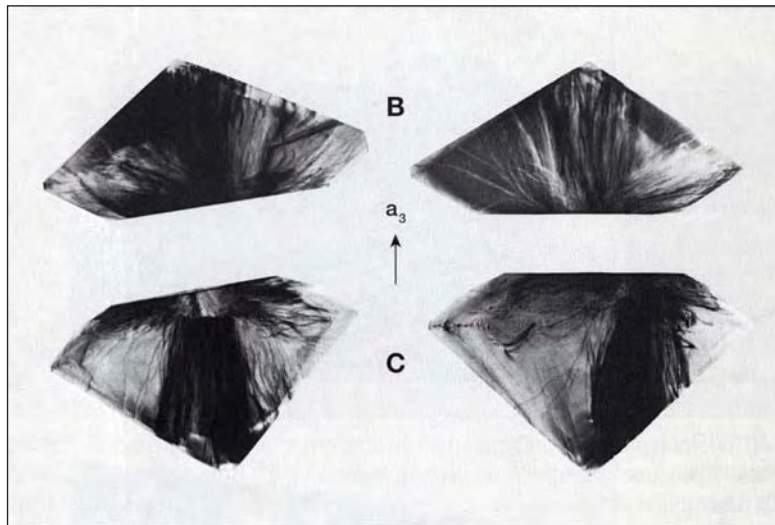
Figure 9. These X-ray topographs show two profile views of sample B (top) and sample C (bottom). The topographs are oriented to show the faceted diamonds as they were positioned in the original crystal, with the a3 axis indicated by the arrow in the center. The topographs on the right show the samples rotated 90° from those on the left; the crystallographic orientation between the upper and lower views is identical. There is a high degree of correlation between the two diamonds in the character and orientation of the dislocations. The core portion is difficult to see in sample B, because most of it has been polished away. Note also that the table facet is inclined about 6°–7° from the crystallographic (100) plane.

the radiating dislocations that are clearly visible on the X-ray topographs of samples A, B, and C could not be resolved on their CL tomographs.

5. In sample A, alternating bright and dark CL zones are straight and parallel to {111}. In both samples B and C, two different types of growth zoning can be distinguished on the CL tomographs. One type is visible between neighboring areas of the second set as short, fairly straight, bright and dark CL zones parallel to <110>. In the second set, bright and dark zones with a zigzag pattern are present within the <100> zones, which correspond to the location of dislocation bundles seen on the X-ray topographs. (Note: Since {100} faces are never present as smooth, flat faces on natural diamond crystals [Sunagawa, 1984b], they are customarily called "cuboid" faces. For simplicity, we refer to them here as <100> zones instead.)

At higher magnification, CL images of the core portions of samples B and C revealed these additional features (figure 12):

Figure 10. These diagrams schematically illustrate the three-dimensional nature of the dislocations revealed by X-ray topography in the three samples. On the left, the appearance and orientation of the dislocations in sample A (bottom) are much different from those in sample B (top). On the right, a perfect match is evident for samples B and C in the presence of a cuboid-shaped core and the analogous dislocation bundles.
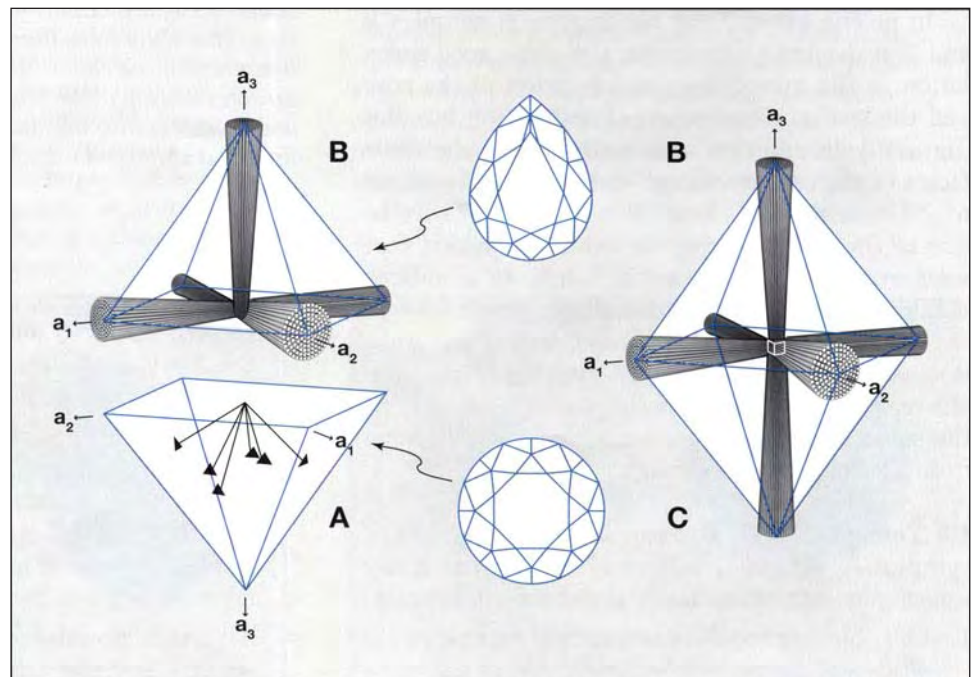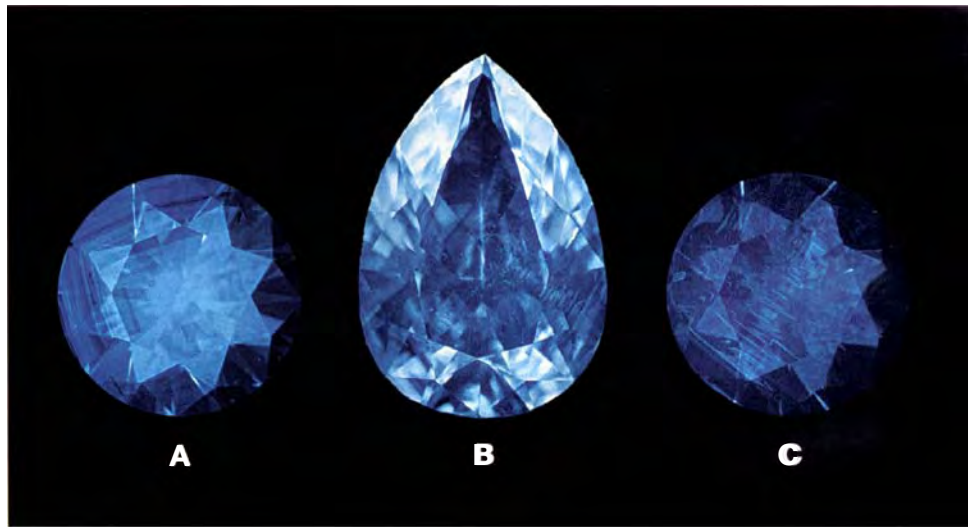
Figure 11. The distribution of CL-emitting centers is visible on these CL tomographs. Note the marked difference between sample A (e.g., straight growth zones, absence of a square-shaped core) and samples B and C (e.g., zigzag growth zones and the presence of a square-shaped core—in the center of the table of sample B and in the upper left of the table in sample C).

6. The distribution of bright and dark areas is less heterogeneous in the core portion than in the surrounding areas.

7. Around the perimeter of the core is a bright cathodoluminescence zone, which indicates a high concentration of CL-emitting centers at this boundary.

8. In the <100> growth sectors, where bundles of dislocations are visible on the X-ray topograph, bright and dark zones in the shape of a zigzag—or short right angles—appear alternately or intermittently. The segments are parallel to <110> (i.e., they consist of segmental {111} planes).

9. In the <110> growth sectors (i.e., in the areas between the neighboring <100> growth sectors), short or long bright CL bands appear parallel to <110>. These bands do not show a zigzag pattern, but rather they have a tabular form. These features correlate to a high concentration of CL-emitting species. The intervening dark bands correlate to zones that lack CL-emitting centers.

10. Both the straight bands and the zigzag segments are parallel to <110> (i.e., to {111} planes). Each straight band or segment corresponds to a small internal {111} face. Since they appear as bright CL bands, the {111} faces are apparently associated with incorporation of CL-emitting species.

Figure 12. At greater magnification (approximately 25×), the CL tomographs of samples B and C show the dark, roughly square-shaped core and surrounding brighter CL-emitting areas. Crystallographic directions <100> and <110> are indicated. Note the bright and dark zigzag patterns in the <100> sectors and the tabular patterns in the <110> sectors.

DISCUSSION

Fingerprinting Faceted Diamonds. Several features observed with X-ray topography and CL tomography prove that samples B and C were cut from the same piece of diamond rough, whereas sample A came from a different crystal. In general, the spatial distribution and orientation of dislocations, the presence or absence of a square-shaped core, and the characteristics of growth banding were distinctive for these samples.

Although the present case is unambiguous, it might be asked whether such fingerprinting is universally applicable. The answer is "yes," since each natural single crystal experienced its own unique growth or post-growth history, which is recorded in its internal imperfections and inhomogeneities. With careful investigation, one can conclusively fingerprint a stone or a set of stones, even if two stones show quite similar internal features.

Applying X-Ray Topography and CL Tomography in Gemology. Crystallographic imperfections and inhomogeneities are distinctive features that can be visualized using instruments available in many standard gemological laboratories (such as the horizontal microscope with immersion; see, e.g., Schmetzer 1996; Smith, 1996). However, X-ray topography allows the visualization of three-dimensional lattice imperfections—such as dislocations—that are not easy to visualize by other methods. CL tomography shows near-surface chemical inhomogeneities two-dimensionally. Both methods can be used to distinguish natural from synthetic diamonds (as well as any other gemstone), since in each case the crystals grow from different media and under different conditions (Lang et al., 1992; Sunagawa, 1995, 1998).

In general, X-ray topography is more informative than CL tomography. Although most major gemological laboratories have the capitalization to install a Lang configuration for X-ray topography (which can cost from $50,000 to about $100,000), the technique requires a thorough knowledge of crystallography and diffraction, and it is somewhat time consuming to adjust the crystallographic orientation of a sample to obtain good topographs.

CL tomography, in combination with optical microscopy, is also affordable (about $25,000) for most major gemological laboratories, and it does not require much background knowledge. Although it cannot reveal the spatial distribution of dislocations as effectively as X-ray topography, it is useful in fingerprinting a stone or a set of stones. Furthermore, CL data can, independent of X-ray topography, conclusively separate natural from synthetic diamonds (Ponahlo, 1992; Sunagawa, 1995).

Growth History. These techniques also provide useful information about the formation of natural diamond crystals. Arguments over the origin of natural diamonds began long ago (e.g., Fersman and Goldschmidt, 1911), and still continue (Frank and Lang, 1965; Lang, 1978, 1979; Lang et al., 1992; Sunagawa, 1984b, 1988, 1995; Sunagawa et al., 1984).

Although we did not identify the CL-emitting species in this study, or determine their concentrations, it is commonly known that blue cathodoluminescence is principally due to nitrogen (probably a combination of band-A and N3 centers) and that CL intensities correspond semi-quantitatively to nitrogen contents (Clark et al., 1992). Higher concentrations of nitrogen are assumed for the zones showing brighter CL images than for the darker zones. The CL observations in the present study indicate that nitrogen incorporation into the growing diamond crystal fluctuated intermittently, with the boundaries between the CL zones representing the positions of growing surfaces at various stages. Such fluctuations are universally observed in natural crystals.

Two distinctly different growth histories were identified for the diamonds in the present study (figure 13). In sample A, alternating bright and dark CL zones form a straight pattern parallel to {111} throughout the stone, which indicates that a simple, unmodified octahedral crystal habit was maintained throughout its entire growth history. Dislocations originate from a central point and are oriented perpendicular to {111}. These indicate that the crystal did not experience an abrupt change in growth parameters to modify the habit. Such a situation corresponds to the growth of crystals under a near-equilibrium condition at a small driving force (low supersaturation or low degrees of supercooling). Dislocation patterns of this type are commonly encountered in octahedral crystals of natural diamond (see, e.g., Frank and Lang, 1965; Lang, 1978). They have been identified as screw-type dislocations in single-crystal octahedral diamonds from Siberia (Sunagawa et al., 1984), which proves that the natural diamond crystals investigated grew by
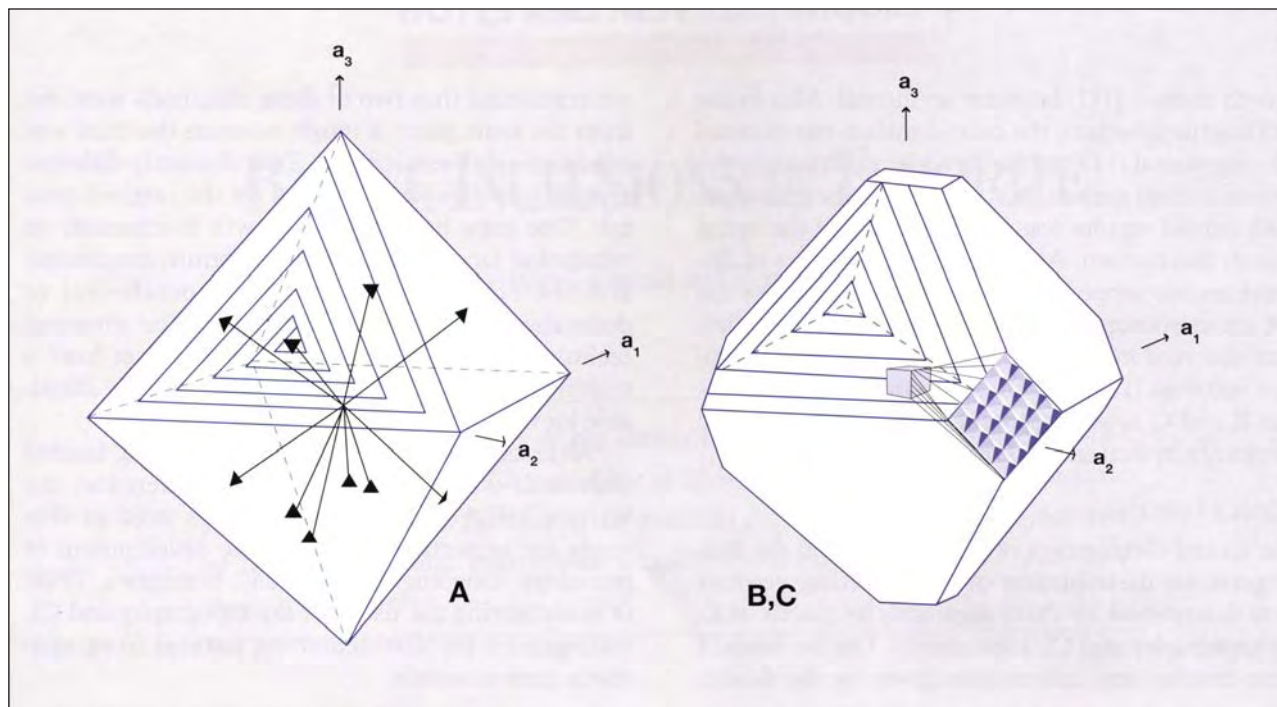
Figure 13. Samples B and C were cut from a crystal with a different morphology—and a more complicated growth history—than sample A. As shown on the left, sample A had a simple octahedral habit, bounded by {111} faces that grew by the spiral growth mechanism from the outcrop of dislocations. Several outcropping dislocations (the straight lines with triangular terminations) are shown, along with only one triangular growth spiral; each dislocation would be expected to produce a similar growth spiral during crystal growth. Samples B and C are assumed to have been cut from a dodecahedroid crystal with a rounded morphology that was due to post-growth dissolution of a crystal that originally consisted of stepped octahedral faces (equivalent to {110} faces) that were truncated by rough cuboid faces (right). The cuboid-shaped core acted as a seed for further growth of the surrounding portion. The straight lines that extend from the core to the cuboid face are dislocation bundles. Only part of the complicated growth history for this crystal is shown.

the spiral growth mechanism. The straight growth bands parallel to {111} are commonly encountered in single-crystal natural diamond, and they indicate a layer-by-layer (including spiral) growth mechanism on {111}, such that the octahedral habit was not modified throughout the growth history (Sunagawa, 1984b). It should be noted that even under such a steady growth condition, the nitrogen partitioning fluctuated, as shown by the alternating bright and dark CL zones. Such a zonation is attributed to local fluctuations in the growth rate.

Samples B and C showed a square-shaped core portion and much denser dislocation bundles in the <100> directions. Since most dislocations originate at the core boundary, there must have been an interruption of growth between the core and the surrounding material. A possible explanation is that the core formed under one set of growth conditions,

and then was transported to a new growth environment where it acted as a seed for further diamond growth. This is the first observation of the presence of a seed crystal in natural diamond crystal growth.

The core took a cuboid form, bounded by rough cuboid surfaces (Sunagawa, 1984a), rather than an octahedral form. Further diamond growth on this seed transformed the morphology from cuboid to octahedral, or dodecahedral truncated by cuboid faces (i.e., that of a mixed habit). At the onset of growth over the cuboid seed, nitrogen was incorporated isotropically (i.e., equally over the seed surface, independent of crystallographic direction) into the crystal, giving rise to a bright CL band surrounding the seed surface. This also implies an abrupt change of growth parameters, which was followed by the appearance and development of {111} faces. In <110> growth sectors, {111} faces are flat; whereas in <100>

growth sectors, {111} faces are segmental. Also in the <100> growth sectors, the cuboid surface transformed into segmental {111} subfaces, while maintaining the general cuboid surface. It is likely that the growth of {100} cuboid sectors was not governed by the spiral growth mechanism. Although a large number of dislocations outcropped on the growing surface, they did not act as sources of spiral growth steps. The difference observed in interface roughness and growth process between {111} and {100} in sample A and samples B and C is in agreement with results reported previously by Sunagawa (1984b, 1995).

CONCLUSIONS

The spatial distribution of dislocations and the heterogeneous distribution of CL-emitting centers were determined for three diamonds by means of X-ray topography and CL tomography. On the basis of these results, and information given by the dealer,

we concluded that two of these diamonds were cut from the same piece of rough, whereas the third was cut from a different crystal. Two distinctly different growth histories were revealed for the original crystals. One grew by the spiral growth mechanism on octahedral faces under near-equilibrium conditions, and the other showed growth of octahedral or dodecahedral forms on a cuboid seed. The advanced techniques employed require that the user have a technical background, but the equipment is affordable for most major gemological laboratories

Although the demand for fingerprinting faceted diamonds will depend on market preference, the writers believe that the techniques used in this study are important for the future development of gemology. Ongoing research (e.g., Sunagawa, 1998) is investigating the use of X-ray topography and CL tomography for distinguishing natural from synthetic gem materials.

REFERENCES

Clark C.D., Collins A.T., Woods G.S. (1992) Absorption and luminescence spectroscopy. In J.E. Field, Ed., *The Properties of Natural and Synthetic Diamond*, Academic Press, London, pp. 35–80.

Davies G. (1979) Cathodoluminescence. In J.E. Field, Ed., *The Properties of Diamond*, Academic Press, London, pp. 165–184.

Fersman A., Goldschmidt V. (1911) *Der Diamant*. Carl Winter's Universitätbuchhandlung, Heidelberg.

Frank F.C., Lang A.R. (1965) X-ray topography of diamond. In R. Berman, Ed., *Physical Properties of Diamond*, Clarendon Press, Oxford, pp. 69–115.

Lang A.R. (1978) Techniques and interpretation in X-ray topography. In S. Amelinckx, R. Gevers, and J. van Landuyt, Eds., *Diffraction and Imaging Techniques in Material Science*, Vol. II, North-Holland, Amsterdam, pp. 623–714.

Lang A.R. (1979) Internal structure. In J.E. Field, Ed., *The Properties of Diamond*, Academic Press, London, pp. 425–469.

Lang A.R., Moore M., Walmsley J.C. (1992) Diffraction and imaging studies of diamond. In J.E. Field, Ed., *The Properties of Natural and Synthetic Diamond*, Academic Press, London, pp. 215–258.

Ponahlo J. (1992) Cathodoluminescence (CL) and CL spectra of DeBeers experimental synthetic diamonds. *Journal of Gemmology*, Vol. 23, No. 1, pp. 3–18.

Scandale E. (1996) *X-ray Topographic Method for Minerals.*

Lecture notes of Short Course on Crystal Growth in Earth Sciences, Santa Vittoria d'Alba, Italy, 14–19 April, pp. 361–374.

Schmetzer K. (1996) Growth method and growth-related properties of a new type of Russian hydrothermal synthetic emerald. *Gems & Gemology*, Vol. 32, No. 1, pp. 40–43.

Smith C.P. (1996) Introduction to analyzing internal growth structures: Identification of the negative *d* plane in natural ruby. *Gems & Gemology*, Vol. 32, No. 3, pp. 170–184.

Sunagawa I. (1984a) Growth of crystals in nature. In I. Sunagawa, Ed., *Materials Science of the Earth's Interior*, Terra, Tokyo and D. Reidel, Dordrecht, pp. 63–105.

Sunagawa I. (1984b) Morphology of natural and synthetic diamond crystals. In I. Sunagawa, Ed., *Materials Science of the Earth's Interior*, Terra, Tokyo and D. Reidel, Dordrecht, pp. 303–330.

Sunagawa I. (1988) Morphology of minerals. In I. Sunagawa, Ed., *Morphology of Crystals*, Part B, Terra, Tokyo and D. Reidel, Dordrecht, pp. 509–587.

Sunagawa I. (1995) The distinction of natural from synthetic diamonds. *Journal of Gemmology*, Vol. 24, No. 7, pp. 485–499.

Sunagawa I. (1998) Imperfections and inhomogeneities in single crystals as a basis to distinguish natural from synthetic gemstones. *Zeitschrift der Deutschen Gemmologischen Gesellschaft*, Vol. 47, No. 1, pp. 45–52.

Sunagawa I., Tsukamoto K., Yasuda T. (1984) Surface microtopographic and X-ray topographic study of octahedral crystals of natural diamonds from Siberia. In I. Sunagawa, Ed., *Materials Science of the Earth's Interior*, Terra, Tokyo and D. Reidel, Dordrecht, pp. 331–349.

BARITE INCLUSIONS IN FLUORITE

By John I. Koivula and Shane Elen

Hemispherical aggregates of the mineral barite were identified as inclusions in fluorite from Illinois. One of these inclusions showed a dramatic pseudo-color change because of its position in the host. The identification of these inclusions was made nondestructively using laser Raman microspectrometry.

During the 1984 Tucson Gem and Mineral Show, one of the authors (JIK) discovered an interesting specimen while examining a large selection of Illinois fluorites for mineral and fluid inclusions. This 247.02 ct partial crystal, which measured 36 mm on its largest dimension, was transparent and had a rich, slightly brownish yellow color. What made it interesting, however, was the presence under a cube face of two prominent white, hemispherical aggregates of an unknown mineral (figure 1). Because no similar inclusions were seen in any of the other fluorite crystals, the unusual specimen was acquired for further investigation.

These inclusions resembled the fibrous white barite aggregates that had been previously observed on fluorite specimens from Illinois (Goldstein, 1997; Ross Lillie, pers. comm., 1998). Because neither inclusion reached the surface of the fluorite, however, conclusive identification at that time would
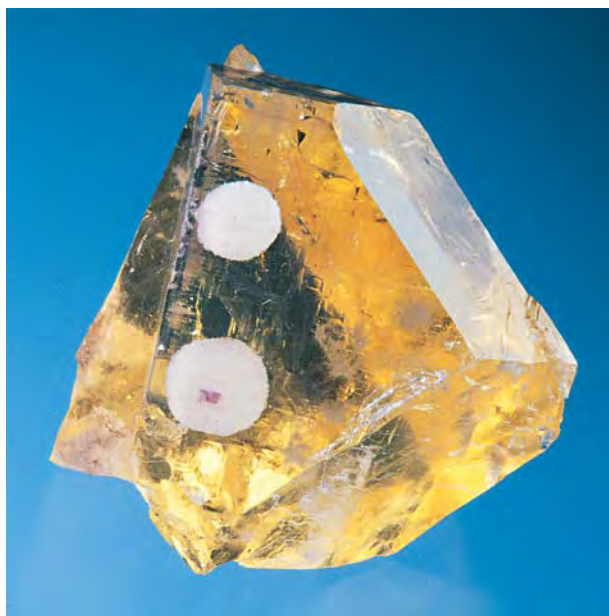
Figure 1. Two large inclusions, which Raman analysis proved to be barite, are easily seen in this 247.02 ct specimen of Illinois fluorite. Photo by Maha DeMaggio.

have required that the host be damaged by cleaving or grinding to expose the inclusions for X-ray powder diffraction and/or chemical analysis. Given the apparent rarity of the specimen, we decided to keep the sample intact until a nondestructive means of analysis became available at GIA.

Figure 2. This 99.49 ct fluorite contains a white 7.5 mm inclusion, also identified as barite, that reflects the color of the surrounding fluorite. Photo by Maha DeMaggio.

More than a decade later, in 1995, gem cutter Michael Gray showed one of the authors (JIK) an unusual 99.49 ct faceted fluorite from Illinois (figure 2) with a white 7.5 mm inclusion that was visually identical to the two inclusions described above. This sample was even more unusual, however, because the inclusion appeared to show a color change from purple in incandescent light to blue in fluorescent illumination (figure 3).

In April of 1996, R. C. Feather described some voids in fluorite from Illinois that had the same shape as the mineral inclusions described here. In that article (p. 12), Mr. Feather speculated that the voids might once have been occupied by the mineral barite because of "the form and the fact that barite is known to occur in the area."

MATERIALS AND METHODS

The large "white" inclusions in both the original 247.02 ct partial crystal and the 99.49 ct faceted fluorite were examined with a standard gemological microscope and analyzed by laser Raman microspectrometry. In preparation for Raman analysis, both samples were first cleaned in acetone and then carefully examined with magnification to position the inclusions as close to the surface as possible and to determine the best angle from which to analyze them. This is necessary to minimize matrix effects from the fluorite host. We used a mounting clay to place the fluorite samples on glass microscope slides during analysis. Because the inclusions were so large, we were able to study them using the 20× objective lens of the Leica targeting microscope, which allowed a greater depth of focus and laser penetration into the fluorite host than the 50× lens we typically use. Further details on the Raman technique as applied to gemology can be found in Schubnel et al. (1992) and Hänni et al. (1997).

Using the continuous scan feature and the 514 nm argon laser of the Renishaw Raman system, we performed 10 complete scans of the inclusions in each of the two samples. The peak-search program employed used the Raman system's software in conjunction with the Renishaw digital spectral library. As a control, we also analyzed a crystal of barite from Colorado under the same conditions.

Figure 3. The 7.5-mm-long barite inclusion shown in figure 2 appears purple in incandescent light (left) and blue in fluorescent light (right). This pseudo-color change is imparted to the white inclusion by reflection from the fluorite host, which shows the actual color change. Photomicrographs by John I. Koivula.
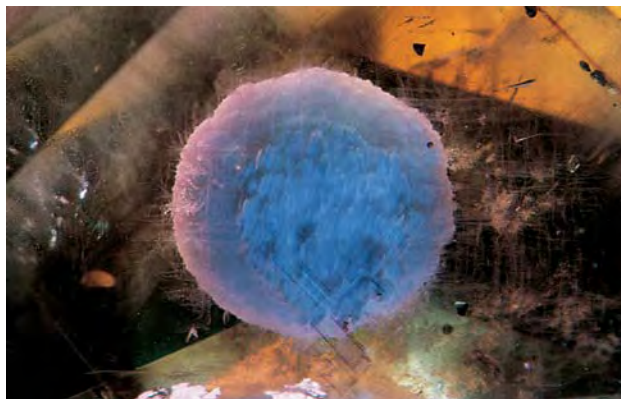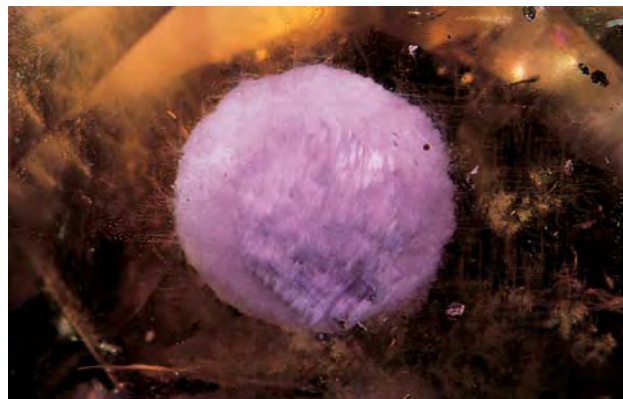
RESULTS AND DISCUSSION

Standard examination with magnification revealed that the color change in the inclusion in the faceted fluorite was not a phenomenon of the inclusion itself; rather, it was caused by the position of the inclusion with respect to the color zoning of the fluorite host. The base of the inclusion rested in a zone of brownish yellow fluorite that comprised the entire pavilion of the stone, giving the fluorite a brownish yellow color face up (again, see figure 2). The upper portion of the inclusion was enclosed in a fluorite color layer that showed a strong purple-to-blue color change. The white inclusion served as an excellent background on which to display this dramatic change of color.

The Raman analysis revealed a spectral match for barite in each of the three inclusions (figure 4). All of the major peaks for barite were present in all of the analyses. Slight differences were noted between the spectra obtained for the barite inclusions and the barite control sample, but these are due to the fluorite matrix and to differences in optical and crystallographic orientation (i.e., anisotropy of Raman spectra).

As noted earlier, voids shaped like barite aggregates have been described and illustrated in fluorite (Feather, 1996). A search of the literature, however, failed to turn up any photographic documentation of actual barite inclusions in fluorite, although Goldstein (1997) briefly mentions them. No description of any association between change-of-color fluorite (Gübelin and Schmetzer, 1982) and barite as an inclusion was found. Therefore, the 99.49 ct faceted gem, which dramatically displays its color change by reflection from a white barite inclusion, may be unique.
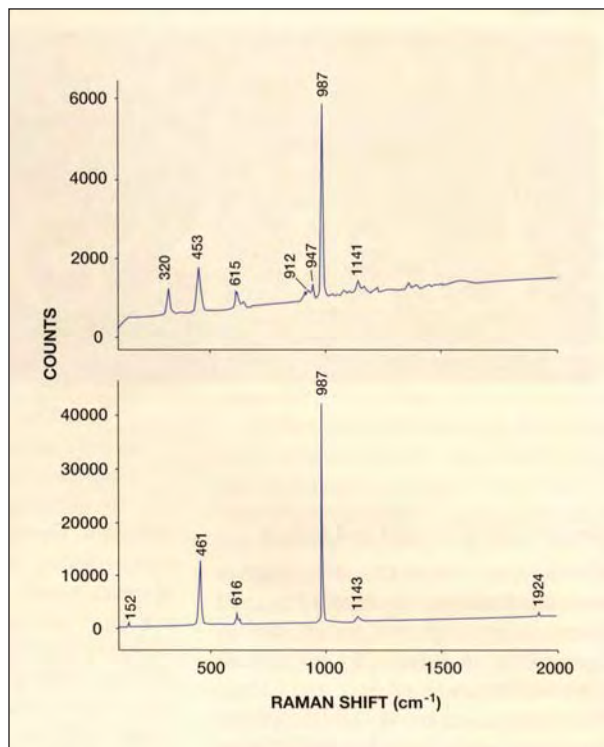
Figure 4. This representative Raman spectrum of the white inclusions in the two fluorite samples (top) is nearly identical to the spectrum for barite that was used as a reference sample (bottom). The additional peaks (e.g., at 320, 912, and 947 cm^{-1}) in the Raman spectrum of the barite inclusions are due to anisotropy of Raman spectra and matrix effects from the surrounding fluorite.

REFERENCES

Feather R.C. II (1996) Inclusion of the month: Phases in fluorite. *Lapidary Journal*, Vol. 50, No. 1, p. 12.
Goldstein A. (1997) The Illinois-Kentucky fluorite district. *Mineralogical Record*, Vol. 28, No. 1, pp. 3–49.
Gübelin E.J., Schmetzer K. (1982) Gemstones with alexandrite effect. *Gems & Gemology*, Vol. 18, No. 4, pp. 197–203.
Hänni H.A., Kiefert L., Chalain J.P. (1997) A Raman microscope in the gemmological laboratory: First experiences of application. *Journal of Gemmology*, Vol. 25, No. 6, pp. 394–406.
Schubnel H.J., Pinet M., Smith D.C., Lasnier B. (1992) La microsonde Raman en gemmologie. *Revue de Gemmologie*, special issue.

Maxixe BERYL, Faded and Fading

Recently, the West Coast laboratory was asked to identify the 8.10 ct light greenish blue gemstone shown in figure 1. The refractive indices of 1.580–1.590 and uniaxial optic character suggested beryl, an identification confirmed by a specific gravity value (measured hydrostatically) of 2.80. Magnification revealed needles, growth tubes, angular growth planes, and pinpoints, thus proving that this was a natural gemstone. The color fell in the typical range for aquamarine, although the refractive indices, birefringence, and specific gravity were slightly higher than expected for that variety of beryl.

The spectrum visible through a desk-model spectroscope did not show the line at 427 nm, which is

Figure 1. This 8.10 ct light greenish blue free-form mixed-cut beryl was of the Maxixe-type, rather than an aquamarine. This color probably represents the result of fading.

related to the iron that causes blue in aquamarine. Instead, we saw four distinct bands between 550 and 700 nm that are characteristic of both natural-color dark blue beryl from the Maxixe mine in Brazil and beryl treated to this color (see K. Nassau et al., "Deep-blue Maxixe-type color center in beryl," *American Mineralogist*, Vol. 61, 1976, pp. 100–107). A visible spectrum obtained with a Hitachi U-4001 spectrophotometer showed bands at 581, 617, 655, and 696 nm, with additional (weaker) peaks at 553, 592.5, 605, and 630 nm. This type of beryl typically shows pleochroism with a stronger color seen along the optic axis direction (the opposite of aquamarine, in which the stronger pleochroic color is seen looking perpendicular to the optic axis). However, the color of this stone was so pale that no pleochroism was observed.

Except in rare cases, dark blue is an unstable color in beryl; it fades in bright light or on exposure to heat, whether it is produced by treatment or by natural irradiation (K. Nassau, "On the identification and fade testing of Maxixe beryl, golden beryl and green aquamarine," *Journal of Gemmology*, 1996, Vol. 25, No. 2, pp. 108–115). It is likely that the light greenish blue color of this 8.10 ct beryl is what remained after such fading. The greenish component in particular can arise when previously irradiated beryl is heated to temperatures under 300°C (G. Mathew et al., "Maxixe-type colour centre in natural colourless beryl from Orissa, India: An ESR and OA investigation," *Journal of Gemmology*, Vol. 26, No. 4, 1998, pp. 238–251). However, we could not prove this nor ascertain whether any additional fading might occur, so we included a comment on the report about possible color instability.

Shortly thereafter, a client submitted three blue beryls, reportedly from Brazil, to the West Coast lab for examination, with permission to carry out fade testing on one of them, a 3.34 ct oval. The gemological properties were within the usual range for beryl, and the spectra were similar to that described above. We compared the samples to Munsell color chips and recorded their hue, tone, and saturation; then we photographed them. The initial appearance of the 3.34 ct oval is shown in figure 2 (left). We placed it in a solar simulator, exposing it to bright light (approximately D65, i.e., daylight-equivalent). After four hours, the color was substantially less saturated and lighter in tone, so the gem appeared paler and grayer. An additional four hours of exposure caused further fading (figure 2, right).

CYW and IR

Figure 2. Before exposure to light, this 3.34 ct oval Maxixe-type beryl was dark blue (left). Eight hours of exposure in a solar simulator caused this stone to fade considerably (right). The faded color is both less saturated and lighter in tone than the original, resulting in an appearance that is both paler and grayer.

DIAMOND

Brown with Green-to-Blue Color Zones

From time to time, both laboratories examine diamonds with a concentration of green to blue at the culet or along the keel that suggests laboratory irradiation (see, e.g., E. Fritsch and J. E. Shigley, "Contribution to the identification of treated colored diamonds: Diamonds with peculiar color-zoned pavilions," *Gems & Gemology*, Vol. 25, No. 2, 1989, pp. 95–101). The East Coast laboratory recently received two diamonds from the same client for colored diamond identification and origin. Each showed an overall brown bodycolor, with concentrated color zones of green or blue. In one diamond, a 1.80 ct round brilliant, the concentration of blue color was extremely noticeable in the face-up position. In the other stone, a 2.00 ct emerald cut, the blue-green zone was smaller and less apparent in the face-up position.

When the emerald cut was examined with magnification in diffused light, the blue-green color concentration along the keel showed no sharp edges (as would be expected from cyclotron irradiation), but there were also no natural radiation stains anywhere on the stone. While it is possible to remove a radiation stain and not the color beneath, a naturally occurring green-to-blue color is usual-ly too shallow for the polisher to accomplish this. Although the presence of a GR1 center in the UV-visible spectrum proved that the diamond had been exposed to ionizing radiation, it was difficult to see whether the color zone followed the facets, which would prove treatment (see Summer 1991 Gem Trade Lab Notes, pp. 108–109). Consequently, we concluded that the origin of color for this diamond is currently undeterminable.

In contrast, when we examined the 1.80 ct round brilliant in diffused light, it was obvious that the blue color zone at the culet followed the faceted shape, a feature that can only result from laboratory treatment. When we looked downward through the upper girdle facets (figure 3), the blue color was clearly visible and separate from the brown color seen throughout the body of the diamond. While it is not uncommon for brown diamonds to be irradiated (usually by an electron beam) to produce a strong blue-to-green color in the face-up position, it appears that the original brown color of this stone was too strong to be entirely masked.

TM and Thomas Gelb

Raman Analysis of Inclusions

During a routine quality analysis, a diamond grader brought to our attention an unusual inclusion in a 0.83 ct marquise-cut diamond. The edge of the otherwise opaque, black-appearing, angular crystal inclusion appeared to have a brown "stain." The grader thought the inclusion could be a diamond crystal with radiation burns on its surface; such stains would make it easy to see, as diamond-in-diamond inclusions are generally invisible because both have the same optical properties.

When the inclusion was examined with polarized light, its morphology and apparent isotropic behavior on thin edges supported this preliminary hypothesis. Because mineral inclusions in diamond often assume the isometric habit of the diamond host, however, the isometric appearance of this or any inclusion in a diamond can be misleading. Furthermore, it is unlikely that an "included diamond" could show radiation stains on its surface, since the natural irradiation of diamond that forms such a "coating" is believed to be a post-growth phenomenon that occurs near the earth's surface.

A detailed microscopic examination of this inclusion—with intense pinpoint fiber-optic illumination—revealed that the crystal actually had a dark red-brown color, which was

Figure 3. The concentration of blue at the culet contrasts strongly with the brown bodycolor in this 1.80 ct round brilliant diamond. Seen here through the crown facets, color zoning that clearly follows the faceted shape of a diamond indicates a treated color. Magnified 22×.
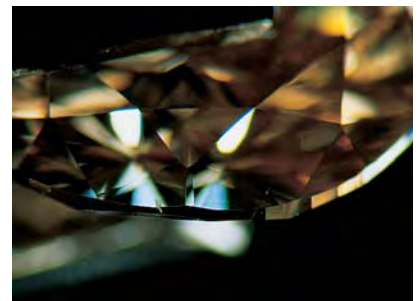
Figure 4. This inclusion in diamond was identified by Raman analysis as chromite that is coated with graphite. Magnified 63×.

clearly visible on thin edges. The majority of the inclusion appeared to be covered with an opaque black material that had a submetallic luster and was bluish gray in reflected light (figure 4).

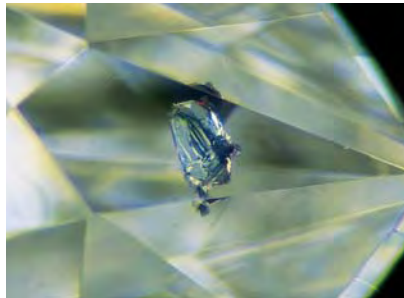Because this inclusion was relatively close to the surface of the diamond, and the overlying facets were well polished, we analyzed it by laser Raman microspectrometry. We detected weak signals for two different mineral components. To resolve the inclusion data, the signal from the host diamond had to be subtracted, which was done by setting the scan parameters to reduce sampling of the large diamond peak at 1334 cm^{-1}.

Using this method, we identified the opaque black material as graphite and the dark red-brown areas as chromite. This suggests that the main mass of this inclusion is chromite, which was coated with graphite. The conversion of diamond to graphite at the interface between a mineral inclusion and its diamond host is relatively well understood, and has even been reproduced in the laboratory (see J. W. Harris and E. R. Vance, "Induced graphitisation around crystalline inclusions in diamond," *Contributions to Mineralogy and Petrology*, Vol. 35, 1972, pp. 227–234). Graphitization is most likely responsible for most of the so-called "carbon spots" observed in gem-quality diamonds.
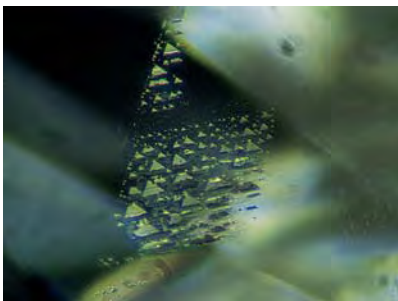
John I. Koivula

With Triangular "Void" Inclusions

Last fall, a former staff member shared a 2.03 ct near-colorless oval-brilliant-cut diamond with staff members in the East Coast lab because of its unusual inclusion pattern (figure 5): a group of "internal trigons" that were all oriented in the same direction and apparently aligned along an octahedral plane. This inclusion scene was reminiscent of a triangular arrangement of numerous triangular voids seen in a 1.74 ct marquise cut diamond that was reported in the Spring 1995 Gem Trade Lab Notes (p. 53).

Careful examination of this inclusion formation indicates that, just like the inclusion pattern previously reported, it represents a phantom octahedral crystal face that is invisible except where decorated by the numerous tiny, flat triangular voids that formed along a growth interface.

Even though these individual triangles are transparent, their high relief and almost silvery metallic luster suggest that they are "voids." Since no cleavage planes or fractures link them to the surface of the host diamond, it is probable that they contain a gas or fluid that was trapped and sealed off during growth. Tiny cleavage "halos" were seen at the edges of some of the triangles. These minute cracks might have resulted from a large difference in pressure between the conditions present when the inclusions formed, and those when the diamond was emplaced in

Figure 5. Numerous triangular voids decorate a phantom octahedral face in this 2.03 ct diamond. Magnified 63×.

the transporting magma; stress induced during mining and faceting might also have caused the cracks.

John I. Koivula

SYNTHETIC DIAMOND, Showing Change of Color

This past fall, a client showed a most interesting synthetic diamond to the laboratories on both coasts. Although the 0.51 ct round brilliant appeared mostly brown (due to both a dark tone and low saturation), it exhibited a color change from a greenish yellow hue in day (or fluorescent) light to an orange hue in incandescent light, as shown in figure 6. This first stone was produced by accident, but the manufacturer has since reproduced the phenomenon in several more synthetic diamonds.

The round brilliant was readily identified as synthetic diamond by standard gemological testing. Magnification showed a cloud of pinpoints in the form of a square under the table, as well as several tiny gray inclusions. Brown graining along cubic directions formed a long, slim hourglass shape in profile view, and some of this graining luminesced green to strong visible light. When viewed with the long-wave UV lamp, this same brown graining fluoresced yellowish green, which was visible through the table as a cross pattern. When exposed to short-wave UV, the body of the stone fluoresced a weak orange, and the green cross persisted. Unlike the colored synthetic diamonds we reported on previously, this one showed a strain pattern (anomalous birefringence) that followed the cubic graining.

Several spectral features indicated that this synthetic diamond had been treated after growth. The infrared spectrum revealed a type IaA diamond, rather than the type Ib that most yellow synthetic diamonds are. Also present were clear, moderate-sized H1a and H1b bands (at 1450 and 4935 cm^{-1}, respectively), which are known to develop following irradiation and heating (A.T. Collins et al.,

Figure 6. Beneath the overall brown color, this 0.51 ct synthetic diamond shows a color change from a greenish yellow hue in daylight (left) to an orange hue in incandescent light (right).

"Spectroscopic studies of the H1b and H1c absorption lines in irradiated, annealed type Ia diamonds," *Journal of Physics C: Solid State Physics*, Vol. 19, 1986, pp. 3933–3944). The infrared spectrum also showed weak absorptions due to hydrogen, an impurity previously unreported in synthetic diamond.

The visible spectrum showed a well-developed N-V center, with a primary peak at 637 nm and related absorptions at 503, 575, and 594 nm. While this center occurs rarely in natural-color diamonds, it is commonly found in those that have been irradiated and heated, most notably treated-color pink to purple diamonds. Although there are some other peaks in the spectrum, this broad feature between about 550 and 637 nm, along with the transmission regions on either side, causes the color-change behavior. (For an explanation of the color-change phenomenon, see Y. Liu et al., "The 'alexandrite effect' in gemstones," *Color Research and Applications*, Vol. 19, No. 3, 1994, pp. 186–191.)

IR

PEARLS

Cultured, with a Faceted Surface

Another interesting item that the East Coast laboratory received for identification was a strand of 10–13 mm light gray cultured pearls that had been fashioned in a most unusual way: All were completely covered by rhombic facets, which gave them a distinct "polished" appearance (figure 7). We had seen similar cultured pearls at the 1997 Tucson gem and mineral shows, as reported in the Summer 1997 Gem News (pp. 146–147).

The X-radiograph substantiated that these were cultured pearls. When we examined them with long-wave ultraviolet radiation, however, we noticed an uneven greenish yellow fluorescence, which was more intense along the facet edges. With magnification, it became evident that all facets were indeed flat and showed very sharp edges. They were completely smooth and had a mirror-like appearance in reflected light; we saw no polishing lines. The characteristic growth or suture lines in the nacre, formed by the edges of the overlapping aragonite platelets, were barely visible: They appeared as very faint lines rather than as narrow grooves. This overall flatness of the surface greatly increased the observed luster.

We also noted that carefully applied pressure from the tip of a needle probe left smooth indentations on the surface of the cultured pearl, similar in appearance to those depressions left on a coated surface. This response may be a result of the extreme smoothness of the polished face, residue left on the surface from polishing, or a superficial coating applied after polishing. *KH*

Figure 7. The faceted surfaces of these 33 cultured pearls (10–13 mm in diameter) were extremely flat and showed very high luster.

Non-Nacreous "Pearls"

By coincidence, last summer our laboratories on both coasts received two groups of symmetrical, oval- to drop-shaped, light pink concretions for examination. Some specimens were evenly colored, but others showed slight color variations (mainly darker bands of color encircling them). The most prominent feature was a "mosaic" pattern that covered the entire surface and gave rise to a sheen-like effect in reflected light (figure 8).

This appearance reminded us of the flame-like pattern seen in some conch "pearls." The sample in figure 8 is particularly attractive, an oval shape that measured approximately 14 × 12 mm in diameter. With 10× magnification, the surface looked fairly smooth. There were no signs of any polishing lines that might indicate that the specimen had been cut and polished to produce its shape. Standard testing verified that the specimen was a carbonate.

An X-radiograph revealed a homogeneous structure, which proved that the specimen was indeed a natural concretion. The surface of the pearl (figure 9) showed a pattern of densely packed polygons, which indicate a radiating prismatic structure; the polygons are cross-sections of the carbonate prisms. According to consult-ing biologist Dr. C. Hedegaard, this geometry contrasts with the stacked shingles of nacre tablets found in common pearls, as well as with the flame-like pattern in pearl formations with crossed lamellar structure (e.g., *Melo melo* and *Strombus gigas* [conch "pearls"]). To our knowledge, various thorny oysters can produce concretions (see Winter 1987 Gem Trade Lab Notes, p. 235). Our client informed us that this unusual concretion came from an oyster found along the Pacific Coast of North America.

KH

SPINEL, with a Darker Core

When you mention high-quality natural red spinel to anyone in the gem or jewelry trade, they usually think of Burma (now Myanmar) as a locality and often, more specifically, of the Mogok region. This is because nature has seen fit to have its finest red spinels "walk hand-in-hand" with its finest rubies in this locality.

In fact, spinel is commonly associated with ruby in many gem deposits worldwide. These two gems are close chemical cousins with a similar paragenesis, and in both cases the red color is caused by chromium. However, whereas ruby from Mogok is known for its distinctive roiled or
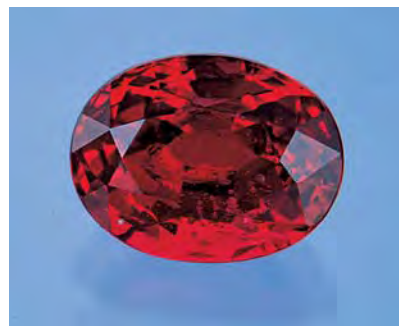
Figure 10. This 1.11 ct spinel from Myanmar appears evenly colored face up, but it is actually strongly color zoned and shows two different refractive index readings.

heat-wave-like color zoning, the red spinels from this area (and spinels in general) do not commonly exhibit color zoning.

It was, therefore, with great interest that we saw distinct color zoning in a 1.11 ct oval mixed-cut red spinel from Mogok (figure 10). The color zoning was not apparent when this gem was examined without magnification; rather it appeared to have a uniform color, as would be expected in a fine spinel. With magnification and standard, darkfield illumination, the color also appeared even. The natural origin of this stone was immediately discernible by the presence of numerous small negative crystals and birefringent mineral inclusions. These crystals appeared to outline one half of an octahedral "phantom" or core which was also delineated by edges that were somewhat rounded or melted looking.

Another interesting feature of this stone was its refractive index. When testing spinel, one generally expects to get a single consistent reading. With this gem, however, the R.I. obtained from the table was 1.732, while testing anywhere else on the crown or pavilion gave a reading of 1.718. Such a variation could easily lead to the erroneous conclusion that the stone was assembled. Since most flame-fusion synthetic spinel is known to have an R.I. of about 1.73,

Figure 8. Note the color bands encircling one end of this 14 × 12 mm calcareous concretion, which was produced by an oyster from the Pacific Coast of North America.

Figure 9. A closer look at the uneven coloration of the "pearl" in figure 8 shows the radiating prismatic structure of the carbonate grains of which it is composed. Magnified 12×.

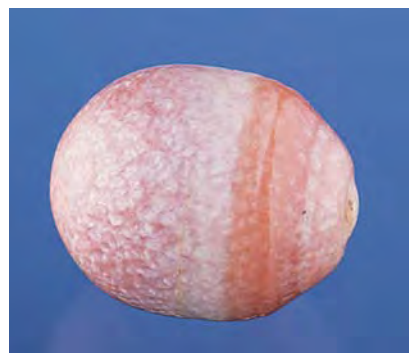and since most natural spinel gives a single refractive index reading of about 1.71 to 1.72, the double reading on this stone could lead one to assume that the table area was composed of synthetic spinel, while the pavilion area was natural.

Given the unusual results obtained with both magnification and the refractometer, we decided to examine the stone further using immersion in methylene iodide and diffused transmitted light. The color zoning became obvious (figure 11), in the form of a deep red, diamond-shaped core that was surrounded by much lighter pink spinel. The stone was then rotated for a profile view of the centralized color zone (again, see figure 11), which was revealed to be a half-octahedron with a large portion exposed on the surface of the table facet. It was now clear that the red core had the higher refractive index of 1.732, while the pink areas had the slightly lower index expected for natural spinel.

Since the properties of this spinel were so unusual, we explored the chemical composition of the sample with energy-dispersive X-ray fluorescence (EDXRF) analysis. Although our instrumentation is not calibrated to give quantitative results for spinel, this method can show if there is more of a particular element(s) on one surface of a faceted stone or crystal than on another. Mike Moon of GIA Research measured significantly more chromium and vanadium on the table facet, where the red octahedral phantom core was exposed to the surface, than on the pavilion.

As a last test, we performed laser Raman microspectrometry on both the table and pavilion surfaces. While the instrument identified both test areas as spinel, the peaks obtained from the darker red table were 50% higher (i.e., more intense) than those generated from the pavilion. Like the obvious differences in refractive index recorded for this stone, this is apparently the result of the greater amounts of chromium and vanadium in the darker red core exposed on the table surface.

This is not where the story ends. Last September, Mike and Pat Gray of Graystone Enterprises in Missoula, Montana, showed this writer a parcel of small, transparent, bright red "cutting rough" spinel octahedra from Myanmar. Microscopic examination of two of these crystals (0.19 and 0.20 ct) revealed distinct, rounded cores of a deeper red color. The low relief of these cores showed that they were very close in refractive index to the surrounding spinel. It was only the strong difference in color that made them readily visible. Another 0.20 ct spinel crystal from this group showed what appeared to be an oblong core surrounded by layers of roiled growth zoning (figure 12), which is more reminiscent of what we expect to see in Mogok rubies.
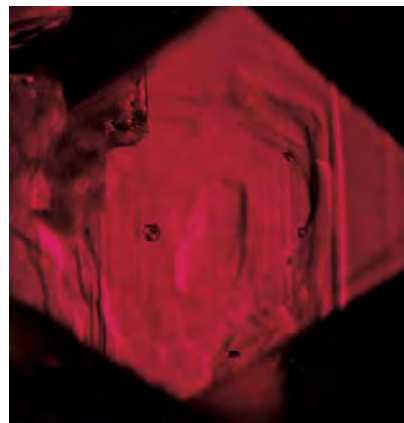
Figure 12. The strong roiled growth zoning around the oblong core in this 0.20 ct red spinel is unusual in spinel, but similar to that seen in Mogok rubies. Magnified 25×.

Since the darker red cores of the two samples seemed to blend into the surrounding crystals with no sign of an interfacial separation—and, unlike the first spinel described above, the cores were not exposed on the surface of either crystal—we used a Becke line method (see. e.g., W.D. Nesse, *Introduction to Optical Mineralogy,* Oxford University Press, New York, 1991, pp. 26–30) to determine that the cores had a higher refractive index than their host.

It is not known how unusual such color-zoned red spinels are. In the parcel of 48 small octahedra, just two with darker red cores were found with magnification alone. Since immersion is not generally used as a testing procedure in the identification of spinel, the color zoning in such stones could easily be overlooked by a less-experienced gemologist. Yet knowledge of such a core could help the cutter produce a darker red stone.

John I. Koivula

Figure 11. Immersion in methylene iodide revealed strong color zoning (left) in this 1.11 ct natural spinel. The profile view (right) shows that the dark red zone (6.82 mm long) is exposed on the surface of the table facet.
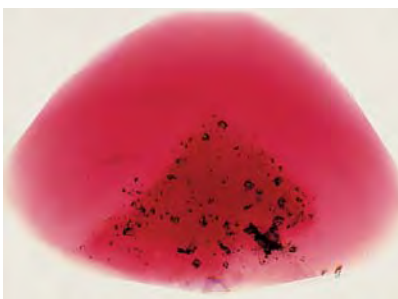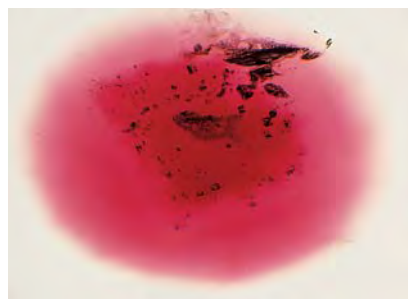
GEM N·E·W·S

Figure 1. Five kimberlite pipes make up the Ekati diamond mine, which is located about 300 km northeast of Yellowknife in the Northwest Territories. Artwork modified from original provided by Outcrop; courtesy of BHP Diamonds Inc.

DIAMONDS

Diamond production starts at Canada's Ekati mine. October 14, 1998, marked the opening of the Ekati diamond mine in Canada's Northwest Territories (NWT). About 125 guests attended the event, including ministers from both the federal and territorial governments, officials of indigenous peoples' groups and municipal governments, executives of several mining companies, and media representatives. Prof. A. A. Levinson (University of Calgary, Alberta) attended on behalf of *Gems & Gemology* and provided the following report.

Several large mining companies began exploring for diamonds in the NWT in the early 1980s, but by 1985 most had withdrawn from the area. However, the indefatigable Charles E. Fipke, who in 1983 incorporated Dia Met Minerals Ltd., continued the arduous and expensive exploration along with his partner, Stewart L. Blusson. In 1985, Fipke found the first diamond indicator minerals (most importantly, "G10" pyrope garnets) in glacial deposits in the vicinity of Lac de Gras (figure 1). He staked the first claims for diamonds in the NWT in 1989. In September 1990, Dia Met and BHP Minerals (a subsidiary of Australia-based Broken Hill Proprietary Ltd.) signed a joint-venture agreement for the NWT Diamonds Project; BHP became operator of the project.

Within a few months, the joint venture had located a likely source of the diamond indicator minerals (which now included chrome diopside) under what was subsequently named Point Lake. Following geophysical sur-

veys, in spring 1991 a core hole was drilled under Point Lake and the first diamond-bearing kimberlite pipe was confirmed (it is presently noneconomic, at a grade of 0.6 ct/tonne with diamonds valued at less than US$40/ct). To date, the joint venture has discovered more than 100 kimberlite pipes, many of which contain diamonds, within its 1,820 km² stake on the north side of Lac de Gras. The economic potential of some of the pipes has yet to be determined. The five kimberlite pipes that now comprise the Ekati diamond mine, in order of their discovery between 1992 and 1995, are Fox, Koala, Misery, Panda, and Sable (again, see figure 1).

Most of the pipes are located under lakes that formed because the kimberlite was eroded more easily than the surrounding granite by advancing glaciers during the last Ice Age. By world standards, these kimberlite pipes are small (e.g., Panda is about 3 ha [hectares], or 7.4 acres), but they can have extremely high grades and/or high values (table 1 and figure 2). (Most kimberlite mines operating today are larger than 6 ha. For example, Mir is 6.9 ha, Venetia is 12.7 ha, and Premier is 32.2 ha.)

By late 1993, it was clear to the joint venture that a viable diamond mine could be developed in the Lac de Gras region. In 1994, BHP Minerals transferred its interest to BHP Diamonds Inc., a newly formed Canadian corporation. In December of that year, BHP Diamonds Inc. notified the Canadian government of its intent to mine the deposit. However, the mine is located in an area of continuous permafrost, with a fragile ecosystem. In July

Figure 2. All of these diamonds were recovered from the Ekati mine. (The largest rough diamond reported thus far weighed 47 ct, but we do not know if it was gem quality.) Photo courtesy of BHP Diamonds Inc.

1995, an extensive environmental impact study was submitted for government review. Following a careful evaluation, the successful conclusion of negotiations with four indigenous peoples' groups, and approval by the Federal Cabinet, all necessary licenses and permits were obtained by January 1997, allowing construction to begin. Close attention was paid to integrating the project with the local communities and the economy of the NWT (for example, about 550 permanent jobs have been created, 30% of which are held by indigenous people.)

The project was named Ekati in 1997, with the ownership distributed as follows: BHP Diamonds Inc. (51%), Dia Met Minerals Ltd. (29%), Charles E. Fipke (10%), and Stewart L. Blusson (10%). *Ekati* means "fat lake" and is the name traditionally used by indigenous people for Lac de Gras. It refers to the white quartz rock found in abundance around the lake, which resembles caribou fat.

Construction of the mine presented numerous challenges because of the remoteness of the area, the lack of permanent roads (a 475 km ice road is available from Yellowknife, the territorial capital, for only 8–10 weeks from mid-January to mid-April), the lack of other types of infrastructure (e.g., electricity), and the harsh climate (temperatures can drop to –50°C in the winter months). Yet construction of a processing plant and supporting facilities, as well as preparation of the first kimberlite for mining (Panda; see figure 3), were completed on schedule in 21 months. This is an amazing engineering and logistical feat, considering the difficulties mentioned above. So far the investment in Ekati totals about US$700 million.

The five kimberlites at Ekati will be mined in a sequence determined by the size and location of each pipe, as well as by the projected value of (and market demand for) the diamonds they contain. This plan is designed to provide a consistent production, both by quality and value of the diamonds. Some ore will be stockpiled in case mining is interrupted by equipment

TABLE 1. Ore reserves and the timetable (anticipated production dates) for mining diamonds at the five pipes comprising the Ekati diamond mine.[a]

Production	Panda 1998–2009	Misery 1999–2013	Koala 2002–2013	Sable 2007–2013	Fox 2008–2015	Total (T) Avg. (A)
Mining reserves (millions of tonnes)[b]	13.4	5.5	17.4	12.9	16.7	66.0 (T)
Grade of kimberlite (ct/tonne)	1.09[c]	4.26	0.76[d]	0.93	0.40	*1.09* (A)
Average value of diamonds (US$/ct)	130	26	122	64	125	*84* (A)

[a] Production schedules are subject to change. All pipes will be mined initially by open-pit methods. Underground mining will occur later at the Panda and Koala pipes. Modified from Dia Met Minerals Ltd. Annual Report 1997-1998. A particular year (e.g., 1999) refers to the fiscal year, which starts in June (e.g., June 1999–May 2000).

[b] Includes both proven reserves (43.5 million tonnes total) and probable reserves (22.4 million tonnes total); 1 tonne = 1,000 kg = 2,204.6 pounds (avdp).

[c] Grade includes the 0.97 ct/tonne material in the underground mining portion of 2.8 million tonnes.

[d] Grade includes the 1.63 ct/tonne material in the underground mining portion of 0.8 million tonnes.

Figure 3. This aerial photograph of the Ekati diamond mine, looking south (with the camp and processing facilities in the distance), was taken in August 1998. The Panda pit (foreground) measures about 900 m in diameter; the kimberlite is the much smaller dark region in the center and lower right of the pit floor. (The area of the pit is larger than the pipe because of the requirements of open-pit mining.) Eventually, the bottom of the pit will be about 100 m wide and 300 m below the present surface, at which time underground mining will commence. Just beyond the Panda pit is Koala Lake, which marks the location of another kimberlite that is scheduled to begin mining in 2002. Photo © Jiri Hermann/BHP Diamonds Inc.

breakdown or extreme weather. Production from Ekati, initially only from the Panda pipe, is scheduled at 9,000 tonnes of kimberlite per day, yielding approximately 10,000 carats of diamonds daily (about enough to fill a large coffee can). Annually this is equivalent to 3.5–4.5 Mct (million carats) of rough gem and industrial diamonds, worth about US$500 million. On the basis of current world production (115 Mct), this will constitute about 4% of the total annual supply by weight and 6% by value. It is planned that, after 10 years, production will be increased to 18,000 tonnes of kimberlite per day, requiring an additional investment of US$80 million. Over the initial 17 year life of the Ekati mine, about 66 million tonnes of ore will be processed from the five kimberlite pipes (again, see table 1), yielding about 72 Mct of diamonds (based on an overall grade of 1.09 ct/tonne). In view of the numerous other kimberlites in the area, some of which almost certainly will be mined in the future, mining in this region is expected to last for at least 25 years.

The rough diamonds will be sorted and evaluated at a specially designed facility near the Yellowknife airport, beginning in early 1999. Initially, all of the rough dia-

monds will be exported to Belgium, to be marketed through BHP Diamonds' sales office in Antwerp, with the assistance of I.D.H. Diamonds NV. It is anticipated that a limited number of cutting facilities eventually will be established in various parts of Canada.

Ekati is the first of what are likely to be several new diamond mines in Canada. The Diavik project, which borders Ekati on the south, is being developed by Rio Tinto PLC and Aber Resources; it is expected to begin production in 2002 with about 6 Mct annually. When the Diavik production is combined with that of Ekati, about 10% of the world's diamonds (by both weight and value) could come from Canada; this is comparable to current production from South Africa.

***Financial Times* Diamond Conference.** *Gems & Gemology* editor Alice Keller attended this one-day conference, which was held in Antwerp, Belgium, on October 28. Three main areas of the diamond business were addressed: supply, manufacture, and demand.

De Beers has a major stockpile of diamonds (which they valued at about $4.6 billion as of June 1998) and can adjust supplies to assure stability for rough diamond prices. Given concerns about diamond demand (see below), the Central Selling Organisation (CSO) will continue to restrict sights, and not all sightholders will receive diamonds at each one. The main sources for stones outside CSO marketing channels have been Russia, Angola, and Australia; Canada is now poised as a fourth source. Despite its own economic crisis, Russia is in a good position to continue diamond mining; however, production is not likely to increase in the near future, and current production is completely absorbed by the CSO and the Russian cutting industry. Mining in Angola is uncertain (and expensive) because of the civil war raging there, which shows no sign of abating. However, Angola has produced several million carats of alluvial stones in recent years, and the first kimberlite pipe to be mined there, Catoca, recovered more than 122,000 carats in one month in 1998. Although Canada's Ekati mine will produce about 3.5–4.5 Mct annually, with no plans by BHP to stockpile goods, De Beers's representatives do not believe that Canadian production will have a significant impact on supply.

Two related economic problems bedevil manufacturers: overcapacity and financial liquidity. Today, the diamond industry is in transition from being supply driven to being demand/marketing driven. India is now the world's leading diamond manufacturer, producing 9 of every 10 fashioned diamonds, with costs as low as $0.75 to cut a small sawn stone. The huge manufacturing capacity there has led to excess inventory. Israel is suffering because so much of their business fed demand in Asia. Rough imports to New York decreased 23% for 1997 compared to 1994, yet diamond jewelry sales in the U.S. continue to rise. However, this increased demand is

primarily for less-expensive goods, rather than for the more important stones cut in New York. Like Israel and New York, the Belgian diamond industry must contend with high wages relative to India. Recent allegations that drug dealers are laundering money through the Antwerp diamond trade may lead to further scrutiny on the part of government authorities.

Diamonds have been adversely affected on the demand side, not only because of the Asian financial crisis, but also because consumers in Japan appear to be putting disposable income into goods other than diamonds. (In Japan, diamonds—especially solitaire rings with certificates—are perceived to be the least profitable part of a jeweler's inventory.) More and more diamond manufacturers look to U.S. consumers to compensate for lost Asian sales. The auction market saw a recent drop in demand: Christie's sold only 50% of the lots offered at its October 1998 sale in New York, and the company responded immediately with a reduced, more selective, December auction. One key to building demand is advertising; in addition to its own branding initiative (still being "test-marketed"), De Beers continues to invest $200 million per annum in "generic" diamond advertising worldwide. Overall, technology is altering the "diamond landscape": improved communications (e.g., the Internet), new instruments, and ongoing research are changing the way diamonds are found, fashioned, and regarded.

COLORED STONES

Colored stone presentations at the International Mineralogical Association meeting. The Fall 1998 Gem News section reported the results of several diamond investigations described at the 17th IMA meeting in Toronto, Ontario, last August. There were also numerous presentations on colored stones, several of which are summarized below.

George Rossman (California Institute of Technology,

Pasadena) delivered a plenary lecture on the origin of color in minerals. The coloration of tourmaline, garnet, and the colored varieties of quartz are due to transition metal ions (often interacting to produce different colors) and microscopic inclusions. Color also can be induced when natural background radiation changes the oxidation state of ionic impurities. D. C. Grenadine (Slippery Rock University, Pennsylvania) attributed the formation of the color centers that produce yellow to brown in silicate minerals such as quartz, topaz, and beryl, to ionic impurities in the presence of aluminum that has substituted for silicon in tetrahedral sites. In two presentations, John Emmett and Troy Douthit (Crystal Chemistry, Brush Prairie, Washington) described the techniques used to treat some gemstones (especially sapphire), which may result in a substantial improvement in color and/or clarity (see, e.g., figure 4) and therefore value.

There were numerous presentations on gem corundum. F. L. Sutherland (Australian Museum, Sydney) presented a model for the origin of two geochemically distinct suites of corundum from alkali basalts, whereby partial melting of the lithosphere over a rising plume of the earth's mantle can lead to repeated eruptions of potentially gem-bearing lava. M. I. Garland and colleagues (University of Toronto) inferred that the alluvial sapphires from southwest Montana came from a crustal metamorphic source, on the basis of their relatively low (40–60 ppm) gallium contents. T. Häger (University of Mainz, Germany) and colleagues studied the trace-element chemistry and inclusions in rubies from two mining areas in Vietnam—Luc Yen (where the rubies are produced by metasomatic processes in marble) and Quy Chau (where pegmatites introduced into sillimanite-bearing schists are responsible for ruby formation). T. Häger also studied the cause of color in sapphire, and noted that magnesium seemed to be required (as well as Fe and Ti) to explain the coloration of heat-treated yellow sapphire. D. Tang (University of Fuzhou, Fujian, China) attributed the blue color of sapphires from Mingxi

Figure 4. Some near-colorless geuda sapphires from Sri Lanka (left) become commercially important after heat treatment improves their color (right). The stones range from 1 to 4 ct. Photos courtesy of John Emmett, Brush Prairie, Washington.
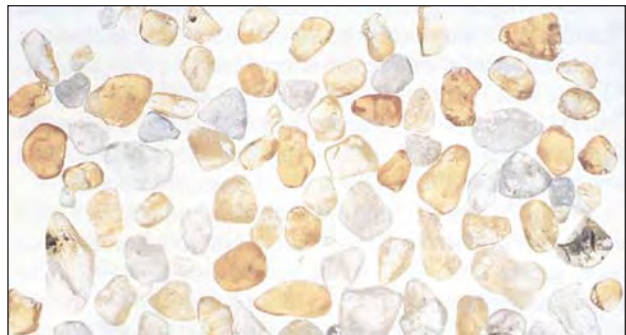
Figure 5. Granitic pegmatites in Afghanistan are renowned for producing large quantities of gem-quality spodumene in a variety of colors. This kunzite crystal is 11.8 cm long. Courtesy of Bill Larson, Fallbrook, California; photo © Jeff Scovil.

(Fujian Province) to a defect cluster containing hydrogen as well as iron and titanium. A. V. Lyutin (Moscow State University, Russia) and colleagues grew flux synthetic rubies with up to 6.38 wt.% Cr_2O_3 from $PbO-V_2O_5-WO_3$ flux. They found that samples grown in this flux, and in Li_2O-WO_3 flux, at 1100°–1250°C, had rather equidimensional shapes.

I. I. Moroz (Hebrew University of Jerusalem, Israel) and G. Panczer (University Claude Bernard, Lyon, France) examined the Raman spectra of emeralds from several deposits, and suggested that this technique might someday be useful to differentiate emerald localities. I. Z. Eliezri (Colgem Ltd., Ramat Gan, Israel) and I. I. Moroz examined the compositions of mica and talc inclusions in emeralds from different sources, and likewise suggested that these compositions might be useful to identify emerald sources. G. Graziani (University of Rome "La Sapienza," Italy) used infrared spectroscopy to investigate several possible sources for ancient Roman emeralds.

A. M. R. Neiva (University of Coimbra, Portugal) and co-workers described the trace-element chemistry of blue, green, pink, and white beryl from Namivo, Alto Ligonha, Mozambique. Z. L. Li and colleagues (Zhong-shan University and Nanjing University, China) characterized zinc spinel and other daughter crystals found in

melt inclusions in pegmatite beryl from Xinjiang, Hunan, and Yunnan Provinces, China. J. M. Evenson (University of Oklahoma, Norman) and colleagues looked at the equilibrium among beryl, aluminosilicates, chrysoberyl, and quartz in an aluminum-rich granitic melt; they found that beryl could crystallize at very low beryllium concentrations in low-temperature-solidifying melts.

T. Lu (GIA Research, Carlsbad) and colleagues described differences between natural and synthetic amethyst, citrine, and ametrine. Some synthetic amethyst can be identified by the orientation of color zones and growth bands, pleochroism, and a characteristic IR absorption peak at 3540 cm^{-1}. I. K. Bonev (Bulgarian Academy of Science, Sofia) suggested that thin microscopic calcite plates acted as seeds for well-formed crystals of "fadenquartz" (quartz crystals containing opaque white strips that might be mistaken for the seed plates in synthetic quartz), which form in Alpine-cleft-type deposits in Switzerland and elsewhere.

Advanced analytical techniques were described in many presentations. M. Gaft (Open University of Israel, Tel Aviv) and G. Panczer illustrated the use of laser-induced time-resolved luminescence spectroscopy to differentiate among luminescence centers with similar emission spectra but different decay times; previously unknown causes of luminescence (mostly involving rare-earth elements) were documented. M. Superchi and E. Gambini (CISGEM, Milan Chamber of Commerce, Italy) discussed the use of infrared spectrophotometry, energy-dispersive spectrometry, and Raman microspectrometry to identify treatments and differentiate between varieties of organic and amorphous gem materials. A. Banerjee (University of Mainz, Germany) and D. Habermann (Bochum University, Germany) used hot-cathode cathodoluminescence to differentiate between natural and cultured freshwater pearls from North America and China, respectively. P. Zecchini (University of Franche-Comté, Besançon, France) and colleagues used reflectance IR spectroscopy, electron microprobe analysis, and X-ray diffraction to determine nondestructively the species, composition, and lattice parameters of gem garnets.

Gem-bearing pegmatites were highlighted by several researchers. K. L. Webber and colleagues (University of New Orleans, Louisiana) calculated the crystallization times of some gem-bearing pegmatites in San Diego County, California; for the famous Himalaya dike at Mesa Grande, they estimated that the pegmatite cooled to 400°C in only five to 14 days. P. Keller (University of Stuttgart, Germany) defined several belts of rare-element pegmatites in Namibia's Central Damara Province; gem tourmaline has been found in some of these pegmatites. B. M. Laurs (GIA *Gems & Gemology*) surveyed the gemstone resources and the geologic setting of kunzite-elbaite-beryl pegmatites in Afghanistan (see, e.g., figure 5), and suggested possibilities for further exploration. A.

B. Rao and M. S. Adusumilli (University of Brasilia, Brazil) gave exploration guidelines for aquamarine- and elbaite-bearing pegmatites in Borborema Province, Rio Grande do Norte, Brazil. C. Kasipathi (Andhra University, India) and A. B. Rao described the source rocks (mostly pegmatites) for many gems (e.g., ruby, alexandrite, tourmaline, topaz, and garnet) in the Khammam, East Godavari, and Visakhapatnam districts of Andhra Pradesh State, India.

Chalcedony with goethite inclusions from Madagascar. On a recent trip to Madagascar, Michel Bricaud of La Rose du Désert, Bagneux, France, acquired a large quantity of an unusual variety of chalcedony (figure 6), some of which was examined by Gem News contributing editor Emmanuel Fritsch at the University of Nantes, France. The material is currently being fashioned into cabochons.

The chalcedony contains abundant tiny, dark spherical aggregates, typically 0.1–0.2 mm in diameter. Their dark brown color contrasts sharply with the white or beige of the matrix, and their small size creates very fine detail in the inclusion patterns. With magnification, these spherules show yellow-brown internal reflections, which suggests that they are goethite.

Chemical analyses of the spherules were performed with a JEOL 5800 LV scanning electron microscope, equipped with an energy-dispersive detector that can detect most light elements, including oxygen (but not, e.g., hydrogen). The only elements detected by SEM-EDX were iron and oxygen, as well as small amounts of silicon from the chalcedony matrix. This chemistry is typical of iron oxides and hydroxides. X-ray diffraction analysis of a fragment of chalcedony particularly rich in the inclusions showed peaks corresponding to goethite, in addition to the quartz peaks. Dr. Fritsch therefore identi-

Figure 6. The tiny black inclusions forming fine patterns in these chalcedony samples from Madagascar (each about 4 cm across) were identified as goethite. Photo by A. Cossard.
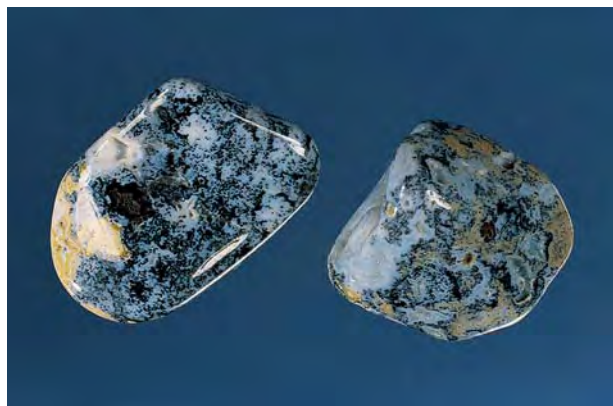
Figure 7. At first, this 1.48 ct colorless iolite was thought to be feldspar. The 18.49 ct iolite block shown on the left was used as a reference standard for Raman analysis. Photo by Maha DeMaggio.

fied the small brown spherules as goethite [α-FeO(OH)] inclusions in chalcedony.

Iolite gemologically indistinguishable from feldspar. The vast majority of gem identifications today—well over 90%—can still be made with the standard methods available to most gemologists and jewelers. However, occasionally we receive gem materials that present especially subtle challenges. The actual identities of these materials often are not even suspected unless so-called advanced testing techniques are used. One example was the faceted genthelvite described in the Fall 1995 Gem News (pp. 206–207), which could not be distinguished from (much more common) pyrope-almandine garnet using standard gem-testing methods.

Recently, we were asked to look at a colorless, transparent oval mixed cut (figure 7), which weighed 1.48 ct and measured $9.31 \times 7.09 \times 4.05$ mm. The stone was initially represented to K & K International of Falls Church, Virginia, as oligoclase feldspar from Sri Lanka. The gemological properties of this stone were typical for plagioclase feldspar in the albite-oligoclase compositional range. Its three refractive indices were $\alpha = 1.531$, $\beta = 1.534$, and $\gamma = 1.541$, yielding a birefringence of 0.010. The optic character and sign were biaxial positive. The specific gravity, as determined hydrostatically, was 2.62 (average of three measurements). The stone was inert to both long- and short-wave UV radiation. When it was viewed with a microscope in polarized light, lamellar twinning was obvious (figure 8); this feature was similar to that commonly seen in plagioclase.

To confirm the stone's identity, we analyzed it with the laser Raman microspectrometer. We were surprised when the Raman spectrum indicated that this colorless
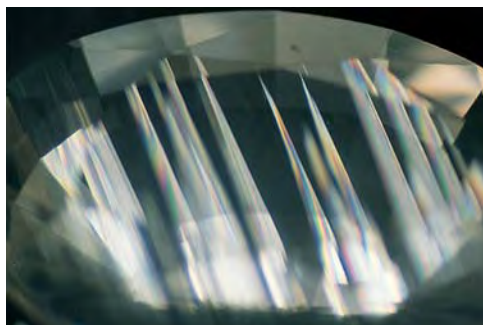
Figure 8. In polarized light, the colorless iolite showed obvious polysynthetic twinning. These two views illustrate the sample at slightly different orientations. Photomicrographs by John I. Koivula.
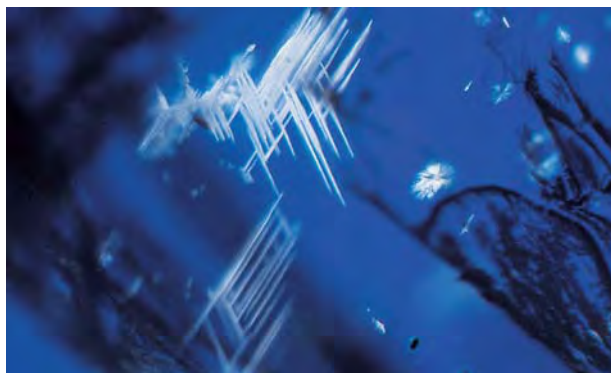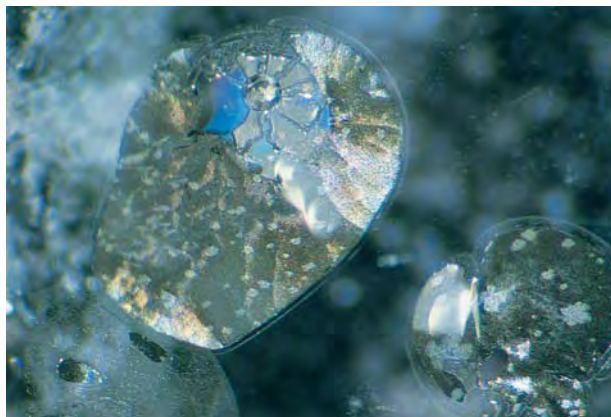

Figure 9. Areas of polysynthetic twinning were also observed in the iolite block shown in figure 7. Photomicrograph by John I. Koivula; polarized light, magnified 20×.

gem was cordierite (iolite). Three different areas of the stone were tested, all with the same result. To corroborate this identification, we performed Raman analysis on an 18.49 ct rectangular block of blue iolite (also shown in figure 7). On the basis of the results obtained, there is no question that the colorless stone is cordierite and not a feldspar, even though the gemological properties of this stone would be consistent with either gem material.

Although lamellar or polysynthetic twinning of cordierite is not mentioned in gemological texts, mineralogy texts do list this structural property as a common feature. For example: "Cordierite may show polysynthetic twinning and birefringence resembling that of plagioclase" (W. R. Phillips and D. T. Griffen, *Optical Mineralogy, the Nonopaque Minerals*, 1981, W. H. Freeman and Co., San Francisco, p. 168). In fact, the blue iolite sample that we used as a Raman standard also showed excellent twinning in polarized light (figure 9).

Because plagioclase and cordierite have similar gemological properties, it is quite possible that these gems could be misidentified, especially samples from a locality that hosts both gem minerals (e.g., Sri Lanka, India, and Madagascar).

New features of Montana sapphires: Gold is where you find it. Since 1992, Marc Bielenberg of Hamilton, Montana, has been involved in an extensive sapphire sampling project on the main drainage and both forks of Montana's Dry Cottonwood Gulch. Those gem-quality, water-worn crystals that were deemed suitable for heat treatment were visually separated from the "rejects,"

Figure 10. Rounded, metallic grains of pyrrhotite are surrounded by decrepitation halos in this sapphire from Dry Cottonwood Creek, Montana. Photomicrograph by John I. Koivula; magnified 25×.

Figure 11. This crystal of clinozoisite in sapphire from Dry Cottonwood Creek displays perfect cleavage; it also hosts a smaller unidentified rod-shaped inclusion. Photomicrograph by John I. Koivula; magnified 35×.

which were mostly smaller stones of apparent lower quality. These reject stones were stored for several years without any further examination.

During the 1997–1998 winter season, when mining activity had ceased, Mr. Bielenberg decided to examine the reject sapphires more closely. While searching for interesting or unusual inclusions, he discovered what later were proved to be (by Raman analysis and X-ray powder diffraction) mineral inclusions of pyrrhotite (figure 10) and clinozoisite (figure 11), which were not previously known as inclusions in Montana sapphires.

A real surprise, however, was the discovery of microscopic grains of gold in the crevices, pits, and cracks of some of these sapphires. The gold had the form of tiny water-worn nuggets (figure 12) rather than flakes. In no instance was gold observed as an actual inclusion in any of these sapphires. Mr. Bielenberg observed gold on the surfaces of 135 of the 600–700 stones he examined. Most of these stones had only one microscopic nugget; the most gold particles found on any one stone was four. Higher magnification shows that, at least in some instances, the gold appears to have been smeared by friction across the surface and into cracks and crevices (inset, figure 12). To confirm the identification, energy-dispersive X-ray fluorescence analysis by Sam Muhlmeister of GIA Research resolved a gold peak from each of two different sapphires.

Because the gold can be removed from the surface of the sapphires with a small probe, it is evident that the grains are not strongly bonded to the sapphires. Apparently, the gold was naturally wedged in place as the stone was moving through its alluvial environment. This discovery suggests that the Dry Cottonwood Creek area might also have potential for gold recovery.

Highly translucent green serpentine from Afghanistan. Franck Notari of GemTechLab in Geneva, Switzerland, provided contributing editor Emmanuel Fritsch and the gemology laboratory at the University of Nantes with several highly translucent yellowish green beads (figure 13). These poorly polished beads came from necklaces that were reportedly purchased in Afghanistan. One bead was sawn in two and polished for gemological testing. Refractive index measurements varied between 1.563 and 1.567, and the specific gravity (determined hydrostatically) was 2.55 ± 0.05. These data are typical for serpentine. Further testing was required to identify the particular species in the serpentine "subgroup" of the kaolinite-serpentine mineral group. Energy-dispersive spectroscopy, with the University of Nantes SEM-EDX system, showed the presence of oxygen, magnesium, and silicon, with lesser amounts of aluminum and iron. (Although oxygen can be detected with this system, hydrogen cannot.) The X-ray diffraction pattern was an excellent match for a monoclinic polytype of antigorite, antigorite-6M, which is a serpentine mineral. The chemical formula usually quoted for antigorite is

Figure 12. A cluster of gold micronuggets is visible in a surface depression on this sapphire from Dry Cottonwood Creek. Photomicrograph by John I. Koivula; magnified 15×. The inset shows a small particle of gold that appears to have been smeared into the surface of the sapphire. Photomicrograph by John I. Koivula; magnified 40×.

$(Mg,Fe^{2+})_3Si_2O_5(OH)_4$; the yellowish green color is probably caused by the iron present.

Etch-decorated topaz. Two interesting samples of colorless topaz were recently sent to the Gem News editors for photodocumentation and gemological investigation of their inclusions (figure 14). Bill Larson, of Pala International, Fallbrook, California, reported that both samples were from the Mogok region of Myanmar.

The cabochon was thought to contain inclusions of the mineral goethite (an iron oxyhydroxide), as suggested by the brown color and acicular habit. When these inclusions were viewed with magnification, however, their

Figure 13. These unusually translucent yellowish green beads, reportedly from Afghanistan, are antigorite, a serpentine mineral. Photo by A. Cossard.

Figure 14. The 26.31 × 20.08 × 13.24 mm (62.68 ct) cabochon of colorless topaz contains etch channels filled with yellowish brown limonite. The crystal (73 mm long) also contains numerous etch channels, but these do not show any evidence of staining. Courtesy of Bill Larson; photo by Maha DeMaggio.

appearance was identical to the so-called "rutilated" topaz that was described and documented in the Summer 1987 issue of *Gems & Gemology* (J. Koivula, "The rutilated topaz misnomer," pp. 100–103). Although the inclusions in the topaz crystal were identical in shape to those in the cabochon, they were colorless. All the inclusions in both samples appeared to reach the surface of their host topaz.

In the earlier *Gems & Gemology* article, Brazilian "rutilated topaz" was actually shown to contain ribbon-shaped (to somewhat more prismatic) etch channels that were stained by limonite. The channels probably formed as surface-reaching fissures during growth of the topaz and were significantly enlarged through later etching by corrosive hydrothermal fluids. The "earthy" yellowish brown limonite was later deposited in the channels by iron-rich groundwaters. Therefore, although the inclusion channels co-existed with the growth of the topaz, the filled inclusions developed after the crystal had formed; these were not solid mineral inclusions that grew at the same time as the topaz. (The channels would be colorless if they were not stained or filled with epigenetic material.) The colorless channels present near the termination of the topaz crystal in figure 14 indicate that this particular crystal may not have been exposed to the same epigenetic solutions that entered the stone from which the cabochon was cut; or perhaps the iron-rich stains were removed during cleaning of the specimen.

Red, pink, and bicolored tourmaline from Nigeria. Tourmaline from Nigeria has been known in the gem trade since at least the middle 1980s (see, e.g., Gem News: Spring 1988, p. 59; Spring 1989, p. 47; Spring 1992, p. 62). These stones originated from tin-bearing pegmatites in Kaduna State, as well as from a pegmatite belt southeast of Kaffi in central Nigeria (J. Kanis and R. R. Harding, "Gemstone prospects in central Nigeria," *Journal of Gemmology*, Vol. 22, No. 4, 1990, pp. 195–202). Gem-quality green, red, pink, and bicolored tourmalines have been recovered. Recently, contributing editor Karl Schmetzer provided information on a new tourmaline find in Nigeria.

In summer 1998, Nigerian traders at Idar-Oberstein offered large parcels of gem tourmaline from a locality west of the town of Ogbomosho, near the border with the country of Benin. More than 100 rough crystals and 10 faceted stones were loaned to Dr. Schmetzer by Karl

Figure 15. These tourmaline crystals come from a new find in Nigeria. Red, pink, colorless, and green zones are typical, but grayish blue zones were also seen. The largest crystal, on the left, measures 49 mm long and 13.5 mm across. Courtesy of Karl Egon Wild Co.; photo by M. Glas.

Egon Wild Co. (Kirschweiler) and Julius Petsch Jr. Co. (Idar-Oberstein). Dr. Schmetzer described the crystals as prismatic in habit (figure 15), with trigonal prism faces *m* {01$\overline{1}$0} and hexagonal prism faces *a* {11$\overline{2}$0}; the dominant trigonal pyramid faces were *o* {02$\overline{2}$1}, sometimes in combination with ditrigonal pyramid *x* {12$\overline{3}$2} faces. The relative size of the terminal face, or pedion, *c* (0001) varied from small to large (figure 16).

Most of the crystals were color zoned purplish red to pink to nearly colorless. In some samples, the growth zones adjacent to the pedion (parallel to the pyramid faces) were medium to intense yellowish green or green; rarely, this end of a crystal was bluish gray (again, see figure 15). The pleochroism for the red and pink zones was colorless to medium pink parallel to the c-axis, and intense pink to red perpendicular to the c-axis. For green zones, it was light yellowish green parallel to the c-axis, and intense yellowish green or green perpendicular to this axis. For the bluish gray zones, pleochroism was light grayish blue parallel to the c-axis, and intense grayish blue perpendicular to this axis.

The faceted stones were evenly colored red or pink (figure 17), bicolored green and pink (and, rarely, blue and pink), or color zoned in various shades of red and pink. The refractive indices and specific gravities varied within relatively small ranges: n_ω = 1.640 and n_ϵ = 1.620 (both ± 0.002); specific gravity = 3.05 ± 0.02. On the basis of visible absorption spectroscopy, Dr. Schmetzer determined that Mn^{3+} was the dominant chromophore in the red and pink samples.

TREATMENTS

On the burning of polymer-impregnated synthetic and natural opals. In polymer-impregnated gem materials (e.g., opal, turquoise, and jade), the question sometimes arises as to how much polymer is present. This is especially a cause for concern with opal, since the refractive index and specific gravity values of the polymer compound(s) commonly used are so similar to those of the opal itself. Furthermore, the two materials are not easily distinguished by visual examination, even with the microscope. Consequently, the amount of polymer present is generally unknown, and might constitute a significant portion of the weight of a sample.

In addition, the Materials Safety Data Sheets provided with polymers state that many are flammable. To study this possible durability concern, as well as to investigate the amount of polymer present in some natural and synthetic opals, Gem News editor Mary Johnson and GIA Gem Trade Laboratory staff gemologist Maha DeMaggio destructively tested seven samples by burning them. Since heat drives off both water and volatile organic materials (such as some of the breakdown products of heated polymers), the approximate amount of these substances present can be measured by weighing the sample before and after heating. Although this test would not be
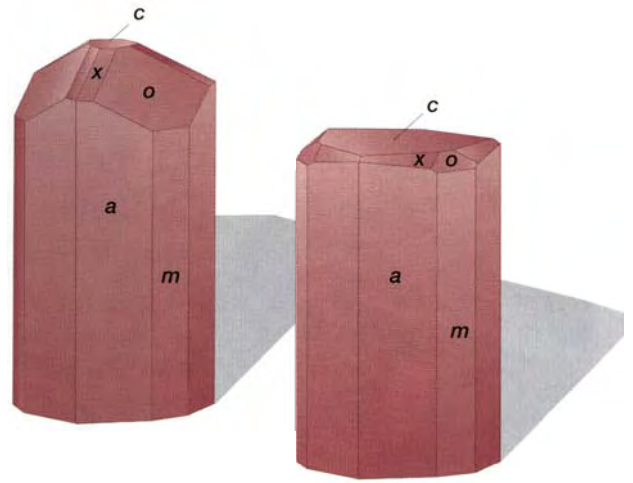
Figure 16. These schematic drawings illustrate the crystal faces seen on the tourmaline crystals recently found in Nigeria. Variations in the size of the pedion c *(0001) face primarily account for the differences in morphology between the two crystals. After drawings by Karl Schmetzer.*

applied in the course of routine gem testing, it does provide some idea of the potential weight component of the polymer in such treated synthetic opal (which, based on earlier research, appears to be largely anhydrous).

The samples used were: one (untreated) "white" Gilson synthetic opal (2.43 ct), one (untreated) "black crystal" Gilson synthetic opal (1.13 ct) [Gilson synthetic opals are not polymer-treated, in our experience], four polymer-impregnated synthetic opals (0.21, 0.65, 1.39, and 8.14 ct), and one polymer-impregnated natural opal

Figure 17. Attractive faceted stones are being cut from the new find of Nigerian tourmaline, such as this 21.10 ct rectangular cushion. Courtesy of Bill Larson; photo by Maha DeMaggio.
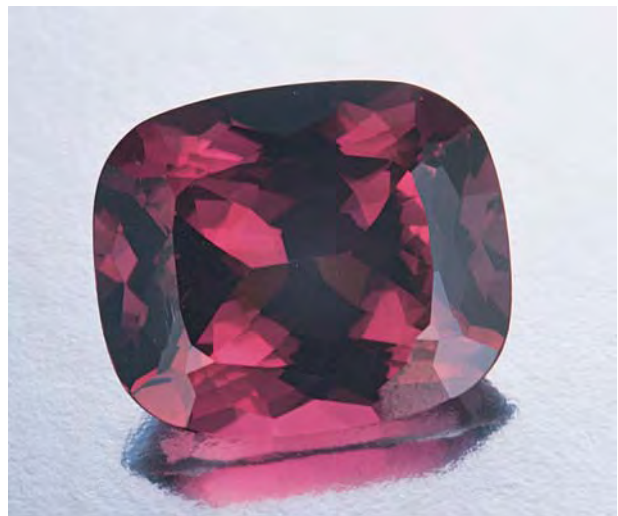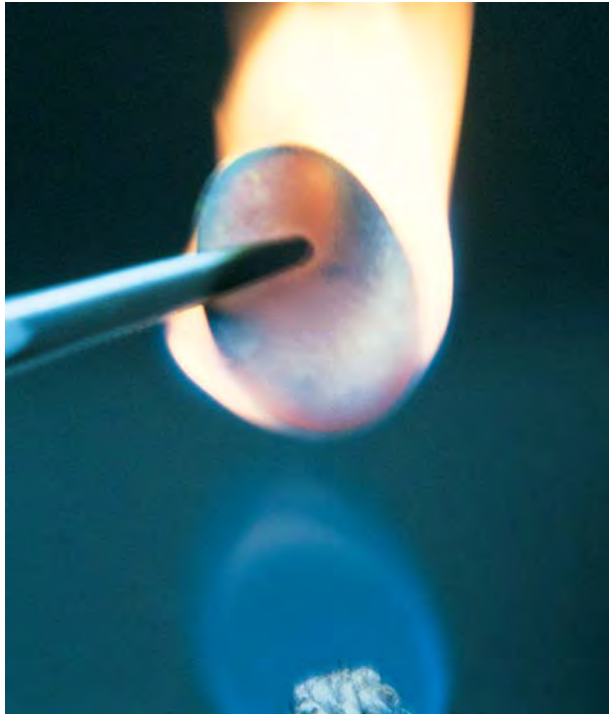
Figure 18. This 8.14 ct polymer-impregnated synthetic opal burned readily in the flame of an alcohol burner. Photo by Maha DeMaggio.

from Brazil (1.14 ct). We attempted to ignite each sample using a match or an alcohol burner; this was done in a fume hood, to avoid exposure to (possibly toxic) combustion gases.

All the polymer-impregnated samples caught fire readily (figure 18), and they continued to burn when removed from the flame. The four polymer-impregnated synthetic opals lost 16%–27% of their weight by burning, with an average weight loss of 21%. Because the resulting residue broke apart easily, we did not attempt

Figure 19. After burning, droplets of charred polymer residue can be seen on the surface of this impregnated synthetic opal; a network of cracks is also visible. Photomicrograph by John I. Koivula; magnified 20×.

to burn the samples all the way through, so these values represent the minimum weight of the polymer in these samples. Subsequent microscopic examination showed deep cracks throughout, as well as charred droplets of exsolved polymer (figure 19). The impregnated natural opal also burned, although somewhat less readily. Because this stone broke apart during examination, weight loss from the burning alone could not be determined. The two Gilson synthetic opals (which had not been polymer-impregnated) reacted the least: The "black crystal" synthetic opal appeared unchanged, while the "white" opal became more transparent. Neither lost weight or caught fire.

In a previous examination of polymer-impregnated synthetic opals ("Kyocera plastic-impregnated synthetic opals," Summer 1995 Gem News, pp. 137–139), we reported the results of heating experiments performed by Jeffery Bergman in Bangkok, who found weight losses of about 20% at 600°C. The results of the simple pyrolysis test reported here are consistent with this finding.

In the 1995 study, scanning electron microscopy revealed that Kyocera polymer-impregnated synthetic opal contains organized aggregates of small silica spheres, as does natural opal. The polymer may stabilize the silica lattice and improve both the durability (under normal wear conditions) and clarity of the synthetic opal. However, the flammability hazard that is now introduced may be a consideration for the wearer of such a piece, as well as for the jeweler (although we would not expect a jeweler to use direct flame in the vicinity of an opal).

Irradiated inclusions in topaz. At the 17th IMA meeting in Toronto, Ontario (reported above), I. L. Komov (State Science Centre of Environmental Radiogeochemistry, Kiev, Ukraine) reported that colorless halite (NaCl), sylvite (KCl), and villiaumite (NaF) crystals in fluid inclusions became yellow, "lilac-colored," and brown, respectively, when exposed to gamma radiation (the host mineral was not specified). Over a decade ago, in 1987, the late Charles Ashbaugh, then at UCLA and collaborating with GIA in Santa Monica, examined one such example. The core of a colorless sylvite in a fluid inclusion in a Nigerian topaz became purple after exposure to ionizing radiation from a linear accelerator ("linac" treatment; figure 20). (The sylvite identification was confirmed by Chuck Fryer of GIA GTL, using X-ray powder diffraction analysis.) The topaz itself turned blue. At the time, Mr. Ashbaugh and John Koivula speculated that the presence of such purple crystal inclusions might prove that a topaz had been irradiated, as sylvite crystals in natural-color near-colorless and brown topaz are near-colorless. Unfortunately, this project was never pursued. However, Dr. Komov's IMA presentation supports these earlier findings. For more on irradiated gems, see C. E. Ashbaugh III, "Gemstone irradiation and radioactivity," *Gems & Gemology*, Winter 1988, pp. 196–213.
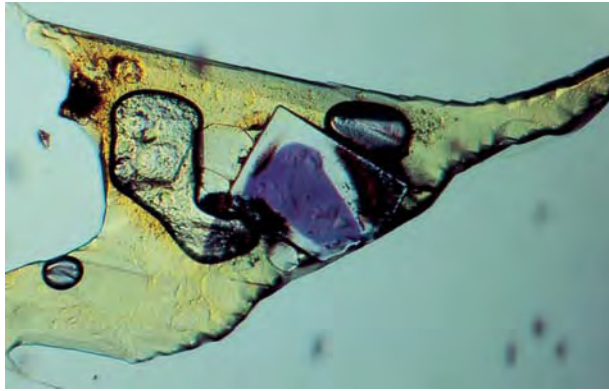
Figure 20. In this linear-accelerator-treated piece of blue topaz, a fluid inclusion contains several phases. The core of the colorless sylvite crystal turned purple from the irradiation. Photomicrograph by J. I. Koivula; magnified 80×.

SYNTHETICS AND SIMULANTS

Obsidian imitation. On a visit to Idar-Oberstein, Germany, one of the editors (JIK) found an attractive glass sphere in one of the many gem and jewelry shops that make this area famous. Represented as "obsidian from Russia," this well-polished sphere was relatively large (approximately 9 cm in diameter) and opaque. The sphere was predominantly a mottled brownish green, with a diffused stripe of lighter green to grayish green through the center. Perhaps the most distinctive feature, however, was the presence of numerous spherical inclusions with a silvery metallic luster that appeared as circles scattered over the entire surface. These inclusions ranged from well under a millimeter to just over 3 mm in diameter. If in fact this object was a natural glass, then it was certainly unusual. The sphere's cost however, made its acquisition for scientific examination impractical.

This "problem" was solved shortly thereafter with the discovery by this editor of a partially polished piece of the distinctive glass in a box of cutting scraps and crystal fragments at the shop. This piece weighed about 213 grams and measured 8.3 cm on its largest dimension (figure 21). It had one large, flat, polished surface, while the opposite side was "rough." The botryoidal appearance, flow structure, and bubble pits on the unpolished surfaces made it obvious that this was not obsidian or any other form of natural glass. It was apparent that this large mass, and the sphere that had been fashioned from the same material, were a form of slag (manufactured) glass.

The refractive index of this glass was 1.606. It showed no fluorescence to UV radiation. No absorption spectrum was visible with incident illumination. The specific gravity was determined hydrostatically to be 2.99, although it was undoubtedly influenced by the numerous metallic-appearing inclusions present.

Chemical analysis showed that this glass contained several elements in addition to the expected silicon. EDXRF chemical analysis (by Sam Muhlmeister of GIA Research) showed the presence of barium, calcium, copper, iron, manganese, potassium, rubidium, strontium, and titanium. A few small fragments were broken off the sample so that the spherical metallic inclusions could be extracted, cleaned, and analyzed separately by EDXRF. These proved to contain primarily manganese, possibly as an oxide.

Diffusion-treated synthetic sapphire. Contributing editor Karl Schmetzer has sent word that greater quantities of diffusion-treated *synthetic* sapphires are showing up on the market in Bangkok, Thailand. Diffusion-treated natural sapphires have been known in the trade since the late 1970s (see, e.g., R. E. Kane et al., "The identification of blue diffusion-treated sapphires," *Gems & Gemology*, Summer 1990, pp. 115–133), but large quantities again became available in recent months. One diffusion-treated synthetic blue sapphire was mentioned as early as 1982 (Summer 1982 "Lab Notes," p. 107), but the treater of that sample might not have known that it was synthetic. The first notice that larger parcels of synthetic sapphires were being treated in this fashion was issued in 1992 (R. C. Kammerling et al., *ICA Laboratory Alert No. 55*, June 2, 1992). Recently, similar large parcels were offered in the Bangkok market, and the appearance of this material at other trading sites is only a matter of time.

Five faceted samples, submitted by gem dealer M. Steinbach, were made available to Dr. Schmetzer for examination. They were comparable in color to good-quality natural sapphire of Sri Lankan origin. Absorption spectroscopy showed that the color of the samples was due to Fe^{2+}/Ti^{4+} charge transfer, which is also common for natural blue sapphire.

No inclusions or growth patterns that are typical of natural stones were observed in any of these samples

Figure 21. Represented as obsidian from Russia, this decorative glass proved to be manufactured. Photo by Maha DeMaggio.

Figure 22. The uneven color distribution between facets and the color concentrations along facet junctions—both typical of diffusion-treated sapphire—are best seen with the samples immersed in methylene iodide. The dark spots on four of the samples are cavities that were found to be filled with synthetic sapphire. Photo by M. Glas.

Figure 23. A dark-blue-appearing synthetic sapphire crystal is seen within a cavity on the surface of this diffusion-treated synthetic sapphire. Photomicrograph by Karl Schmetzer; magnified 50×.

when viewed with the microscope. Two of the samples revealed a number of tiny gas bubbles, indicating that they were Verneuil-grown synthetic sapphires. However, Dr. Schmetzer did not observe any of the curved color banding that is also typical of Verneuil-grown synthetics, and would have been expected if the color were inherent in the material (instead of being due to diffusion treatment).

As described in the references cited above, the diffusion treatment of either natural or synthetic sapphires can be identified (often macroscopically) when the sample is immersed in methylene iodide (or observed using diffuse transmitted white light). This was the case for the present samples, all of which showed an uneven coloration from one facet to the next (figure 22). This pattern is caused by variation in the thickness of the diffusion layer on different facets that results from the repolishing that is always necessary after diffusion treatment. In most of the samples, a greater color concentration was also observed along facet junctions (also visible in figure 22). Four of the samples had cavities on the surface that were filled with a dark-blue-appearing solid material (figures 22 and 23). In two of these samples, some of the cavities were only partially filled. With SEM-EDX analysis, Dr. Schmetzer found that the material in each cavity was actually a tiny synthetic sapphire crystal.

ANNOUNCEMENTS

Indonesian South Sea Pearl auction. Philmore USA and PT Philmoremas have organized a group of Indonesian South Seas pearl producers, whose harvests will be sold at ISSPA 1999. This is the first such auction to be held, and will occur on February 8–9, 1999, at the Hong Kong Convention and Exhibition Centre. For further information, contact Philmore USA representative Stephen
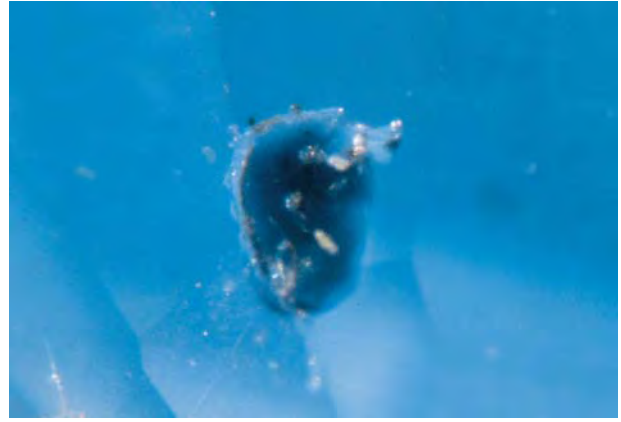
Church at 836 Woodshire Lane K-6, Naples, Florida 34105; phone 941-263-9371; FAX 941-263-9371; e-mail schurch241@aol.com.

Congratulations to *Gems & Gemology* authors Kurt Nassau, James E. Shigley, and Shane McClure. Their Winter 1997 article "Synthetic moissanite: A new diamond substitute" won a Certificate of Achievement from the American Society of Association Executives 1998 Gold Circle competition. This is the 10th award that *Gems & Gemology* has won in this competition since 1992.

Note. The entry "'Wild Life' assembled natural gemstone cabochons" in the Fall 1998 Gem News section was contributed by Emmanuel Fritsch.

ERRATA:

1. *The photograph of Dr. George Rossman and Richard T. Liddicoat in the Fall 1998 Gem News (p. 230, figure 23) was taken by Judy Colbert.*

2. *In the Fall 1998 Gem News entry "Color-change pyrope-spessartine garnet, also from Madagascar" (pp. 222–223), the positions of the UV-visible absorption bands were listed incorrectly. The correct wavelengths for the Mn^{2+} bands are 408, 413, 422, and 483 nm, and the Fe^{2+} bands are at 459 and 503 nm.*

3. *On p. 164 of the Hemphill et al. article "Modeling the Appearance of the Round Brilliant Cut Diamond: An Analysis of Brilliance" (Fall 1998), the source for the information given in table 3 on the European Gemological Laboratory (EGL) should have been listed as Federman, 1997.*

Book Reviews

Susan B. Johnson & Jana E. Miyahira, Editors

BULGARI

By Daniela Mascetti and Amanda Triossi, 225 pp., illus., publ. by Abbeville Press, New York, NY, 1996. US$75.00*

Bulgari is a welcome addition to the growing body of jewelry history literature. Not only are the luscious photos of sumptuous jewels a feast for the eyes, but the book is also a lucid and thorough portrayal of this prominent jewelry company.

Each of the 12 chapters focuses on a specific aspect in the development of Bulgari's distinctive style. Chapter one traces the history of the Bulgari firm from its modest beginnings in a small Greek village near the Albanian border to international success by following the life of Sotirios Bulgari, the founder of the firm. Sotirios, the only surviving child of a Greek silversmith, was born in 1857. His steady progress from silversmith to fine jeweler was the base on which the Bulgari firm was built. This chapter also shows how each successive generation contributed to the growth of Bulgari and describes some of their important clients and significant jewelry sales.

The next chapter, The Evolution of the Bulgari Style, demonstrates Bulgari's transition from following jewelry fashion (between 1920 and 1950) to leading it (from the 1960s to the present). We are shown how Bulgari designers introduced smooth, rounded elements that gave a sense of volume to their jewelry and incorporated colored gemstones for chromatic effect. Bulgari also chose to use more yellow gold for important pieces, in response to their customers' desire for jewelry that could be worn at any time of day and for any occasion.

The authors go on to address three important design innovations introduced by Bulgari that are now part of their signature style: the integration of ancient coins in jewelry, the use of modules, and the use of a flexible band called a *tubogas*. During the 1960s, Bulgari revived the style of setting ancient coins in jewelry, which had been out of fashion since the end of the 19th century. The company also introduced the concept of using modules—simple, interlocking elements made of precious metals and/or carved gems assembled in different combinations to make necklaces, earrings, bracelets, and rings. The *tubogas*, named for its resemblance to a gas-pipe, is a flexible band of interlocking thin strips made without solder, used by Bulgari for collar necklaces, bracelets, watch bands, and rings.

Manufacturing aspects include discussion of the sense of volume that is built into each piece with metalwork and gems, the selection and cut of gemstones used by Bulgari, and the production of their jewelry, from design concept to finished product. These chapters are particularly interesting for the jeweler/gemologist. Each of Bulgari's line of luxury items has its own chapter: Silver and Precious Objects, Watches, and Perfumes. The book closes with a chapter titled the Bulgari Image, which is an enlightening examination of how Bulgari has carefully crafted the image they present to the public through advertising and store design.

The authors and the art director deserve special merit for the visual impact of this book. The jewelry is laid out and photographed so the reader can truly appreciate its magnificence, and many important jewels are shown from front *and* back to illustrate the beautiful gallery work and clasps. Also, close-up details provide an immediate understanding of Bulgari's manufacturing excellence.

The exceptional illustrations and the in-depth text make this book a useful reference for jewelry historians, collectors, and appraisers. Yet it is also an enjoyable read for anyone interested in a taste of luxury.

ELISE B. MISIOROWSKI
Jewelry Historian
Los Angeles, California

COLLECTING AND CLASSIFYING COLORED DIAMONDS: An Illustrated Study of the Aurora Collection

By Stephen C. Hofer, 742 pp., illus., publ. by Ashland Press, New York, NY, 1998. US$300.00*

This heavy, lavishly illustrated book delivers more than 700 pages on the various aspects of colored diamond collecting, with an emphasis on the observation, determination, and classification of a stone's color. The book is based on the 260 stones of the Aurora collection, which has been displayed at the American Museum of Natural History in New York.

A brief introduction precedes a catalog of the entire Aurora collection. Each gem is illustrated, and its weight, dimensions, shape, cutting style, and color description indicated. Following the catalog is a concise discussion of important considerations in colored diamond collecting. Rarity is addressed at some length, as it is pivotal to the estimation of value. This naturally leads to a discussion of value, which is illustrated by a table of auction prices according to diamond color. Then the major section devoted to color begins, with comments first on color observation and

grading, then on how to determine face-up color (see below). The longest of the 12 chapters (at nearly 200 pages, a book in itself) is devoted to color classification. It is organized by color (white, gray, black, purple, pink, red, orange, brown, yellow, "olive," green, blue, and colorless) and emphasizes the various nuances. Three appendices complete the book: (1) cut and color determination graphs; (2) a glossary and an extensive bibliography; and (3) a list of diamonds sold at auction, classified by color.

This is clearly not a book on colored diamonds in general, as it is strongly biased toward collecting and classifying. One feels that the book was written for the pleasure of sharing knowledge, rather than as a scholastic or scientific treatise. As such, it fulfills its purpose remarkably well. The collector will find all sorts of interesting information, as well as attractive color photographs that can also be used for reference.

The book's size (approximately 32 × 24 × 6 cm, or $12\frac{1}{2} \times 9\frac{1}{2} \times 2\frac{1}{2}$ inches) and cost may be intimidating to some, but the overall quality of the production is excellent. The 700-plus color photos, a number of them by world-renowned photographer Tino Hammid, are of high quality, as are the numerous line drawings and color sketches. One of the great merits of this book is that the photos of groups of colored diamonds include a colorless diamond for visual reference. One wishes this could have been done for the catalog section; although pictures of colorless diamonds are available for comparison, these photos were not necessarily taken under the same conditions as those of the colored diamonds.

The text is easy to read, even when it comes to the more delicate aspects of color science (such material was enhanced by contributions from Nick Hale, a professional color scientist). Mr. Hofer should be commended for his remarkable bibliography, which provides an excellent base for further research. References

to other authors are numerous and offer a welcome support to the text.

The value of the text is limited, however, by the fact that Mr. Hofer makes no particular effort to compare his views with those of major players in the field. For example, the use of the catalog as a reference for collectors is significantly limited by the fact that it does not provide GIA color grades (although, as most auction houses and colored diamond dealers agree, this is the most widely accepted color grading system in the industry today). The author offers his own system to estimate color, with new concepts such as the CAMP ("colour-area micro pattern") and the weighted average face-up color, but the relationship between these parameters and the color terms used to describe the diamonds is not clear. Mr. Hofer also insists on giving each of the Aurora collection stones a common name, but such qualifiers as *jade*, *heliotrope*, "*manilla*," and *lead* are uncommon for colored diamonds, to say the least.

This beautiful, well-documented book is certainly a must-have for gem book and colored diamond collectors. Its superb documentation base will be an asset for scholars as well. However, in addition to the idiosyncrasies in the discussion of color, the fact that there is little on practical concerns such as the separation of natural from treated or synthetic colored diamonds in this work makes it less useful for the gemologist outside the collector community.

EMMANUEL FRITSCH
Institut des Matériaux de Nantes
Nantes, France

THE NATURE OF DIAMONDS

Edited by George E. Harlow, 278 pp., illus., publ. by Cambridge University Press, New York, NY, 1998. US$29.95* (softbound)

The Nature of Diamonds is the companion text for a special American Museum of Natural History exhibi-

tion of the same name. Its stated focus is to provide a well-illustrated overview of the diverse topics related to diamond. It is successful in this endeavor—both in content and in illustration.

In *The Nature of Diamonds*, leading scientists, gemologists, and cultural observers cover virtually every aspect of this cherished gem. The reader experiences a panoramic view, ranging from how diamonds form to their economic, social, and technological incarnations. Whether your interest in diamonds leans toward the romantic, the symbolic, or the scientific, you will enjoy the diversity of subject matter and the expanse of photos and illustrations.

Individual essays address three broad categories: science, history, and utility. Beginning with the science of diamonds, chapters examine diamond's unique mineralogy, the causes of color (both natural and artificial), the extreme environments required for formation, and a global timeline of sources and production. Subsequent chapters explore the role of diamonds throughout history, their diverse mythology and literary presence, and their evolving cultural status. Remaining chapters highlight diamond mining and processing, provide a brief excursion into the gemologist's world of identifying and grading gem diamonds, and give insights into the role of diamonds in modern technology.

Additional sections encompass a pictorial guide to the world's greatest diamonds and the diamond treasures of Russia. Two monographs cover the history of diamond cuts and the fascinating story behind the evolution of today's symbol of love and marriage, the diamond ring. Each chapter includes an ample bibliography.

The book's editor (and one of the subject specialists) characterizes *The Nature of Diamonds* as an overview of the expansive world of diamonds. However, it accomplishes far more than his modest statement might convey. This compendium of essays

penned by renowned experts, punctuated with numerous illustrations and photographs, and packaged with valuable bibliographical references, is an important resource for any library.

Whether you cherish diamonds for their status, their economic and social legacy, or their unique scientific applications, you will be entertained and enriched by *The Nature of Diamonds*.

SHARON WAKEFIELD
Northwest Gem Lab
Boise, Idaho

GLOSSARY OF GEOLOGY, 4th Edition

Edited by Julia A. Jackson, 769 pp., publ. by the American Geological Institute, Alexandria, VA, 1997. US$110.00

Over the past few decades, the scope of gemology has expanded considerably, particularly in the areas of geology and analytical techniques. As a result, today's gemologist needs a more solid technical vocabulary than ever before. For geology and related fields (e.g., geophysics), the *Glossary of Geology* has been the best available dictionary of specialized terms in English since its first edition was published in 1957. The fourth edition continues this tradition of excellence. The *Glossary* now contains about 37,000 entries, of which 3,400 are new and 9,000 have been updated, expanded, or revised since the publication of the third edition only 10 years ago.

The 4,000-plus mineral names constitute the largest single group of entries in the *Glossary*. Therefore, it is not surprising to find such terms as *benitoite, californite, chrysoprase, demantoid, rhodolite,* and *tanzanite*, although some gem variety names such as *tsavorite* are not included. Among the more traditional gemological terms, *diaphaneity, enhancement, melee,* and *Tolkowsky theoretical brilliant cut* do appear, but manufactured materials such as cubic zirconia, GGG, and YAG are grouped together under *diamond simulant*.

There are also entries for most of the analytical techniques likely to be encountered by gemologists, such as infrared absorption spectroscopy, Raman spectrometry, and X-ray fluorescence (XRF) spectroscopy; only ED[energy dispersive]XRF was not present from among my arbitrary selection of terms.

Without hesitation, I recommend this *Glossary* to all gemologists as the most authoritative work of its type in English. Given the history of the *Glossary* and the size of this fourth edition, it is not likely that another edition will appear for at least a decade, which makes this volume a good long-term investment.

A. A. LEVINSON
University of Calgary
Calgary, Alberta, Canada

GEM AND JEWELLERY YEAR BOOK 1997–98

Edited by V. V. Kala and A. Kala, 697 pp., illus., publ. by International Journal House, Jaipur, India [diaworld@jpl.vsnl.net.in], 1998. US$35.00 (surface), US$50.00 (air)

Thirty-five years ago, India was an insignificant player in the diamond world, constituting less than 5% of any aspect of the industry. Today, it dominates in the manufacturing sector by virtue of its production of about 40% by value and 70% by weight of the world's polished diamonds, and by being home to at least 90% of the world's diamond cutters and 20% of De Beers's sightholders. Further, India-based companies are garnering strength in downstream jewelry manufacturing and retailing. The gem and jewelry industry is now a vital component of the national economy, having become India's second-largest source of foreign exchange—at 18%, surpassed only by textiles. How did this all occur? How do Indian diamantaires view the industry? And, what is the prognosis for India's influence on the diamond industry in the next millennium?

These are not easy questions to

answer, but some indications can be gleaned by perusing *Gem and Jewellery Year Book 1997–98*. Now in its 19th year of continuous publication—primarily for the gem and jewelry industry in India—this sourcebook is little known elsewhere. It is primarily concerned with the diamond industry, a reflection of the fact that polished diamonds account for the bulk (93%) of India's gem and jewelry exports.

The book is divided into three parts. Part I (358 pp.) covers a vast amount of material from the mining to retailing of diamonds. Topics include: a review of recent highlights in the Indian diamond industry; industry statistics that are difficult to obtain elsewhere; descriptions, with photographs, of new Indian-made manufacturing tools and technology; a "Who's Who," with brief profiles and photographs, of 171 Indian gem and jewelry luminaries worldwide; and glimpses of 38 world diamond mining and consuming countries from an Indian perspective. Part II (132 pp.) consists of nine appendices, ranging from a list of worldwide gem and jewelry organizations to a listing of India's diplomatic and trade representatives abroad. Part III (198 pp.) contains lists (with addresses and specialties) of over 3,500 selected international exporters and importers—from 55 countries—for gemstones, jewelry, pearls, and synthetic stones.

This volume clearly indicates that India has built up a formidable gem and jewelry infrastructure, particularly with respect to diamonds. It is also clear that the Indian diamantaires have the knowledge, finances, and ability to expand their influence. Those in the international gem industry who choose to ignore this unique and valuable handbook, with its wealth of information and subliminal implications, do so at their own risk.

A. A. LEVINSON
University of Calgary
Calgary, Alberta, Canada

Gemological
ABSTRACTS

COLORED STONES AND ORGANIC MATERIALS

The color of money. M. Lurie, *Colored Stone*, Vol. 11, No. 3, 1998, pp. 42–44, 46, 48, 50.

Besides being a source of national pride and Colombia's fifth-largest export commodity, emerald represents a livelihood for an estimated 300,000 people in Colombia. With the pending creation of an emerald bourse, the government is hoping that increased demand (which has been down in recent years) will push Colombian emerald exports into the same class as the country's coffee and oil exports.

In light of these high expectations, the article discusses the production capabilities of Colombia's top three emerald mines: Muzo, Cosquez, and Chivor. Muzo and Cosquez have historically been the richest mines, with Cosquez producing more than Muzo in recent years. Chivor's potential, though, is still largely untapped, and it has turned out some exceptionally high-quality material. Chivor specifically has benefited from modernized methods and foreign investment. *Stuart Overlin*

Opals: Gems of lore and luster. G. Butler, *Rock & Gem*, Vol. 27, No. 10, October 1997, pp. 16–18.

Intrigue has surrounded opal since ancient times. It was once thought to possess great medicinal value, particularly for the glands. It was also considered the bearer of certain magical qualities—ensuring fidelity, enhancing memory, making the wearer invisible, and serving as an

aid to psychic visions and out-of-body consciousness, to name a few.

Included in this article is a description of opal by Roman scholar Pliny the Elder, who ranked it second in value to emerald. The article shifts to the modern age with a discussion of opal's occurrences and gemological properties, and in closing it illustrates the ongoing, still mystical appeal of opal's "fire."   *Stuart Overlin*

Oxygen isotope systematics of emerald: Relevance for its origin and geological significance. G. Giuliani, C. France-Lanord, P. Coget, D. Schwarz, A. Cheilletz, Y. Branquet, D. Giard, A. Martin-Izard, P. Alexandrov, and D. H. Piat, *Mineralium Deposita,* Vol. 33, 1998, pp. 513–519.

There are ambiguities in identifying the geologic and geographic origins of cut emeralds by conventional gemological means such as color, transparency, or inclusions. This problem led the authors to investigate the usefulness of oxygen isotope ($\delta^{18}O$) data from emeralds. Samples (no specific number given) from 62 locations in 19 countries were studied. This is a destructive technique, for which 5–10 mg of sample is needed for the isotope analysis.

Three groups of oxygen isotope data are delineated, each of which generally corresponds to specific geologic environments and, in some cases, to specific countries, districts, or even deposits. The first two groups have relatively low oxygen isotope values ($\delta^{18}O$ = +6.2 to +7.9‰, and $\delta^{18}O$ = +8.0 to +12.0‰), and the majority of these deposits formed in association with granitic pegmatites. Most of the isotope values in these two categories overlap and cannot be used alone to identify unambiguously either individual deposits or country of origin. However, a few individual deposits can be identified by using solid and fluid inclusion information in conjunction with the isotope data. The third group, with higher oxygen isotope values ($\delta^{18}O$ > +12.0‰), consists of emeralds associated with faults and shear zones (e.g., from Colombia and Afghanistan). The oxygen isotope values in this group can be differentiated from one another, allowing identification of the specific geographic source (country, district, or mine) for such emeralds. Because geographic origin may influence the value of some gem-quality emeralds, the oxygen isotope method merits further research as a possible tool in identifying country of origin.   *JL*

A reexamination of the turquoise group: the mineral [*sic*] aheylite, planerite (redefined), turquoise and coeruleolactite. E. E. Foord and J. E. Taggart Jr., *Mineralogical Magazine,* Vol. 62, No. 1, 1998, pp. 93–111.

The term *turquoise* applies not only to a mineral species but also to a group of minerals with similar chemistry and structure, of which turquoise is the best known. The group includes six (mostly rare) species (planerite, turquoise, faustite, aheylite, chalcosiderite, and an unnamed Fe^{2+}-Fe^{3+} analogue) that have the general for-

mula $A_{0–1}B_6(PO_4)_{4–x}(PO_3OH)_x(OH)_8 \cdot 4H_2O$, where x = 0–2. This paper summarizes the elemental site occupancies of the six species, and gives crystallographic (e.g., unit cell) data for all members of the group and X-ray diffraction data for some (planerite, turquoise, and aheylite).

The established species, many of which may be blue or green, are indicated in the following table:

Mineral name	A-site cations	B-site cations
Planerite	vacant	Al
Turquoise	Cu	Al
Faustite	Zn	Al
Aheylite	Fe^{2+}	Al
Chalcosiderite	Cu	Fe^{3+}
Unnamed	Fe^{2+}	Fe^{3+}

A complete solid solution exists between planerite and turquoise, and solid solutions exist to varying degrees between chalcosiderite and turquoise, and between faustite and turquoise; these substitutions affect the color.

Study of the turquoise group is hindered by the lack of pure material and the extremely small crystal size, which account for the difficulty in obtaining accurate optical and other physical data. Nevertheless, data are given for planerite (density of 2.68 g/cm^3, hardness of 5 on the Mohs scale, mean R.I. ~ 1.60) and aheylite (density of 2.84 g/cm^3, biaxial (+), mean R.I. ~ 1.63).

The samples studied by these authors are from Bolivia, Russia, and the U.S. (Pennsylvania, Virginia, and Arkansas). The authors suggest that, mineralogically, light blue or blue-green "turquoise" from many worldwide localities may be planerite rather than the species turquoise. [*Editor's note:* The authors did not study material from the classic Persian locality for which the species is named, nor from other gemologically important localities in Arizona and New Mexico. To the best of our knowledge, the International Mineralogical Association has not yet made any rulings on the basis of this study.]
                                         RAH

Tanzanite takes off. R. B. Drucker, *Jewelers' Circular-Keystone,* Vol. 169, No. 4, April 1998, pp. 76–80.

Since its discovery in 1969, tanzanite has risen in popularity to the point that some believe it is the fourth most important colored gemstone after emerald, ruby, and sapphire. In only 30 years, tanzanite has gone from being a collector's specimen to a successfully marketed retail gemstone. It has overcome the stigma of being "too soft," in part because the industry has learned how to set and care for the material properly.

The price of tanzanite has fluctuated widely since its discovery. Prices reached their peak in 1984, at $750 per carat (wholesale) for extra-fine goods. Then, supply overtook demand and prices declined, reaching a low in 1993 of $200 per carat for the same quality of goods. Ironically,

this great price decrease became the main contributor to tanzanite's current popularity and a 50% price rise in the past five years. The lower cost attracted the attention of both mass marketers (e.g., TV retailers) and traditional jewelers and, consequently, consumers.

At present there is no synthetic tanzanite on the market, and the various simulants available can be detected with routine gemological tools (such as a refractometer); visual detection alone is difficult and not recommended. Buying tips are briefly discussed, with saturation being the key to fine color. *JY*

Time travelers. R. Weldon, *Professional Jeweler*, Vol. 1, No. 6, July 1998, p. 50.

Amber [defined as tree resin that is both fossilized and over one million years old—otherwise it is copal] with prehistoric insects and other organic inclusions offers a beautiful window into the past, and it may provide clues to our own civilization. The best-known sources are in the Baltic region (including Russia) and the Dominican Republic. The price of amber takes into consideration several factors: the rarity of the trapped organic matter (shown is a prized specimen that contains a scorpion); the visibility, size, and location of the inclusions; the condition of the amber (including the amount of crazing); the geographic origin; and the color (deeper colors, such as red, are most desirable). *MM*

DIAMONDS

Chameleon diamonds. M. Van Bockstael, *Antwerp Facets*, December 1997, pp. 46–47.

A new awareness of chameleon-type diamonds followed the sale at auction of an important 22 ct stone in 1996. Chameleon diamonds are characterized by a repeatable color change and strong phosphorescence. Unlike the color change in alexandrite, which is seen when the stone is viewed with different light sources (day [fluorescent] or incandescent light), the color change in chameleon diamonds may be observed only when the stone: (1) is heated; (2) is exposed to light after an extended period of time (days or weeks) in the dark (e.g., a safe); or (3) is exposed to strong ultraviolet (UV) illumination (in this case, gentle heating may be required to return the diamond to its original color).

There are at least three different types of chameleon diamond. The first changes from greenish yellow "olive" to bright yellow. The second is seen in some Argyle pink diamonds that change briefly to brownish pink with strong UV illumination. The third (observed in only one diamond) involves a change from faint pink to colorless after exposure to UV radiation.

While the color changes are rapid and/or brief, the typical greenish yellow phosphorescence of chameleon diamonds is relatively long, lasting up to several minutes. The phosphorescent behavior, "chameleonism," and the occurrence of H3 color centers in these diamonds may all be related. For the purposes of grading chameleon diamonds, the reported color is the one that is most stable, that is, the color of the stone after it has had ample time to equilibrate to normal lighting (and temperature) conditions. *Kim Thorup*

De Beers beats BHP to Russian diamonds. J. Helmer, *Business Review Weekly*, Vol. 20, No. 10, March 29, 1998, p. 30.

De Beers has obtained the right to develop the Lomonosov diamond field, one of the world's richest undeveloped diamond deposits [consisting of five diamond-bearing kimberlite pipes]. It is located near Arkhangelsk in northern Russia. Soglasiye De Beers Mining Investments, a joint-venture company, has acquired at least 40%—more than 23 million shares—of Severalmaz, the Russian company that holds the license to develop the field. The Australian company BHP apparently was the only other serious foreign contender.

With an initial outlay of less than $8 million, De Beers now has firm control over foreign investment in the Russian Arkhangelsk diamond fields, and is planning to spend an additional $50 million on feasibility studies and mine development. De Beers has overcome the political and bureaucratic obstacles, and is confident about solving the technical problems of mining the marshy terrain that is close to ecologically sensitive fish-breeding grounds. *Lori Ames*

Diamonds in California. E. B. Heylmun, *International California Mining Journal*, Vol. 66, No. 11, July 1997, pp. 18–20.

"A few hundred" diamonds have been officially recorded as found in California, and possibly thousands have been discarded in the course of alluvial gold mining. Most of the recorded diamonds are yellow, chipped, and flawed; about 20% have been gem quality. Rarely, they are brown, green, blue, or "red." It is easy to overlook diamonds while panning for gold, and the ones that have been found owe their discovery primarily to fortuitous flashes of light. Many California alluvial diamonds are coated with a paint-like substance that obscures their identity; however, they may retain the octahedral morphology characteristic of diamond.

Although no kimberlite has been identified in California, ultramafic rocks such as peridotite, eclogite, and serpentinite are present in the Klamath, Coast Range, and Sierra Nevada Mountains. These rocks may be the diamond hosts. Most of the diamonds have been found in placers in the Mother Lode region of the Sierras, but this recovery may reflect the relative rates of prospecting in source areas. Within the Mother Lode, diamonds have been found at Cherokee Flat (more than 400 diamonds, to 6 ct), Thompsons Flat, French Corral (where the largest stone, weighing 7.25 ct, was found), Foresthill, Smiths Flat, Fiddletown, and Volcano. Several small diamonds have been found associated with platinum in the Klamath Mountains, especially near the junction of the

Trinity and Klamath Rivers, in Tertiary channel deposits and weathering surfaces. Small-to-microscopic diamonds have been found in beach sands from the Oregon border down to Monterey.   *MLJ*

Emplacement and reworking of Cretaceous, diamond-bearing, crater facies kimberlite of central Saskatchewan, Canada. D. A. Leckie, B. A. Kjarsgaard, J. Block, D. McIntyre, D. McNeil, L. Stasiuk, and L. Heaman, *Geological Society of America Bulletin*, Vol. 109, No. 8, 1997, pp. 1000–1020.

Over 70 kimberlites have been identified in the very large (30 × 45 km) Fort à la Corne kimberlite field in Central Saskatchewan, interspersed with sedimentary rocks. Although the kimberlite phases contain diamonds (0–23 ct/100 tonnes), no economic deposit has yet been identified. These kimberlites are unusual because they do not have the cone shape characteristic of kimberlites from South Africa and most other localities; rather, they are shaped like sheets or saucers and lack diatreme or root zones. Therefore, only crater facies kimberlites are present, with large diameters and shallow depths. The absence of competent barrier rocks (e.g., basalts) in the sedimentary layers near the surface enabled the kimberlite magma to erupt easily without forming the typical cone shape.

Drill cores were obtained from one of the kimberlites, the Smeaton (950 m in diameter; 130 m at its thickest area, tapering to only 20 m at its edges), by the Geological Survey of Canada for research purposes. The Survey's studies show that about 101 million years ago the kimberlites exploded onto the Earth's surface in at least two periods of volcanism. The rock materials erupted into the atmosphere and eventually formed air-fall deposits of various types. These were subsequently intermixed with both marine and terrestrial sediments during such processes as erosion and shoreline changes. Micro-diamonds are found in some of the air-fall deposits, which can only be interpreted to mean that diamonds were literally "falling from the sky"!   *AAL*

It's a rough world. K. Nestlebaum, *Rapaport Diamond Report*, Vol. 21, No. 1, January 9, 1998, pp. 59, 61, 65.

The success of a rough diamond buyer depends on the buyer's ability to recognize and sort different types of rough, and to determine their value. This must be done quickly, using only a few pocket instruments or simple tools. This article describes the various factors a buyer must consider in evaluating rough diamonds, using the major categories of form, shape, and color.

Twelve different forms are described (e.g., closed stones, near-gems, macles, cleavables). On the basis of shape, goods are categorized as sawable, nonsawable, and fancies. Sawables, of which well-formed octahedra and dodecahedra that finish into rounds are the best examples, are more valuable than nonsawables because of their greater finished weight retention. Elongated or distorted crystals will finish into fancies (e.g., emerald cuts) that are generally less expensive than rounds. Three categories of color are recognized. "Colorless," the top category, is equivalent to the gemological color grades D to F; "tinted" refers to the color grades G to I; and "colored" includes the more saturated yellows, browns, and other fancy-color stones.

Another factor in determining the value of rough diamonds is size. Specially designed sieves are used to separate the various sizes. Sieve sizes begin at about 50 stones per carat and increase up to about three stones per carat.

Most of the rough offered for sale is presorted and packaged as a Central Selling Organisation "sight." During a sight offering, the rough buyers (sightholders) can examine goods under the best conditions. Another outlet is the Antwerp rough market, a 60-year-old bourse where diamonds from mines outside of De Beers's control are traded; it is open to all buyers. Rough buyers can also purchase goods in certain source countries, where they commonly must make important decisions under less-than-ideal lighting conditions. No matter where rough is purchased, its ultimate value cannot be determined until it has been cut and polished.   *JY*

Making the cut: The journey from rough to polished. K. Nestlebaum, *Rapaport Diamond Report*, Vol. 21, No. 5, February 6, 1998, pp. 51, 65.

This article follows rough diamonds to their polished state through the following stages: cleaving, sawing, bruting, cross-cutting (creating four facets above and four facets below the girdle), and, finally, brillianteering (placing the remaining facets). The importance and value of the skilled diamond cutter is emphasized. It concludes that even though automation has been in existence and improving for certain aspects of the cutting process (e.g., laser sawing) for the past three decades, finer stones continue to be cut by traditional methods. Modern machinery cannot make the decisions and judgments necessary for each individual stone, especially the more valuable ones.   *JY*

Trans Hex—The miner to marketer. C. Gordon, *Diamond International*, No. 52, 1998, pp. 57, 58, 61, 62.

Trans Hex currently produces about 200,000 carats of diamonds annually in South Africa, primarily from several alluvial deposits along the Orange River and in Namaqualand. This represents 2% of South African diamond production. Much of Trans Hex's production is of very high quality: Orange River goods can be worth $600 per carat. Because the established deposits are rapidly becoming depleted, Trans Hex is developing new alluvial deposits, the most promising of which are marine concessions in the Atlantic Ocean. Through Canadian-registered Trans Hex International, exploration for new diamond deposits is under way in Brazil, Indonesia,

Namibia, Angola, and several West African countries.

Trans Hex markets its own diamonds using a unique, and very successful, sealed-tender system. It holds "sights" in which potential buyers can view parcels. Top buyers are attracted because they can submit bids for the particular types of rough diamonds that suit their needs. This is distinctly different from the CSO "box system," in which sightholders have limited options in their selection of rough diamonds. *AAL*

Unusual diamonds and unique inclusions from New South Wales, Australia. H. O. A. Meyer, H. J. Milledge, F. L. Sutherland, and P. Kennewell. *Russian Geology and Geophysics* [Proceedings of the Sixth International Kimberlite Conference], Vol. 38, No. 2, 1997, pp. 305–331.

Alluvial diamonds in eastern Australia were mined intermittently from 1852 to 1922, primarily in the Copeton/Bingara area of New South Wales (400 km north of Sydney). These diamonds are enigmatic because they cannot be related to any conventional primary source, such as a kimberlite or lamproite. Although the many sophisticated studies (e.g., carbon and nitrogen isotopes) that have been made uncovered some unique characteristics of these diamonds, none succeeded in determining their provenance. After reviewing pertinent data, this paper continues the search by examining a selection of 65 documented diamonds collected between 1989 and 1992. The studies include: mineral inclusions, carbon and nitrogen isotope data, external features, cathodoluminescence (CL) characteristics, and estimation of nitrogen content and aggregation by infrared spectroscopy.

Important results are: (1) There are two major populations of New South Wales diamonds, one white (low nitrogen, complex CL zoning) and one yellow (high nitrogen, no CL zoning); (2) morphologically, there are almost no octahedra, which suggests substantial resorption and/or transportation over long distances; (3) previous conclusions with respect to the unusual isotopic characteristics and mineral inclusions of these diamonds are confirmed, and an augite inclusion—characteristic of an eclogitic origin—was identified; and (4) the diamonds formed in the temperature range of 1,180°–1,240°C. Notwithstanding these comprehensive data, no new hypothesis for the origin of the eastern Australia diamonds is presented. *AAL*

GEM LOCALITIES

Chrome diopside & chrome enstatite: Rare gemstones. W. D. Hausel, *International California Mining Journal*, Vol. 67, No. 7, March 1998, pp. 23–24.

The bright green chromium-rich varieties of diopside and enstatite are rare gem materials that can be found in Wyoming and nearby states, in association with kimberlite indicator minerals (e.g., pyrope) as well as diamonds. Gem-quality chromian diopside up to 5 cm (2 in.) long has been found in the State Line district (along the Colorado-Wyoming border) and in the Green River Basin in southwestern Wyoming. Today the latter is a better place to find both chromian diopside and chromian enstatite because of easier access. These materials can be recovered from stream sediments with careful use of a gold pan. The sizes and quality of individual faceted (or facet-grade) pieces are not mentioned in this article.

MLJ

Micro-PIXE analysis of trace element concentrations of natural rubies from different locations in Myanmar. J. L. Sanchez, T. Osipowicz, S. M. Tang, T. S. Tay, and T. T. Win. *Nuclear Instruments and Methods in Physics Research B*, Vol. 130, 1997, pp. 682–686.

The authors analyzed 130 untreated rough rubies from nine metamorphic localities in Myanmar, including Mogok and Mong Hsu, using micro proton-induced X-ray emission (PIXE). The concentrations of chromium, titanium, vanadium, iron, copper, and gallium—the most abundant trace elements—were determined for a 200 × 200 μm area on each stone. In a unique approach, the authors used the trace-element mapping capability of the instrument to eliminate inhomogeneities, such as inclusions, from the analyses for the areas examined.

The measurements revealed that, with the exception of gallium, there were large variations in the trace-element chemistry of rubies from the different localities, as well as for rubies from the same locality. Nevertheless, some consistent differences were also found. Using statistical analysis, including tree clustering and factor analysis, the authors determined that the origin of rubies from six of the nine localities could, indeed, be determined using this technique. *Sam Muhlmeister*

Neue Edelsteinvorkommen (New gem deposits). U. Henn and C. Milisenda, *Uhren Juwelen Schmuck*, January 1998, pp. 51–53 [in German].

Tanzania emerged as a great producer of colored gemstones in the second half of this century. Most of the important localities (e.g., Longido, Lake Manyara, Merelani, and Umba) are in the northern part of the country; they produce a great variety of gems, the most important being tanzanite, corundum (ruby and fancy-color sapphires), garnet (particularly rhodolite and tsavorite), tourmaline, emerald, alexandrite, spinel, and quartz. Diamonds are mined from the Mwadui kimberlite pipe, also in the north. Historically, gemstone occurrences in the south have been rare.

In 1994, however, large and rich gem deposits were found in southern Tanzania in the vicinity of Tunduru, about 80 km north of the border with Mozambique. An estimated 80,000 "illegals" have been working the alluvial deposits in the vicinity of the Muhuwesi and Mtetesi Rivers, mostly by primitive methods. Although the primary sources of the gem minerals have not been found,

the fact that some crystals are only slightly rounded indicates short transport distances. This article discusses the history of the discovery and the development of gemstone trade in this area, the geologic setting of the deposits (in the Proterozoic Ubendian-Usagaran System of metamorphic rocks), and the most important gem materials found to date. These include blue and fancy-color sapphires, ruby, many colors of spinel, garnet (rhodolite, hessonite, and color-change), and chrysoberyl (cat's-eye and alexandrite). *PB*

New gemstone occurrences discovered in Wyoming. *International California Mining Journal*, Vol. 67, No. 6, February 1998, pp. 7–8.

"Gem-quality" cordierite [iolite] and peridot have been discovered in Wyoming by the state Geological Survey. The cordierite is transparent and violet-blue; it is found as mineral grains up to 5 cm (2 in.) long in rock in the central Laramie Mountains, near Wheatland. The peridot occurs in rock (to 2.5 cm across) or as smaller loose pieces; it is transparent and "olive-green." The Survey recovered about 13,000 carats of peridot from alluvial sources in the Leucite Hills, near Rock Springs. Also, two additional kimberlite pipes have been located in the Green River Basin, but no diamonds have yet been found in either. *MLJ*

Pearls and pearl oysters in the Gulf of California, Mexico. D. McLaurin, E. Arizmendi, S. Farell, and M. Nava, *Australian Gemmologist*, Vol. 19, No. 12, 1997, pp. 497–501.

For more than four centuries, Mexico's Gulf of California was a major source of colored pearls, but overfishing and pollution have greatly reduced production since the latter part of the 1800s. This situation is now being reversed with research into pearl culturing and the establishment of pearl farms. This article describes the cultivation procedures of the I.T.E.S.M. Perlas de Guaymas pearl farm in Bacochibampo Bay, near Guaymas, which started operations in 1996. The farm uses a suspended culture system and new, Mexican-developed grafting technology. In 1997, the farm produced 30,000 mabé pearls, and projections for 1998 were to double this quantity. [*Editor's note*: For further information on Baja California pearls, see M. Cariño and M. Monteforte, "History of pearling in La Paz Bay, South Baja California," *Gems & Gemology*, Summer 1995, pp. 88–105.] *Scott Rebhun*

A study of Korean precious serpentine. W.-S. Kim and S.-H. Cho, *Journal of Gemmology*, Vol. 26, No. 3, 1998, pp. 156–164.

A new deposit of gem-quality serpentine was discovered in 1995 in Booyo County, South Korea. The deposit forms along both contacts of a garnet vein that cross-cuts a body of serpentinite (a rock consisting almost entirely of serpentine-group minerals). The gem-quality serpentine is semi-translucent, with a uniform deep green color; it has

a hardness of about 5, a resinous and waxy luster, a specific gravity of 2.57–2.58, and a refractive index of about 1.56. The color changes from deep green to orange-pink when the material is heated at 850°C.

X-ray powder diffraction analysis identified the gem serpentine as antigorite (a mineral in the serpentine group). Eye-visible black inclusions (magnetite) are dispersed throughout the material. Important trace elements include chromium, nickel, and cobalt. The serpentine, marketed domestically as "Booyo Precious Serpentine," is fashioned into cabochons, pendants, buttons, beads, and rings. *MM*

JEWELRY HISTORY

Electron microprobe analysis and X-ray diffraction methods in archaeometry: Investigations on ancient beads from the Sultanate of Oman and from Sri Lanka. C. Rösch, R. Hock, U. Schüssler, P. Yule, and A. Hannibal, *European Journal of Mineralogy*, Vol. 9, 1997, pp. 763–783.

Beads from graves of the Samad Culture (300 BC to 900 AD), excavated in Oman, are made of: natural minerals and rocks (serpentine, talc, and chlorite-containing rocks of local origin, which are soft and can be carved, and almandine-pyrope garnets believed to be imported from Sri Lanka or India); metal (pure silver and gold, or these elements alloyed with copper); glass (reddish brown, sodium-rich, colored by copper dissolved in the glass matrix); "Egyptian Blue" (a synthetic material produced in Egypt since the third millennium BC); and synthetic enstatite (formed by heating carved Mg-silicates, such as talc, to 1,000°C with a resultant increase in hardness and durability).

Beads from an ancient craftsmen quarter of the old kingdom of Ruhuna (third to fifth centuries AD), from recent excavations in Tissamaharama, Sri Lanka, have a few similarities to those from Oman, particularly with respect to the garnets, which suggests that there was commerce between these civilizations in ancient times. However, the potassium-rich reddish brown glass beads from Sri Lanka are distinctive, because they are colored by tiny droplets of cuprite (Cu_2O) and completely lack PbO. This is the first study of its type on beads from ancient Oman and Sri Lanka. *AAL*

Mineralogy of the Louvres Merovingian garnet cloisonné jewelry: Origins of the gems of the first kings of France. F. Farges, *American Mineralogist*, Vol. 83, 1998, pp. 323–330.

The garnets in cloisonné jewelry from a burial site in Louvres (North Paris), France, dated to around the fifth or sixth century AD, were examined using the proton-particle induced X-ray emission (p-PIXE) method. This technique allows archeologists, art historians, and others to measure the chemistry of such irreplaceable artifacts nondestructively. The 118 cloisonné items examined

were from the tombs of Frankish aristocrats, four female and one male; the pieces included brooches, bracelets, and pendants of gold and/or silver construction.

Three types of garnets were identified in the jewelry. Type I, found in the majority of the cloisonnés, is rhodolite, with a chemical composition between almandine (iron) and pyrope (magnesium); the source might have been South India–Sri Lanka. Type II garnet is pyrope, possibly from Scandinavia, central Europe, or South India–Sri Lanka. Type III garnet is chromium-rich pyrope, and the most likely source for this rare mineral is Bohemia. Sri Lanka, then known as Ceylon, was a major source of garnets in the early Middle Ages, and these cloisonnés testify to the extent of Ceylonese trade with Europe at the time. The author proposes that the use of pyrope and rhodolite, rather than the geologically more common almandine garnet, in the Louvres cloisonnés may mean that the Franks had gemological knowledge far more advanced than current historical scholarship suggests.

JL

JEWELRY RETAILING

Consumers discover the other 'C.' R. Bates and R. Shor, *Jewelers' Circular-Keystone*, Vol. 169, No. 9, September 1998, pp. 144–145.

"Ideal Cut" diamonds are becoming more popular, particularly among the affluent and college-educated, because of increased advertising and publicity. Today they account for 5%–7% of diamond sales, up from 1%–2% a decade ago. However, there is concern that diamond cut is becoming commoditized, thus increasing the risk for deception. Those who overgrade color and clarity are also likely to misrepresent cut. Terms such as "near-Ideal," "superior" cut, and "fine" cut are confusing to the consumer, but nonetheless are common in the trade. It has also been reported that certain grading laboratories are labeling stones as "Ideal" even when they fall outside commonly accepted proportions. Such practices may render the term "Ideal" meaningless in the future.   *MM*

Gifts Incorporated. J. D. Malcolmson, *JQ Magazine*, Vol. 77, 1998, pp. 25–34 passim.

Today's jewelers work in a very competitive market. Not only must they compete with "traditional" retailers, but they also must deal with giant mass marketers. One area of retailing that is not yet saturated is corporate sales. Not long ago, such an area might not have been very lucrative, but conditions have changed. The austerity that followed the consumerism of the 1980s has given way to a more carefree attitude toward corporate gifts of jewelry, either as rewards to valued employees or as incentives to customers.

To succeed in corporate sales, a jeweler must have an organization that can deliver the product on time and to the customer's specifications. Otherwise a special occasion could be missed, causing the jeweler to lose a repeat customer. It is also important to offer products with name value. A Rolex-brand watch, for instance, communicates an extra sense of appreciation to the recipient of a corporate gift. Jewelers who already have a good understanding of the gift-giving market and products in general will benefit most quickly from such sales. Developing such a corporate clientele may be difficult, but the rewards—repeat customers of high-end merchandise—can be quite gratifying.   *JEM-S*

It's a Guy Thing. A. Cardella, *American Jewelry Manufacturer*, Vol. 43, No. 8, August 1998, pp. 50–54.

Men's jewelry has historically been one of the most elusive markets to tap, but industry forecasters, designers, manufacturers, and retailers agree that the market is enjoying a gradual resurgence. Some of the factors contributing to this resurgence are a strong economy that has sparked luxury spending, a more image-conscious man, and a changing economic dynamic in which wives tend to be financially independent, leaving husbands with more money to spend on themselves.

The key to predicting what men will buy is understanding why they buy jewelry in the first place. Men shop differently from women: They usually do not buy a piece of jewelry simply because they like it. Salespeople should stress the practical function of the piece, not just its appearance. Men are also symbol oriented—often more so than women, notes one forecaster—and will purchase jewelry that reflects personal interests such as golf, sailing, or their alma mater. Today's symbolism also extends to spiritual, religious, Gothic, and astrological symbols in men's jewelry.

The wrist and hand are the focal points of the men's market, and bracelets and rings remain the strongest-selling items. Less-traditional items such as earrings are still largely unproven, while forecasters predict that necklaces will surge in the coming seasons. Sales of platinum jewelry for men are up, with rings and bracelets leading the way.   *Stuart Overlin*

Selling the diamond dream. *Diamond International*, No. 51, 1998, pp. 57, 58, 61, 62.

Adapted from a talk presented by De Beers's Consumer Marketing Division director Stephen Lussier, this article discusses the company's approach to consumer marketing and evaluates both current and future prospects. Central to the De Beers approach is the "diamond dream": the unique, emotional power of diamond as a cultural symbol of prestige, elegance, and love. Because the value of diamond jewelry is largely symbolic rather than practical (i.e., you don't need it for transportation or nourishment), the company's Marketing Division spends $200 million a year maintaining and building the diamond dream. These promotions have successfully expanded the consumer base for diamonds by developing new occasions (the diamond anniversary band), attracting

new consumers (young, single Japanese women in the early 1980s), repositioning products (the evolution of the "Riviera" bracelet into the more casual "tennis" bracelet), and establishing new markets (the emergence of the diamond wedding ring in Far East societies).

Three factors make the current environment a challenging one for diamond sales: the decline in the Japanese market, the economic crisis in the East Asian markets, and the strength of the dollar. Yet there is optimism, based on: the stability of the Western markets (particularly the American market), growth in a region De Beers calls "Asia Arabia," promising results thus far in the Indian and Chinese markets, and the enduring desire for diamonds. It is this "addictive" allure of diamonds that the company can always rely on, even when the markets are having difficulties. *Stuart Overlin*

Turmoil hits jewellery. *Mining Journal, London*, Vol. 331, No. 8497, September 11, 1998, p. 204.

The economic crisis in Asia has had a major effect on demand for gemstones and precious metals. In Japan, jewelry sales for the first six months of 1998 were down 16% from the same period the previous year. Gold jewelry sales were down 18%, and platinum jewelry was down 15%. Sri Lanka has also been hard hit as a producer of colored stones: Gem exports fell 73% (from 992.6 to 266.3 Sri Lankan rupees) in the first five months of 1998 relative to the same period the year before. Seventy percent of Sri Lanka's gem exports go to Asia. However, the American market remains strong, and exports to the United States rose 31.6% in January through May 1998 compared to the same period a year earlier. *MLJ*

PRECIOUS METALS

Jewellery is now the largest application of platinum. *South African Mining, Gold, and Base Minerals*, May 1, 1998, p. 43.

The demand for platinum jewelry is strong and going up. In 1997, more than 2 million ounces of platinum were used in jewelry. During that same year, consumption "doubled in China and rose 55% in the U.S." This has taken pressure off the industry to rely on Japan as the main sales market. An important reason for the success of platinum has been an aggressive marketing campaign by the Platinum Guild International that is based on quality and value rather then price. *Scott Rebhun*

SYNTHETICS AND SIMULANTS

The death of Kashan. R. Weldon, *Professional Jeweler*, Vol. 1, No. 6, July 1998, p. 46.

Kashan flux-grown synthetic rubies first appeared about 30 years ago and were highly regarded for their fine quality. Nevertheless, the Dallas-based company went out of business in the mid-1980s. Three years ago, Kashan Created Ruby was revived, but once again it has ceased production because of competition from now-abundant (especially in smaller sizes) natural rubies from Mong Hsu (Myanmar), as well as the preference among manufacturers for the less-expensive flame-fusion synthetics. Over its 30-year history, Kashan produced 44,528 carats of cut rubies; Mong Hsu churns out 45,000 carats of rough rubies *daily*. In addition, there are more than 40 other active ruby mines worldwide. *AAL*

Growing carats. R. Weldon, *Professional Jeweler*, Vol. 1, No. 1, February 1998, pp. 47–48.

Small amounts of gem-quality synthetic diamonds, most of which are yellow and in small sizes, are presently known to the trade, but futurists believe that they will become more abundant, larger in size, and relatively inexpensive.

This short article, packed with pertinent information about synthetic diamonds, contains predictions primarily from Tom Chatham (Chatham Created Gems), who is gearing up to manufacture gem-quality synthetic diamonds in the U.S. using Russian expertise. He is striving for eventual production from his facilities of 10,000 carats a month (of J color and SI clarity), and expects that goods in the 1 ct range will sell for about $500 per carat. Alex Grizenko (Russian Colored Stone Co.), another proponent of synthetic gem diamonds, predicts that commercial goods will reach 6 ct. At present, his Russian suppliers produce yellow and "tangerine" synthetic diamonds, and some green material. *Anne M. Blumer*

High-pressure synthesis of high-quality diamond single crystals. Yu. N. Pal'yanov, Yu. M. Borzdov, A. G. Sokol, A. F. Khokhriakov, V. A. Gusev, G. M. Rylov, and N. V. Sobolev, *Diamond and Related Materials*, Vol. 7, 1998, pp. 916–918.

Recent techniques in the growth of synthetic diamonds and assessments of crystal defects are summarized. The synthetic diamond crystals were grown using the temperature gradient method, and X-ray topography was used to reveal crystal lattice dislocations. The dislocations are similar to those found in natural diamonds, and the authors claim that the dislocations in their synthetic diamonds take up a smaller volume of the crystal (10%–35%) than defects in natural diamonds. Ultraviolet transparency in the UV spectral regions reached 400 nm, and the synthetic crystals studied had weak absorption characteristics throughout the visible spectrum that are similar to those in previously studied annealed synthetics. The authors state that synthetic diamonds are increasing in "quality and purity" as work continues; their size was not reported. *JL*

TREATMENTS

Concern about treatments rises. B. Sheung, *Jewellery News Asia*, No. 163, March 1998, pp. 49–52.

Treatment of South Seas and Tahitian pearls to improve

their appearance has increased, and industry leaders are concerned that this may affect consumer confidence. Treatments recognized on the market today include bleaching, polymer coating, dyeing, and irradiation. The percentage of pearls being treated is not known; however, it is estimated that as much as 30% of white South Seas pearls are bleached, and up to 80% of golden South Seas pearls are color enhanced. Some in the pearl trade feel that treated South Seas pearls have a place in the market because the greater availability makes them more accessible to more consumers. Others respond that treatment will erode consumer confidence and the prestigious image associated with South Seas pearls. However, most agree that disclosure of treatment is vital. The article mentions some techniques for recognizing the various treatments.   *JEM-S*

Filled diamond tested by Raman spectroscopic system. C.C. Yuan, *China Gems*, Vol. 7, No. 2, 1998, pp. 53–54 [in Chinese].

Fracture-filled diamonds were studied by Raman spectroscopy. An argon ion laser beam (0.005 mm in diameter) focused on filled fractures revealed two types of filling material. One, lead glass, shows a broad Raman peak in the range of 830–930 cm^{-1}. The other, believed to be resin, gives a series of peaks in the 1100–3000 cm^{-1} range. This article illustrates that Raman spectroscopy is a powerful technique for identifying materials used to fill diamonds and other gemstones.   *Taijin Lu*

MISCELLANEOUS

Green mining. S. Frazier and A. Frazier, *Lapidary Journal*, Vol. 51, No. 9, December 1997, pp. 45–48, 50, 64.

In the past, mining technology was concerned solely with retrieving minerals from the ground at a profit, without much regard for environmental matters. Gold mining, for example, once polluted the environment of the western United States with mercury, which was used to recover the gold from the ore. In addition, the hydraulic methods used for gold mining destroyed California hillsides. Copper mining at Butte, Montana, has dispersed dangerous heavy metals into the atmosphere, soils, surface water, and groundwater. Such practices are no longer tolerated in many countries, and all future mining must be environmentally friendly, even though this process may be expensive, time consuming, and difficult to engineer. These problems are now easier to solve, however, because of new mining technology and a better understanding of mineral deposits.

"Green mining" (i.e., environmentally responsible mining) is currently being practiced at many locations in North America. The article cites as examples a gold and myrickite (a red cinnabar–opal–chalcedony mixture) mine in northern California, and the Sweet Home rhodochrosite mine in Colorado. The mining of gems, crystals, and fossils—like that for metals and all other earth resources—is now commonly accompanied by a demand for environmental protection.   *MD*

Shipping safely. C. Marandola, *American Jewelry Manufacturer*, Vol. 43, No. 8, August 1998, pp. 56, 58–61.

Jewelry is intrinsically vulnerable to loss during shipping, but precautions taken before a package is sent can control losses and keep insurance rates down. This article details four specific steps, gleaned from industry experts:

(1) *Establish internal procedures*. A chain of custody, with as many people involved as possible, simplifies pinpointing where the loss occurred. The following should be documented: description of the items, value, destination, type of packaging, and carrier. Instruct employees not to share even casual information with pick-up drivers.

(2) *Package to minimize theft*. Use ordinary-looking but sturdy brown or white cardboard boxes, no smaller than an adult shoebox, securely sealed with gummed reinforced paper mailing tape, pressure-sensitive tape, or tamper-evident tape. The box should be new; used ones are easier to tamper with. Placing a smaller box within a larger box reduces loss from slit packages. Include an itemized packing slip inside the box *and* send a copy separately. The labeling on the package should not denote jewelry or precious metals (use initials rather than company names). Adding weight to the box diverts suspicion of light and valuable contents. Use labels that cannot be easily replicated and affix them well.

(3) *Follow consistent shipping guidelines*. Research the shipping company's reliability and hiring practices. Avoid shipping to known jewelry zip codes (47th Street in New York and Hill Street in Los Angeles). Armored truck and first-class registered mail are safest. Services such as UPS, FedEx, and Express Mail are riskier because they can be targeted by thieves at a central point. Also, shipping early in the week means packages will not have to sit in a warehouse until Monday morning.

(4) *Prepare for loss*. This section addresses insurance limitations and extent of coverage through shippers and insurance agents. As a general rule, insurance should cover 110% of the item's value, plus freight and incidentals.   *Carole Johnson*